UCLouvain
Institut de recherche
en mathématique et physique

Quadruple Splitting Functions in QCD

Doctoral dissertation presented by

Martin Michel

in fulfilment of the requirement for the degree of Doctor in Sciences.

Thesis Committee

Dr. C. Duhr *(supervisor)*	CERN
Prof. F. Maltoni *(supervisor)*	UCLouvain
Prof. V. Lemaitre *(president)*	UCLouvain
Prof. C. Degrande	UCLouvain
Prof. V. Del Duca	ETH Zürich
Dr. L. Tancredi	Oxford U.

2020

Acknowledgements

This thesis presents the work I have conducted during the last four years, and which could not have been done without the help and support of many people. These few lines are an attempt at listing and showing my gratitude to all those who contributed to my research.

First and foremost, I would like to thank Claude who guided me and offered precious advice during these four years. His experience and near encyclopaedic knowledge proved many times to have the exact answers I needed.

At CP3, there are many people who deserve an acknowledgment, in particular: Bram and Robin, who were always there whatever the matter, whether it was physics, administration, technicalities or just fun, which I considered as my "CP3 big brothers"; Zhengwen, Liam, Matteo, and Samuel for all the chats, the help they provided, the lunch and coffee breaks; Carinne and Jérome who solved my numerous administrative and IT troubles. On the CERN side, I would like to thank the other members of the team: Sophia, Brenda, and Lorenzo, for the discussions during the weekly meetings and their warm welcome each time I went to Geneva.

A huge thank you also to my external collaborators from Zürich: Vittorio, Achilleas, and Rayan. It was a pleasure to work with them and I learned a great deal in this collaboration.

Furthermore, I would like to thank my thesis committee who took the time to read and comment the manuscript so that this improved version could see the day.

Finally, I thank my friends and family, those who did not contribute directly to my work but were nevertheless always there for me: my parents who were always supportive of my projects; my many siblings who brought joy even to the darkest days; in particular, my big brother Christophe whose experience, advice, discussions, disagreements, debates, and others have shaped a lot of my decisions in life; my uncle who will recognise itself, for its running gag of encouragement; my friend Son for his exemplary perseverance and open-mindedness; my housemates who suffered my doubts and tribulations and shared my smallest victories; and my former flatmates for making my weekends and holidays much more memorable.

Abstract

The infrared divergences of QCD have always rendered computations in perturbation theory difficult, making integrating the corresponding regions of phase-space delicate. In the current efforts to bring the state-of-the-art computations in QCD to N^3LO, it is then crucial to develop a subtraction scheme at that order. Such a project requires the knowledge of the soft and collinear behaviour of QCD amplitudes, which is made easier by the universal factorisations that happen in these limits. For squared amplitudes in the collinear limit, the universal pieces are known as *splitting functions*.

In this thesis, we compute the quadruple collinear splitting functions, adding an essential piece to the effort of the community to build a subtraction scheme at N^3LO in QCD. We review how to compute such functions, and detail their symmetries as well as their colour structure. In addition, we check the soft and collinear limits of the splitting functions as both a way to verify our results and to explore these specific regions of phase-space.

Contents

Introduction

Reductionism and the Standard Model

Throughout its History, the successes of science, and in particular physics, have relied thoroughly on the concept of *reductionism*, the idea that any process in nature should be explainable by more fundamental laws. The very meaning of this concept is debatable, but for what concerns physics, or any theory expressed in the language of mathematics, the goal is to have as few and as simple equations as possible describing as many processes as possible.

One of the earliest and yet gorgeous incarnation of reductionism was the unification by Isaac Newton at the end of the XVII$^{\text{th}}$ century of the phenomena of weight and the motion of the planets under the same law of universal gravitation. In a single strike, Newton swept the overcomplicated Ptolemy's geocentric model with its many spheres to combine it with the everyday notion of weight. Later, James Clerk Maxwell managed to brilliantly reveal electricity and magnetism as the two faces of the same coin, yet again boiling down two seemingly completely different phenomena of nature to a more encompassing one. At the end of the XIX$^{\text{th}}$ century, matter was believed to be continuous and all the properties of a certain material could be summarised by some constants: conductivity, elasticity, permittivity, viscosity, and so on. Time, and quantum mechanics, will prove that all these numbers are mere consequences of the atomic and molecular structures of a particular material, which can, in principle, explain these.

These few examples perfectly illustrate how important the role of reductionism was in History, and surely its task is not done yet. Our modern understanding of nature to this day states that our surrounding is mostly made of *atoms*. Through different combinations and ways of assembling, molecules, crystals, and others, these tiny building blocks and their laws are responsible for all the phenomena we see in our lives. However, to get a grasp on atomic laws requires to explore its structure. Even though ancient greeks, who named atoms, thought they were unbreakable and undividable, it was proved that atoms actually are made up of negatively charged particles called *electrons*, orbiting a nucleus, which itself is an arrangement of neutral and positively charged particles, respectively called *neutrons* and *protons*. We could notice once again the action of reductionism here, or use it once more to probe the structure of protons and neutrons. Indeed, at the end of the XX$^{\text{th}}$ century, these two particles, as well as hundreds or others (which are collectively named *hadrons*, protons and neutrons being hadrons themselves), turned out to be made of smaller particles, called *quarks*. In particular, protons and neutrons are made of two types of quarks: the *up* and *down* quarks. Nowadays, electrons and quarks are suspected to be undividable, but if lessons are to be learned from History, should we hold so firmly to this belief ?

Although the description of the *a priori* most fundamental building blocks of the Universe is very satisfying, it would be incomplete without the addition of their *interactions*. Relativity imposing a finite speed to the propagation of information, including for example the change of position of the sources of any force, interactions are elegantly represented in particle physics by the exchange of a mediating particle travelling through space at finite speed. This paradigm adds a certain number of new fundamental particles to the game, e.g. the *photon* which carries the *electromagnetic* interaction or the *gluon* which allows quarks to interact through the *strong* interaction. We can also mention the *weak* interaction, which is mediated by the so-called W and Z *bosons*, and which can be unified with electromagnetism to form the *electroweak* interaction. To this already complex set of particles, we add the *electron neutrino*, a massless neutral particle involved in radioactivity (note that we now know that neutrinos actually have a really small mass, even though this mass is not accounted for in the basic SM). Finally, a last particle, the *Higgs boson*, is needed for mathematical consistency and was thankfully discovered in 2012 at the *Large Hadron Collider* (LHC). The icing on the cake is provided by making three copies, called *generations*, of the set quarks-electron-neutrino, each one identical in every point to its predecessor, except being heavier. This set of particles and their interactions forms what is called the *Standard Model* of particle physics (SM) and is the commonly accepted theory to this day. In the end, it is made of twelve matter particles, called *fermions*, three interactions, carried by *bosons*, whose strengths are fixed by so-called *coupling constants*, and the Higgs boson. For a more detailed introduction of the SM, see for example [1].

fermions			bosons
u up quark	c charm quark	t top quark	γ photon
d down quark	s strange quark	b bottom quark	$W^{\pm}$ W boson
e electron	μ muon	τ tau	Z Z boson
ν_e electron neutrino	ν_μ muon neutrino	ν_τ tau neutrino	g gluon
			H Higgs boson

Table 1: The particle content of the Standard Model

Despite the fact that the SM is performing extremely well when comparing its predictions to experimental results, it is most probably not the ultimate theory of nature. Some phenomena, like gravity, are still not included in this theory. More worryingly, nobody has been able to provide a mathematically consistent quantum theory of gravity, which should reasonably be the first step before even thinking about describing it in the same framework as the other fundamental interactions. In addition, the SM seems to depend on too many free parameters to be a fundamental theory: in such a theory, one would expect all parameters to be mere epiphenomena of more fundamental processes described by a really small set of fundamental parameters. In particular, the masses in the SM seem all over the place and span many orders of magnitude without any apparent pattern. One could also mention dark matter, this mysterious missing mass needed to explain for example galactic rotation speeds, that has no description in the SM despite representing most of the matter in the Universe. To answer all those questions and solve these puzzles requires of course the proposal of new ideas, but also and perhaps mainly to test the SM and try to find where it fails. This requires in turn to better understand the mathematical structure of the SM interactions as well as improve our ability to explicitly make computations in the SM.

Scattering amplitudes and Feynman Diagrams

Particle interactions in the SM are encoded in so-called *scattering amplitudes* (or just amplitudes). These mathematical functions only depend on the kinematics and the quantum numbers, e.g. the electric charge, of the ingoing and outgoing particles and encompass all the information about the interaction. For example, the probability of a certain event happening is obtained by taking the modulus square of the amplitude associated with this event.

Consider a process during which m particles, with momenta p_i, interact to produce n particles, with momenta q_j. We can associate to the initial and final situations a quantum state, respectively $|\text{in}\rangle$ and $|\text{out}\rangle$. By the laws of quantum mechanics, the probability is then obtained by projecting the *in* state to the *out* state, and squaring the result. A convenient way to compute this is to first consider that these states are not interacting with each other: they are free states, which allows to have explicit expressions for these external states, since the solutions

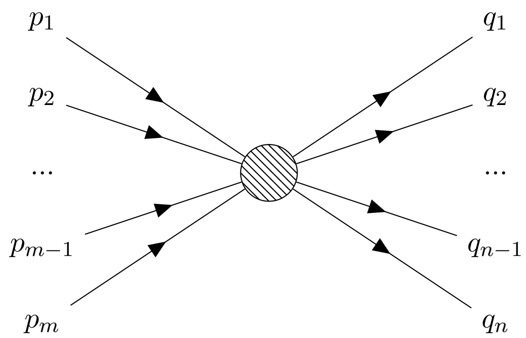

Figure 1: Illustration of a generic scattering event (time goes from left to right)

of the free equations are known. To ensure that the external states are free, we consider these states as being asymptotic states, meaning that the *in* state starts at time $t = -\infty$ and the *out* state is at time $t = +\infty$. The operation of mapping the initial state to the final state is then represented by the action of an operator S, which is essentially the exponential of the interaction terms of the Lagrangian density of the theory, and the action of this operator on the asymptotic *in* state projected on the asymptotic *out* state is known as the S-*matrix*.

Although this procedure for computing amplitudes is clearly defined, in practice though, the problem of exponentiating the Lagrangian density of the SM is not possible within our current knowledge. It is then useful, when computing observables with these amplitudes, to simplify this operation by doing an expansion of the exponential. This method is called perturbative expansion and is justified when the subsequent terms are smaller and smaller such that a finite number of terms in this expansion is enough to have a good approximation of the desired result. If such an expansion in the computation of an observable is performed, we call the first non-zero term the leading order (LO), the next one next-to-leading order (NLO), the third next-to-next-to-leading order (NNLO), and so on (starting from the fourth order, we start to put exponents for the N, so NNNLO will be noted N^3LO). A nice feature of this technique is that one can represent the expansion via the famous *Feynman diagrams*.

In these diagrams, each vertex and each line represent a mathematical expression, depending on the theory of interest, and the problem of computing a scattering amplitude is replaced by the graph-theoretical problem of drawing all diagrams connecting the $m+n$ external points. Once this step is done, we replace by the corresponding mathematical object each part of each diagram and we sum all of them. Since more vertices correspond to higher orders in the expansion, we can truncate the series by limiting the number of vertices allowed in the diagrams that we draw. In the SM, each vertex comes with a power of some coupling constant, meaning that higher powers of the coupling constants correspond to higher power in the expansion. It is important to notice that for a fixed process (hence a fixed number of external points), the more vertices we have the more closed *loops* the diagram possesses. The obvious conclusion from this remark is that the simplest diagrams have no loops; this type of diagram is called a *tree-level* diagram (see figure 2 for examples), which is the type of diagrams we focus on in this thesis.

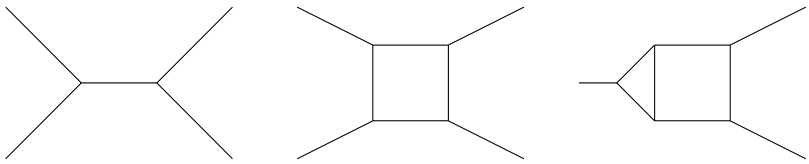

(a) tree-level diagram **(b)** one-loop diagram **(c)** two-loop diagram

Figure 2: Some examples of diagrams

Precision physics and QCD infrared divergences

As we mentioned before, the SM is performing extremely well when comparing its theoretical predictions to experimental results. Nevertheless several theoretical hints suggest that the SM is not complete. One way to move forward is to push the theory-experiment comparison further and look for tiny deviations. For this reason a part of the particle physics community has now entered a precision physics era, whose challenges for experiments are as big as they are for computations. Indeed, the current state of the art for these computations is two-loop diagrams with two incoming and two outcoming particles and going further than this involves very large expressions and requires some cutting-edge mathematical tools.

For example, as the last discovered particle in the SM, the measurements of the Higgs boson properties [2–5] have become a paradigm to the precision program previously mentioned. One measurable observable is *cross-section* which is basically the squared amplitude for the process integrated over the whole phase-space. In hadron colliders, such as the LHC, which make collisions of bound states of quarks, the largest Higgs boson production channel is *gluon fusion*, where the Higgs boson and the two colliding gluons couple via a heavy-quark loop. This process is known up to NLO with full quark mass dependence [6, 7], while it has been computed up to N^{3}LO in the limit where the mass of the quark in the loop is infinite [8, 9] (this effective theory is often called *Higgs Effective Field Theory* or simply HEFT), which allows one to reach a 5% level accuracy [10]. The second largest production mode for the Higgs boson in hadron colliders is from vector-boson fusion, where two W or Z bosons collide to produce a single Higgs boson [11] or two Higgs boson [12], and is known at N^{3}LO in the *deep inelastic scattering* limit (DIS). Also the cross-section for the production of a Higgs boson in *bottom quark fusion* in the five flavour scheme is known at N^{3}LO in α_s [13].

To go beyond inclusive cross-sections with hadronic initial states requires to measure and compute differential distributions. Only very few are known at N^{3}LO accuracy: the Higgs rapidity distribution, computed in the HEFT [14, 15], the Higgs rapidity and transverse momentum distributions in vector boson fusion in the DIS approximation [11], and jet production in DIS [16]. More differential distributions, like the Higgs transverse momentum distribution [17] or Higgs production in association with a jet [18, 19], are known in the HEFT at NNLO in α_s. They usually involve (two-loop) $2 \to 2$ scattering amplitudes, and sector-decomposition [20, 21], slicing [22–24] or subtraction [25–53] methods at NNLO, to deal with the computation of the cross-section where the phase-space integration of the (double and single) real radiation is performed with generic acceptance cuts. With some abuse of terminology, we shall generically refer to those methods as *subtraction methods*.

Despite the recent progress in computing cross-sections and differential distributions at N^{3}LO in the strong coupling constant, extending these results to more general observables and processes requires further developments on the theory side, both for the computation of the purely virtual three-loop corrections and for the development of subtraction methods at N^{3}LO. Indeed, on the one hand, so far there is no complete 2-to-2 three-loop scattering amplitude known in QCD, only the three-loop gluon-gluon scattering amplitude in $\mathcal{N} = 4$ super-Yang-Mills theory is known [54] (though the structure of the infrared singularities is known for generic massless three-loop amplitudes [55, 56]). On the other hand, the tenet of the subtraction methods is the universal behaviour of the QCD scattering amplitudes in the infrared, soft and/or collinear, limits. Indeed, if we consider, as it is the case in this thesis, the theory of *Quantum ChromoDynamics* (QCD), which is the part of the SM which concerns only the strong interactions and its actors: gluons and quarks, but with massless quarks, we encounter two type of *infrared* (IR), or low energy, divergences. The first type occurs when one or more particles have evanescent energy, meaning in the limit where its energy goes to zero, and is called *soft* divergence. The second type concerns two or more massless particles going, in the limit, in the same direction; these divergences are dubbed *collinear*. In these limit, it becomes difficult to resolve individual particles, as they their energy is so tiny in the soft limit or they are basically just one cluster of particles in the collinear limit. Understanding the behaviour of the amplitudes in these limits at a given order is therefore a necessary ingredient to develop a subtraction scheme at that order.

At NLO, the infrared behaviour of amplitudes is simply contained in the tree-level currents, with two collinear partons or one soft parton. At NNLO, this behaviour is embodied in the tree-level currents, with three collinear partons or two soft partons [57–60]; and in the one-loop currents, with two collinear partons or one soft gluon [61–65]. The

NNLO counterterms for unresolved double-parton and single-parton configurations are then built out of those universal infrared currents.

The infrared behaviour of amplitudes at N^3LO is embodied in the tree-level currents, with four collinear partons [59, 66, 67] or three soft partons [68]; in the one-loop currents, with three collinear partons [69, 70]or two soft partons; and in the two-loop currents, with two collinear partons [71–73] or one soft gluon [74–76]. In this list, only the one-loop current with two soft partons and the tree-level current with four collinear partons are not known. In this thesis, we are interested in the four collinear partons current.

Thesis Outline

This thesis aims at studying the quadruple collinear behaviour of squared amplitudes in QCD at tree-level and exploring all possible limits of the arising splitting functions. It is organised in five chapters as described below.

In Chapter 1, we describe the textbook notions this work uses thoroughly as well as set up all our definitions. In particular, a clear presentation of QCD from its central symmetry principle and the rules to compute Feynman diagrams within QCD are given. A particular emphasis is made on the notion of *gauge invariance* and how the choice of a particular gauge is of importance.

Chapter 2 is mainly dedicated to the state of the art on splitting functions. After some brief example, we start by parametrising the collinear momenta, and explain how the limit is formally taken. A detailed proof of the factorisation is then at the centre of this chapter, and both possible cases (quark or gluon parent) are discussed. The tensor structure of the splitting functions is made apparent and other general properties of these objects are presented.

Afterwards we enter the core of the thesis with Chapter 3, where the quadruple collinear splitting functions are presented. Unfortunately, due to the sheer size of the results, none are written in this thesis, but they are rather available online [77]. Instead, for each splitting function, we discuss the Feynman diagram that contribute as well as the symmetries of the result. These symmetries and how they can help in the computations are thoroughly explained.

In Chapter 4, we explore the properties of the splitting functions obtained previously. More specifically, we look at a special limit, called *sub-collinear*, where a subset of the set of collinear particles undergoes a second collinear limit. In this limit, we find that the splitting functions factorise in either two lower order splitting functions, or one lower order splitting function and a new function that we call *splitting tensor*, which is closely related to a splitting function. Once again, we show our parametrisation of the limit as well as present a proof of the factorisation and some further discussion, including a presentation of the splitting tensors.

Finally, in Chapter 5, we consider another limit of the splitting functions: the *soft* limit, where one or more gluons have evanescent energies. After parametrising the limit, we study the behaviour of our results in the cases of one or two partons going soft.

This work is base on the following publications [78, 79]:

- V. Del Duca, C. Duhr, R. Haindl, A. Lazopoulos, M. Michel, *Tree-level splitting amplitudes for a quark into four collinear partons*, *JHEP*, vol. 02, p. 189, 2020;
- V. Del Duca, C. Duhr, R. Haindl, A. Lazopoulos, M. Michel, *Tree-level splitting amplitudes for a gluon into four collinear partons*, 7 2020.

1 | Notions of QCD

Quantum ChromoDynamics (QCD) is the currently established theory of the strong interaction. This model provides a framework for the interaction of quarks and gluons, which are the building blocks of protons and neutrons. Protons and neutrons in turn are the building blocks of atomic nuclei, through an interaction called *strong nuclear interaction*, which is just a residual of the strong interaction. From this point of view, the strong interaction, via the insights that QCD allow, explains the structure of atoms and matter. But it is also central to the understanding of high energy collisions that happened shortly after the dawn of time or these days in large experimental setups, such as the LHC.

This chapter introduces all the useful QCD concepts for this thesis. We start by reviewing the symmetry group underlying this theory: *SU(3)*. After some comment on the Dirac algebra and the conventions used in this thesis, we move on to derive the QCD Lagrangian entirely from symmetry principles. We then present a convenient way to actually make computations in QCD, namely Feynman diagrams and the Feynman rules for QCD. In particular, we emphasise on the specific class of diagrams we are interested in for the scope of this thesis: tree-level diagrams. Finally, we make some comments on gauge invariance and the specific gauge choice used throughout this thesis, the axial gauge.

1.1. The group *SU(N)*

Before exploring the ramifications of the theory of QCD, one needs to further examine its main symmetry group: *SU(3)*. We present in this section in more generality the family of *SU(N)* groups. For a given positive integer number N, the group *SU(N)*, called the special unitary group of degree N, is the Lie group of $N \times N$ unitary matrices of determinant 1. Its algebra consists on $N \times N$ Hermitian matrices, meaning that the conjugate transpose of these matrices is the original matrix ($A^\dagger = A$), with trace zero. This algebra has a dimension of $N^2 - 1$ and the generators for its representations are noted t^a_{bc}, where the index a which runs from 1 to $N^2 - 1$ labels the different generators, while the indices b and c run from 1 to the dimension of the specific representation and allows the matrix t^a_{bc} to act on fields in this particular representation. The generators also define the so-called structure constants of the group f^{abc} as they need to satisfy the following commutation relation:

$$[t^a, t^b]_{de} = i f^{abc} t^c_{de}, \tag{1.1}$$

where the square brackets denote the commutator, namely $[A, B]_{ij} = A_{ik}B_{kj} - B_{ik}A_{kj}$. In this equation, the structure constants of the group f^{abc} are antisymmetric in all indices, and a summation over c (from 1 to $N^2 - 1$) is implied.

The most standard choice of generators for this algebra are the matrices T^a_{ij} which form the *fundamental representation*. The commutation relation for these generators is given by eq. (1.1). We usually normalise this representation such that

$$\mathrm{Tr}\left(T^a T^b\right) = T_R \delta^{ab}, \tag{1.2}$$

where T_R is commonly chosen as $\frac{1}{2}$, and δ^{ab} is the Kronecker symbol.

Another common choice of representation for the $SU(N)$ algebra is to use the structure constants f^{abc} themselves. Indeed, if we use $t^a_{bc} = i f^{bac}$

as a generator in eq. (1.1), we find

$$f^{dac}f^{bce} - f^{dbc}f^{ace} = f^{abc}f^{cde} \;\Leftrightarrow\; f^{dac}f^{bce} + f^{dbc}f^{aec} + f^{abc}f^{ced} = 0, \tag{1.3}$$

which is simply the *Jacobi identity*, a very well-known identity that structure constants need to satisfy. This representation goes by the name of *adjoint representation.*

Independently of any representation, we can find a *Casimir operator*, which is an element of the algebra which commutes with all the generators. The specific values that this operator takes on different representations are simply called *Casimir constants* or just *Casimirs.* It is easy to establish that $t^a_{ij}t^a_{jk}$ verifies that property since

$$\begin{aligned}[t^b, t^a t^a]_{ij} &= [t^b, t^a]_{ik}t^a_{kj} + t^a_{ik}[t^b, t^a]_{kj} \\ &= if^{bac}t^c_{ik}t^a_{kj} + t^a_{ik}if^{bac}t^c_{kj} \\ &= if^{bac}\{t^c, t^a\}_{ij}\end{aligned} \tag{1.4}$$

needs to be zero as f^{bac} is antisymmetric but the anticommutator $\{t^c, t^a\}_{ij} = t^c_{ik}t^a_{kj} + t^a_{ik}t^c_{kj}$ is symmetric. This implies that the Casimir operator takes a constant value on each representation.

We can hence define a Casimir for the fundamental representation, $\mathcal{C}_F$, and one for the adjoint representation, $\mathcal{C}_A$:

$$T^a_{ik}T^a_{kj} = \mathcal{C}_F\ \delta_{ij}, \tag{1.5}$$

$$f^{adc}f^{cdb} = \mathcal{C}_A\ \delta^{ab}. \tag{1.6}$$

In *SU(N)*, these two quantities are linked to N by means of the following relations:

$$\mathcal{C}_F = T_R\,\frac{N^2-1}{N} \qquad \text{and} \qquad \mathcal{C}_A = N. \tag{1.7}$$

1.2. Dirac algebra

We keep introducing some basic tools with the Dirac Algebra. This algebra is actually a *Clifford Algebra* and is generated by D matrices (in a D-dimensional space-time), called gamma-matrices γ^μ, where the index μ runs from 0 to $D-1$. These matrices obey the following anti-commutation relation:

$$\{\gamma^\mu, \gamma^\nu\} = 2\eta^{\mu\nu}\mathbb{1}, \tag{1.8}$$

where the symbol $\mathbb{1}$ is the unity matrix in this algebra and $\eta^{\mu\nu}$ is the Minkowski metric, which is defined throughout this thesis as

$$\eta^{\mu\nu} = \begin{pmatrix} 1 & 0 & 0 & 0 \\ 0 & -1 & 0 & 0 \\ 0 & 0 & -1 & 0 \\ 0 & 0 & 0 & -1 \end{pmatrix}. \tag{1.9}$$

Note that since this is the only metric we use in the thesis so that no confusion can arise, we often note it generically $g^{\mu\nu}$. This definition of the Minkowski metric is actually in 4 dimensions, but throughout this thesis, we work in D dimensions. The definition of eq. (1.9) is then simply generalised by keeping a 1 for the time component, a (-1) for all the space components, and zeros off the diagonal.

The gamma-matrices are more than often contracted with D-dimensional vectors in expressions such as $\gamma^\mu v_\mu$ (with v_μ a generic vector), which justifies the need for a more convenient notation, called Feynman slash notation:

$$\not{v} = \gamma^\mu v_\mu. \tag{1.10}$$

Finally, note that eq. (1.8) together with the notation of eq. (1.10) implies that

$$\{\not{v}, \not{w}\} = 2\ v \cdot w\ \mathbb{1}, \tag{1.11}$$

where the dot $\cdot$ indicates the pseudo-scalar product of Minkowski space ($v \cdot w = v_\mu \eta^{\mu\nu} w_\nu$). In particular, we have

$$\not{v}\not{v} = v^2\ \mathbb{1}, \tag{1.12}$$

with $v^2 = v \cdot v$.

1.3. Gauge invariance and the QCD Lagrangian

With all the information of the previous sections, one can at last turn to QCD. The theory of QCD accounts for the strong interaction whose actors are quarks and gluons. The whole theory is invariant under the group *SU(3)*, meaning that the Lagrangian density must show this property too. More precisely, we build the QCD Lagrangian by starting from the Dirac Lagrangian for a fermion (here, the quarks are fermions), which simply describes a free fermion:

$$\mathcal{L}_{Dirac} = \bar{\Psi}_i \left(i\not{\partial} - m_i \right) \Psi_i, \tag{1.13}$$

∂_μ is the derivative in space-time $\frac{\partial}{\partial x^\mu}$ and a summation over i is understood. In eq. (1.13), Ψ_i is the quark field of flavour i and has mass m_i. The flavours of the quarks can, for the purpose of QCD only, be viewed as six different families of quarks, which all share the same properties, except their mass. In particular, one key element in this thesis is that flavour is conserved. As it was defined in the previous section, $\not{\partial}$ is simply $\gamma^\mu \partial_\mu$, using Feynman slash notation.

We then introduce a *SU(3)* transformation of the quark fields:

$$\Psi_i(x) \to V(x)\Psi_i(x). \tag{1.14}$$

In this equation, the transformation matrix $V(x)$ is a unitary 3×3 matrix acting on *colour* space. Note that this transformation depends on space-time, as reminded by the variable x. The behaviour of this matrix for infinitesimal transformations is dictated by the generators of the fundamental representation T^a:

$$V(x) = 1 + i\alpha^a(x)T^a + \mathcal{O}(\alpha^2). \tag{1.15}$$

By unitarity of $V(x)$, it is immediate to realise that the mass term in the Dirac Lagrangian $\bar{\Psi}_i\Psi_i$ is invariant under this transformation. However, the term with a derivative is not invariant and requires the introduction of a new field, called a *connection*, to be so. We hence introduce the *covariant derivative* as

$$D_\mu = \partial_\mu - ig_s A^a_\mu T^a, \tag{1.16}$$

where g_s is the *coupling constant* of QCD and the connection field A_μ^a transforms (infinitesimally) as

$$A_\mu^a \to A_\mu^a + \frac{1}{g_s}\partial_\mu \alpha^a + f^{abc} A_\mu^b \alpha^c. \tag{1.17}$$

It is now possible to show that the covariant derivative transforms just the same as the fields themselves transform, i.e.

$$D_\mu \Psi_i(x) \to V(x) D_\mu \Psi_i(x). \tag{1.18}$$

These definitions allow to introduce a gauge-invariant Dirac Lagrangian as

$$\mathcal{L}_{GI} = \bar{\Psi}_i \left(i \not{D} - m_i \right) \Psi_i. \tag{1.19}$$

To go one step further, one can now promote the connection field A_μ^a to a physical field (as it actually becomes the gluon field) and try to add a kinetic term for this field in the Lagrangian. After some calculations, one can figure that the correct term for the gluon field is the following bosonic Lagrangian

$$\mathcal{L}_{Gluon} = -\frac{1}{4} G_{\mu\nu}^a G_a^{\mu\nu}, \tag{1.20}$$

where $G_{\mu\nu}^a$ is called the *field-strength tensor* of the gluon and is given by

$$G_{\mu\nu}^a = \partial_\mu A_\nu^a - \partial_\nu A_\mu^a + g_s f^{abc} A_\mu^b A_\nu^c, \tag{1.21}$$

where f^{abc} are the structure constants of *SU(3)* as explained previously and g_s is again the (same) coupling constant of QCD. Note that in the effort to make a gauge-invariant kinetic term for the gluon, we introduced a triple and a quadruple coupling of the gluon field with itself, called self-couplings.

Adding this bit to the gauge-invariant version of the Dirac Lagrangian, we finally get the full classical QCD Lagrangian:

$$\mathcal{L}_{QCD} = \bar{\Psi}_i \left(i \not{D} - m_i \right) \Psi_i - \frac{1}{4} G_{\mu\nu}^a G_a^{\mu\nu}. \tag{1.22}$$

In this thesis, we work with massless quarks so that all m_i are put to zero. Note that to obtain this Lagrangian, we limited ourselves to operators of dimension 4 which are CP-invariant.

1.4. Feynman rules

In Quantum Mechanics, perhaps the most central object is the so-called *scattering amplitude*. Indeed, this mathematical function encodes all the information about the process of interest. Let us consider any scattering process where some particles interact with each other, perhaps creating new particles or simply colliding. We can attribute a quantum state to the system before the event, mathematically at negative infinity in time, and another quantum state for after the event, at positive infinity in time. We call these two states respectively $|\mathrm{in}\rangle$ and $|\mathrm{out}\rangle$. With these states at hand, the scattering amplitude is given by the projection of initial state to the final state, according to the laws of Quantum Mechanics. This mapping is realised by the action of the operator S, also called *scattering matrix* or more simply *S-matrix*, which is obtained by exponentiating the interaction part of the Lagrangian density of the underlying theory. Separating the trivial part where no interaction happens in this matrix, $S = \mathbb{1} + i\mathcal{T}$, the amplitude $\mathcal{M}$ is defined as

$$\langle \mathrm{out}|\mathcal{T}|\mathrm{in}\rangle = \delta^{(4)}\left(\sum_i p_i - \sum_i q_i\right)\mathcal{M}, \tag{1.23}$$

where the Dirac delta ensures momentum conservation (incoming particles have momenta p_i and outcoming ones have momenta q_i).

Although this procedure of computing amplitudes is clearly defined, it is in practice oftentimes impossible to have an analytic expression for the exponential of the Lagrangian density (within the scope of our current knowledge). Actually this is the case for most theories ! To deal with this problem, a convenient way around is to perform an expansion of the scattering matrix in terms of the coupling constants of the theory. The idea behind this procedure is to stop computing the infinitely many terms of the expansion after a certain (finite) number, hence truncating the series, and hoping that the remaining terms account only for a small deviation from the exact result.

Having performed the expansion of the scattering matrix, one then needs to compute individually each consecutive term in the series (up to a certain point). When doing that, we can observe some patterns and reformulate the procedure of computing these terms in a graphical way. This method introduced by Richard Feynman uses aptly named *Feynman diagrams* and consists in placing dots for the initial and final states and then drawing all possible diagrams linking these points together. To each element in these diagrams we assign a mathematical expression that can be directly computed form the Lagrangian density. The lines in the diagrams are called *propagators* and their expressions for (massless) QCD are given in figure 1.2, unless the line connects with an initial or a final state point in which case we use the expressions of figure 1.1. We usually draw spring-like lines for gluons and straight lines with arrows for quarks. The intersections of the lines are called *vertices* and are given for QCD in figure 1.3.

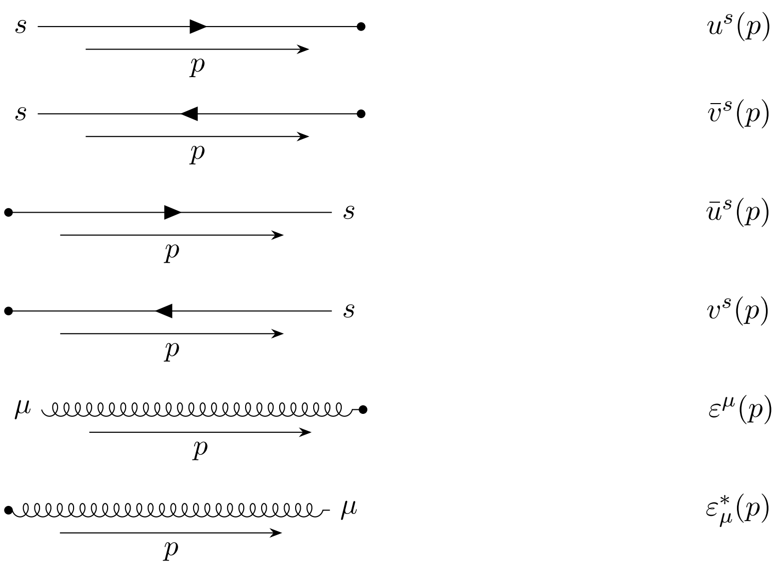

Figure 1.1: Feynman rules for all external states in QCD (u^s and v^s are solutions to the free Dirac equation, such that $\sum_s u^s(p)\bar{u}^s(p) = \not{p}+m$ and $\sum_s v^s(p)\bar{v}^s(p) = \not{p} - m$, with $\bar{u} = u^\dagger\gamma^0$)

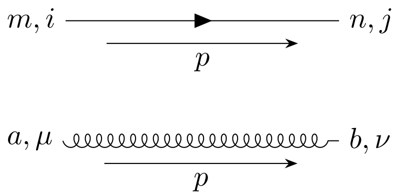

$$\frac{i\not{p}_{ji}}{p^2}\delta_{mn}$$

$$\frac{d^{\mu\nu}(p)}{p^2}\delta_{ab}$$

Figure 1.2: Feynman rules for all propagators in (massless) QCD

Vertices come with some power of the coupling constants, so that we can actually organise our diagrams as contributing to a certain order in the series by the number of vertices. So, to compute an amplitude up to a certain order, one must compute all diagrams with such a number and types of vertices that it doesn't exceed some given number. Then all we have to do is simply add up all the diagrams, with their respective mathematical expressions. Since increasing the order at which we are computing the amplitude increases the number of vertices, for a given process (and hence a given number of initial and final points), higher orders correspond to a larger number of *loops* (by loop, we mean a closed cycle, a set of propagators that one can follow and end on the starting point). Hence another way of sorting Feynman diagrams is by the number of loops they have. In this thesis, we are only interested in the most basic family of Feynman diagrams, *tree-level* diagrams, which simply have no loop. To summarise, in this thesis, we compute tree-level amplitudes, which are approximation of the scattering amplitudes at the lowest order, by drawing all allowed diagrams with no loops, replacing with the expressions given by figures 1.1, 1.2 and 1.3, and summing all of it together.

Finally, if one wants to compute a *squared amplitude*, that we define as the modulus squared of the amplitude summed over all external states, one must for each ingoing or outgoing state multiply by the sum over all possible polarisation states (more precisely, we average over ingoing states and sum over all possible outgoing ones), which means a factor of $\not{p}$ for a quark (of momentum p) or of $d^{\mu\nu}(p)$ for a gluon (of momentum

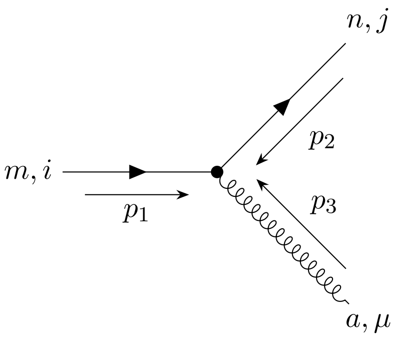

$$ig_s\gamma^{\mu}_{ji}T^{a}_{mn}$$

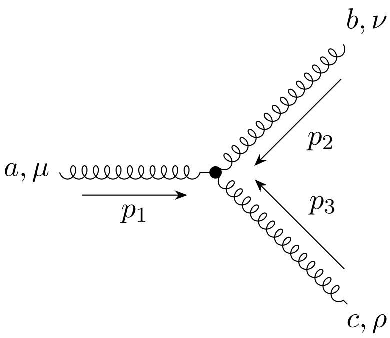

$$\begin{aligned} g_s f^{abc}\Big(&\eta^{\mu\nu}(p_1 - p_2)^{\rho} \\ &+\eta^{\nu\rho}(p_2 - p_3)^{\mu} \\ &+\eta^{\rho\mu}(p_3 - p_1)^{\mu}\Big) \end{aligned}$$

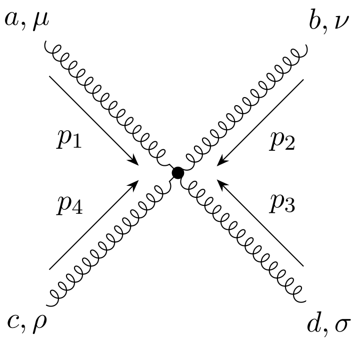

$$\begin{aligned} -ig_s^2\Big(&f^{abe}f^{cde}(\eta^{\mu\rho}\eta^{\nu\sigma} - \eta^{\mu\sigma}\eta^{\nu\rho}) \\ &+f^{ace}f^{bde}(\eta^{\mu\nu}\eta^{\rho\sigma} - \eta^{\mu\sigma}\eta^{\nu\rho}) \\ &+f^{ade}f^{bce}(\eta^{\mu\nu}\eta^{\rho\sigma} - \eta^{\mu\rho}\eta^{\nu\sigma})\Big) \end{aligned}$$

Figure 1.3: Feynman rules for all vertices in QCD

p). The last tensor is called the spin-polarisation tensor of the gluon and more details about this tensor are given in the next section.

1.5. Physical gauge choice and orthogonality

The QCD Lagrangian we described in eq. (1.22) is actually not the most general Lagrangian we could have presented. Indeed, one difficulty arises form the polarisation of the gluons. These are usually described by the polarisation vector $\varepsilon_h^\mu(p)$, where h is the helicity of the gluon and p its momentum. The helicity is closely related to the spin of the gluon, since it is the projection of the spin along the direction of the momentum of the gluon. As massless spin-1 particles, gluons have two possible helicities (in 4 dimensions, $D-2$ in D dimensions). But the polarisation vector $\varepsilon_h^\mu(p)$ seems to have D degrees of freedom as a vector in the D-dimensional space-time, while the fact that they are massless particles forbids any propagation in the longitudinal and temporal directions, meaning they should only possess $D-2$ degrees of freedom. The solution to this puzzle is gauge invariance: these extra degrees of freedom are gauge-dependent and will not change any physical observable. In practice, one often adds a gauge-fixing term to the QCD Lagrangian, so that there is no gauge degrees of freedom left. Amongst all possible gauges, one can consider the *physical gauges* in which case, as their name imply, we work with the physical degrees of freedom of the gluons only. These gauges all have in common that the polarisation vectors of the gluons are transverse to their momenta as well as to an auxiliary vector n, such that there is no longitudinal nor temporal propagation of the gluons:

$$\begin{aligned} \varepsilon_h^\mu(p)\ p_\mu &= 0, \\ \varepsilon_h^\mu(p)\ n_\mu &= 0. \end{aligned} \tag{1.24}$$

A special case of these physical gauges are *axial gauges*, where the tensor $d^{\mu\nu}(p,n)$ in the gluon propagator (c.f. figure 1.2) reads [80]

$$d^{\mu\nu}(p,n) = -\eta^{\mu\nu} + \frac{p^\mu n^\nu + n^\mu p^\nu}{n\cdot p}, \tag{1.25}$$

and is called the *spin-polarisation tensor* of the gluon. Note that now our spin-polarisation tensor in this gauge depends on the light-like auxiliary vector n, which is also orthogonal to the spin-polarisation tensor as $d^{\mu\nu}(p,n) = d^{\mu\nu}(n,p)$, but this dependence can of course not appear in any physical result. Since we always use n as the second vector in the definition of the spin-polarisation tensor, we often write $d^{\mu\nu}(p)$ instead of $d^{\mu\nu}(p,n)$.

The spin-polarisation tensor appears for any gauge. Indeed, in general, for a gluon propagator of polarisation $\varepsilon_h^\mu(p)$, where the index h stands for the different states of polarisation, called helicity, the spin-polarisation tensor is defined as follows:

$$d^{\mu\nu}(p) = \sum_{h=1}^{D-2} \varepsilon_h^\mu(p)\ \varepsilon_h^{\nu *}(p), \tag{1.26}$$

where we sum over all physical polarisations. If the gluon is a physical one, as it is the case in our choice of gauge, this tensor must be orthogonal to the momentum of the gluon: $d^{\mu\nu}(p)p_\mu = 0 = d^{\mu\nu}(p)p_\nu$, since the polarisation vectors are themselves orthogonal to the momenta of their respective gluons (c.f. eq. (1.24)). Note that, due to its orthogonality to p and n, the spin-polarisation tensor acts as a projector on the sub-space of phase-space orthogonal to these vectors.

A important implication of our choice of gauge is that, in a physical gauge, any amplitude with (at least) a gluon stripped of the gluon polarisation vector can be chosen to be orthogonal to the momentum of this gluon. For example, if we consider an amplitude $A_h(p)$, which depends on an external gluon of helicity h and momentum p, one can define an amplitude with Lorentz indices $A_\mu(p)$ by stripping the polarisation vector:

$$A_h(p) = A_\mu(p)\ \varepsilon_h^\mu(p). \tag{1.27}$$

In our gauge choice, we can now project the polarisation vector $\varepsilon_h^\mu(p)$ unto the sub-space transverse to the momentum of the gluon p without changing it, since it is already transverse to p and n:

$$\varepsilon_h^\mu(p) = -d^{\mu\nu}(p,n)\ \varepsilon_{\nu,h}(p). \tag{1.28}$$

This allows to redefine our amplitude with Lorentz indices $A^\mu(p)$ by projecting it unto this same physical subspace

$$A_h(p) = A_\mu(p)\ \varepsilon_h^\mu(p) = -A_\mu(p)\ d^{\mu\nu}(p,n)\ \varepsilon_{\nu,h}(p) = \hat{A}^\nu(p)\ \varepsilon_{\nu,h}(p), \tag{1.29}$$

which is then explicitly transverse to the momentum of the gluon:

$$\hat{A}^{\nu}(p)\; p_{\nu} = -A_{\mu}(p)\; d^{\mu\nu}(p,n)\; p_{\nu} = 0. \tag{1.30}$$

Note however that this is not a new definition of the amplitude, it is rather a different but equivalent form of the amplitude, that exists because of gauge invariance.

These new tools allow to trade helicity indices (indicating in which polarisation state a gluon is) to Lorentz indices when needed. Let us consider for example, the contraction of two amplitudes, with one external gluon (incoming or outcoming). When operating this contraction, one must sum over all $D-2$ helicity states of the gluon:

$$\sum_{h=1}^{D-2} A_h\; B_h. \tag{1.31}$$

However, we can factorise from any amplitude with an external gluon its polarisation vector $\varepsilon_h^{\mu}(p)$. This implies that we can rewrite our contraction as

$$\sum_{h=1}^{D-2} A_h\; B_h = \sum_{h=1}^{D-2} \hat{A}_{\mu}\; \hat{B}_{\nu}\; \varepsilon_h^{\mu}(p)\; \varepsilon_h^{\nu}(p) = \hat{A}_{\mu}\; \hat{B}_{\nu}\; d^{\mu\nu}(p,n), \tag{1.32}$$

which now depends on n.

It turns out that this is enough to cancel all but the first term in the expression of the spin-polarisation tensor in axial gauge (cf. eq. (1.25)) so that the contraction of the two amplitudes can finally be written as (because of eq. (1.30))

$$\sum_{h=1}^{D-2} A_h\; B_h = -\hat{A}_{\mu}\; \hat{B}_{\nu}\; g^{\mu\nu} = -\hat{A}_{\mu}\; \hat{B}^{\mu}. \tag{1.33}$$

Obviously, this little trick can be extended to any number of gluons. We then go through the same reasonings and get to

$$\begin{aligned}
&\sum_{h_1,\dots,h_r=1}^{D-2} A_{h_1\dots h_r} B_{h_1\dots h_r} \\
&= \sum_{h_1,\dots,h_r=1}^{D-2} \hat{A}_{\mu_1\dots\mu_r}\ \hat{B}_{\nu_1\dots\nu_r}\ \varepsilon_{h_1}^{\mu_1}(p_1)\ \varepsilon_{h_1}^{\nu_1}(p_1)\dots\varepsilon_{h_r}^{\mu_r}(p_r)\ \varepsilon_{h_r}^{\nu_r}(p_r) \\
&= \hat{A}_{\mu_1\dots\mu_r}\ \hat{B}_{\nu_1\dots\nu_r}\ d^{\mu_1\nu_1}(p_1,n)\dots d^{\mu_r\nu_r}(p_r,n) \\
&= (-1)^r \hat{A}_{\mu_1\dots\mu_r}\ \hat{B}^{\mu_1\dots\mu_r}
\end{aligned} \tag{1.34}$$

This equation implies that we can effectively change from helicity indices to Lorentz ones without too much of an afterthought, as long as the tensors we are contracting are orthogonal to the momenta of the corresponding gluons. In the rest of the thesis, we will always assume that the amplitudes live on the physical sub-space where all gluons are transverse to their momenta without putting a hat on the amplitudes.

1.6. Dimensional regularisation

We finish this section by giving some insights on dimensional regularisation. As we mentioned in section 1.4, higher orders in perturbation theory are obtained by computing Feynman diagrams that involve loops. These loops are translated as integrations over the momenta of the particles flowing in the loops. Unfortunately, these integrals are known to diverge. One solution that was found for this problem is to change the dimension of space-time from 4 to D, with D a complex number. Now, the divergent integrals in which we integrated over 4-dimensional momenta in a 4-dimensional phase-space become functions of the dimension of space-time as a complex number, allowing us to use all the tools of complex analysis, including analytic continuation. Dimensional regularisation computes the integrals in points of the complex plane where it is not divergent and then analytically continues them to $D = 4$ to obtain a finite result.

We could simply not care about this problem as all the computations and all the proofs in this thesis are at tree-level, hence no loops. However, since we want our results to be used to build counter-terms to the singularities that appear at higher orders, this problem affects us indirectly. The consequences are mainly that all our vectors are now D-dimensional as well as the Minkowski metric. Apart from that, we also have to rescale the strong coupling constant. Indeed, we don't want its physical dimension (in units of energy) to depend on the dimension of space-time. We thus make the substitution :

$$g_s \to \mu^\epsilon g_s, \tag{1.35}$$

where ϵ is defined by $D = 4 - 2\epsilon$ and μ now carries all the dimensionality of g_s. In this thesis, we use the conventional dimensional regularisation (CDR) scheme, for which the quarks and gluons have 2 and $D-2$ helicity states respectively.

2 | Splitting Functions

One of the many interesting properties of QCD amplitudes is their behaviour in the infrared limits: the soft limit where one or more partons have evanescent energies and the collinear one where two or more partons tend to go in the same direction. It is this last limit that we are mainly interested in. More specifically, it can be shown that any QCD amplitude (or squared amplitude) factorises in the limit where two or more partons approach a common direction at the same rate. Perhaps more importantly, this factorisation involves a universal factor, called splitting function, which encapsulates the entirety of the collinear behaviour of the process; the other factor contains no more information about the individual collinear partons.

In this section, we first detail how the collinear limit is defined by parametrising the momenta of the collinear partons. After having established the result we want to prove and defined all sorts of useful quantities, we turn to the first ideas of the proof of the factorisation at tree-level, which makes use of a particular gauge choice. Finally we finish the proof by specialising to the two different cases where the parent parton is either a quark or a gluon, as the tensor structure in the two cases is widely different.

This section is based mainly on references [34, 58, 81].

2.1. First example

In order to properly introduce the subject of collinear limits of QCD amplitudes, let us first consider a really simple example. In this example, we have a certain number of partons involved in a QCD process and two among them we call r and s. Of all the tree-level diagrams for this amplitude, at least one has the two partons r and s connected to a same vertex (see figure 2.3).

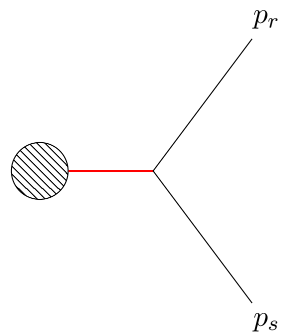

Figure 2.1: Generic diagram with partons r and s connected to the same vertex, the blob encompasses all the rest of the diagram

The lines in this diagram can be quark or gluon lines, but that does not really matter for what follows. All that matters is that this vertex connecting the two partons is linked to the rest of the diagram (represented by the blob) by the red propagator, which in both quark and gluon cases features a factor of $\frac{1}{p^2}$, where p is the momentum carried by the propagator: in this case, $p = p_r + p_s$. This means that this diagram has a factor of

$$\frac{1}{(p_r + p_s)^2} = \frac{1}{p_r^2 + 2\ p_r \cdot p_s + p_s^2} = \frac{1}{2\ p_r \cdot p_s}, \tag{2.1}$$

where we have used the fact that both partons have zero mass, and hence $p_r^2 = 0 = p_s^2$ (in massless QCD). Using this fact, we can rewrite their momenta as $p_r = E_r\,(1, \vec{v}_r)$, where E_r is the energy of parton r and $\vec{v}_r$ is a 3-dimensional vector of unit norm, and of course we do the same thing with parton s. This leads to the following expression of the propagator in eq. (2.1):

$$\frac{1}{2\, p_r \cdot p_s} = \frac{1}{2E_rE_s(1 - \vec{v}_r \cdot \vec{v}_s)} = \frac{1}{2E_rE_s\,(1 - \cos(\theta_{rs}))}, \tag{2.2}$$

where the middle dot $\cdot$ here stands for the scalar product in 3-dimensional Euclidian space, and θ_{rs} is thus the angle between the directions of partons r and s. There are two instances in which the propagator in eq. (2.2) diverges. The first one happens when either one of the partons energy (E_r or E_s) goes to zero and is called a soft divergence. The second one materialises when the angle between the two partons θ_{rs} goes to zero, or in other word when the two partons go in the same direction, and is called a collinear divergence.

While this simple example might seem too simplistic, it is actually easy to generalise. If the propagator is not just connecting two partons but rather a propagator going to another subpart of the diagram (cf. fig 2.2), such that its carried momentum is the sum of m massless momenta p_i ($i = 1, \ldots, m$), then its expression would read

$$\frac{1}{\left(\sum_{i=1}^{m} p_i\right)^2} = \frac{1}{2\sum_{i,j=1}^{m} p_i \cdot p_j} = \frac{1}{2\sum_{i,j=1}^{m} E_iE_j\,(1 - \cos(\theta_{ij}))}. \tag{2.3}$$

Again this expression becomes divergent if either one of these is true: all E_i (but one) for $i = 1, \ldots, m$ are zero, or all θ_{ij} for $i, j = 1, \ldots, m$ are zero (note that these are only the conditions for this specific propagator to be divergent, the conditions for the diagram to be divergent are less demanding). However, these are not the only cases where the expression in eq. (2.3) is divergent; we could also have a mix of the two types of divergences aptly called soft-collinear divergences. For example, if $m = 3$, the propagator is divergent if parton 1 is soft, hence $E_1 = 0$, and partons 2 and 3 are collinear, hence $\theta_{23} = 0$.

2.2. Parametrisation of the collinear limit

Before proving the theorem underlying this whole thesis, one needs to establish some conventions, and in particular properly define in which

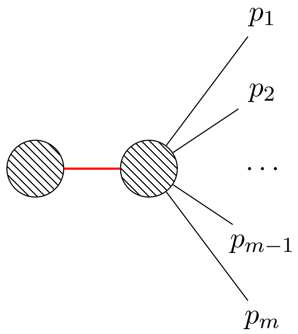

Figure 2.2: Generic diagram with partons 1 to m all connected to the rest of the diagram by the same propagator (in red)

manner the collinear limit is approached. In this chapter, and all the following ones, we consider a scattering process in massless QCD in which n particles (gluons or massless quarks) interact. Among those n particles, m are collinear. We first parametrise these m momenta p_i as all being proportional to some collinear direction p with the addition of a small transverse momentum k_i, explicitly,

$$p_i = x_i p + k_i \qquad\qquad i = 1, \ldots, m. \tag{2.4}$$

Note that by definition all transverse momenta are orthogonal to the collinear direction: $p \cdot k_i = 0$. We also choose the collinear direction to be a null-vector, so $p^2 = 0$.

However, this parametrisation is in contradiction with the fact that all the momenta are on-shell and should square to zero since we are dealing with massless particles. To circumvent this difficulty, we simply add a third piece that ensures that all particles are massless:

$$p_i = x_i p + k_i - \frac{k_i^2}{2x_i} \frac{n}{n \cdot p} \qquad\qquad i = 1, \ldots, m. \tag{2.5}$$

In this last equation we introduced a new light-like vector n , called auxiliary vector. This vector is orthogonal to all transverse momenta but can not be orthogonal to the collinear direction. The collinear limit is then defined as the limit in which the transverse momenta all approach zero at the same rate. It is worth to note that this definition of the collinear limit is frame-independent: it only depends on the collinear direction p and the transverse momenta k_i. In particular, it is independent on the choice of n, which merely indicates how the collinear direction is approached but does not interfere with the behaviour of the amplitude in the limit. This parametrisation of the collinear limit is often called a *Sudakov decomposition*.

The variables x_i and k_i in eq. (2.5) are a priori totally unconstrained. Nevertheless, a basic counting of the number of degrees of freedom seems at odds with basic kinematics. Indeed, for m independent light-like vectors in D-dimensional space-time, one expects $m(D-1)$ degrees of freedom. However, our parametrisation seems to rely on $m(D-1)+2$ degrees of freedom: m for the variables x_i, $m(D-2)$ for the transverse momenta k_i, and 2 for p and n. This apparent paradox is solved by noticing that the collinear limit is not affected by longitudinal boosts in the direction of the parent parton $P=\sum_{i=1}^m p_i$ (the parent parton is the initial parton that splits into the m collinear ones). It is therefore more convenient to replace the variables x_i and k_i by new ones which are invariant under such boosts, respectively called z_i and $\tilde{k}_i$. Their expression in terms of the former variables is the following:

$$z_i = \frac{x_i}{\sum_{j=1}^m x_j}, \tag{2.6}$$

$$\tilde{k}_i = k_i - z_i \sum_{j=1}^m k_j. \tag{2.7}$$

It is immediate to observe that this new set of variables satisfy $\sum_{i=1}^m z_i = 1$ and $\sum_{i=1}^m \tilde{k}_i = 0$, reducing the number of degrees of freedom to the expected amount.

With this parametrisation now complete, we can express any kinematic quantity in terms of the set $\{z_i, \tilde{k}_i, p, n\}$. For example, for the sub-energy $s_{ij}=(p_i+p_j)^2$, we obtain

$$s_{ij} = -z_i z_j \left(\frac{\tilde{k}_i}{z_i} - \frac{\tilde{k}_j}{z_j}\right)^2, \tag{2.8}$$

and similarly for more complex sub-energies defined in general as

$$s_{i_1 i_2 \dots i_t} = \left(\sum_{j=1}^{t} p_{i_j} \right)^2 . \tag{2.9}$$

It is oftentimes useful to define

$$t_{ij,k} = 2\frac{z_i s_{jk} - z_j s_{ik}}{z_i + z_j} + \frac{z_i - z_j}{z_i + z_j} s_{ij}. \tag{2.10}$$

Finally, one can rewrite eq. (2.5) in a way that explicitly uses boost-invariant variables as

$$p_i = z_i P + \tilde{k}_i + \mathcal{O}(k^2), \tag{2.11}$$

where the last term is proportional to the auxiliary vector n. Indeed, inserting the definitions of eq. (2.6) into eq. (2.11), we get

$$\begin{aligned} p_i &= z_i P + \tilde{k}_i + \mathcal{O}(k^2) \\ &= \frac{x_i}{\sum_{j=1}^{m} x_i} \sum_{j=1}^{m} (x_i p + k_i) + \left(k_i - \frac{x_i}{\sum_{j=1}^{m} x_j} \sum_{j=1}^{m} k_j \right) + \mathcal{O}(k^2) \\ &= x_i p + k_i + \mathcal{O}(k^2), \end{aligned} \tag{2.12}$$

which gives back eq. (2.5).

2.3. Definition of the splitting functions

We are now considering the amplitude for the process of n particles interacting in massless QCD, in the limit where m ($m \leq n-3$) among those are collinear to the direction p. In order to take this limit, we simply rescale $k_i \to \lambda k_i$ and look for the Laurent series in λ at $\lambda = 0$. We note the n particles flavour, spin and colour indices respectively as f_i, s_i and c_i. We then write the amplitude for the interaction of these n particles as

$$\mathcal{M}_{f_1 \dots f_n}^{c_1 \dots c_n; s_1 \dots s_n}(p_1 \dots p_n). \tag{2.13}$$

It is well known that in the collinear limit that we presented beforehand, the leading term in the Laurent series of such an amplitude factorises as [82–84]

$$\begin{aligned}\mathscr{C}_{1\dots m}\mathcal{M}^{c_1\dots c_n;s_1\dots s_n}_{f_1\cdots f_n}(p_1,\dots,p_n) = \\ \mathbf{Sp}^{c,c_1\dots c_m;s,s_1\dots s_m}_{f,f_1\cdots f_m}\mathcal{M}^{c,c_{m+1}\dots c_n;s,s_{m+1}\dots s_n}_{f,f_{m+1}\cdots f_n}(Xp,p_{m+1}\dots p_n),\end{aligned} \quad (2.14)$$

where $X = \sum_{i=1}^m x_i$. Here the symbol $\mathscr{C}_{1\dots m}$ indicates that we keep only the leading term in the Laurent series, so that this equality is only valid up to terms that are power-suppressed in the collinear limit. In this equation, f, c, and s denote respectively the flavour, colour, and spin of the parent parton. Note that in QCD, with only quarks and gluons, the flavour of the parent is unequivocally determined by those of the other particles in the collinear set. We therefore often suppress the dependence on f. The tensor $\mathbf{Sp}^{c,c_1\dots c_m;s,s_1\dots s_m}_{f,f_1\cdots f_m}$ is called a splitting function and encapsulates the collinear behaviour of the amplitude, as it carries only the information about the collinear set, and most importantly no other function on the left hand side of eq. (2.14) depends on the collinear momenta or quantum numbers.

As the amplitude factorises in the collinear limit, so does the squared amplitude. The squared amplitude is defined as the modulus squared of the amplitude summed over all colour and spin indices:

$$|\mathcal{M}_{f_1\dots f_n}(p_1\dots p_n)|^2 = \sum_{\substack{(s_1,\dots,s_n)\\(c_1,\dots,c_n)}} \left|\mathcal{M}^{c_1\dots c_n;s_1\dots s_n}_{f_1\cdots f_n}(p_1,\dots,p_n)\right|^2. \quad (2.15)$$

The squared amplitude behaves in the collinear limit as

$$\begin{aligned}\mathscr{C}_{1\dots m}\,|\mathcal{M}_{f_1\dots f_n}(p_1,\dots,p_n)|^2 = \\ \left(\frac{2\mu^{2\epsilon}\,g_s^2}{s_{1\dots m}}\right)^{m-1} \hat{P}^{ss'}_{f_1\cdots f_m}\,\mathcal{T}^{ss'}_{ff_{m+1}\cdots f_n}(Xp,p_{m+1},\dots,p_n),\end{aligned} \quad (2.16)$$

where g_s is the strong coupling constant, μ is the scale introduced in dimensional regularisation, and ϵ is the dimensional regulator ($D = 4-2\epsilon$, with D the dimension of space-time). The tensor $\mathcal{T}^{ss'}_{ff_{m+1}\cdots f_n}$ is defined in a pretty similar way to a squared amplitude (cf eq. (2.15)), only with no summation over the spin indices of the parent parton:

$$\mathcal{T}^{ss'}_{ff_{m+1}\dots f_n} = \sum_{\substack{(s_{m+1},\dots,s_n)\\(c,c_{m+1},\dots,c_n)}} \mathcal{M}^{c,c_{m+1}\dots c_n;s,s_{m+1}\dots s_n}_{ff_{m+1}\dots f_n} \left[\mathcal{M}^{c,c_{m+1}\dots c_n;s',s_{m+1}\dots s_n}_{ff_{m+1}\dots f_n}\right]^*, \tag{2.17}$$

where for the sake of clarity we have suppressed the momenta on which the amplitude depends. Due to colour conservation, there is no non-trivial colour correlations in eq. (2.16) and we thus sum over the colour indices of the parent parton. On the contrary, spin correlations may arise non trivially so that the tensor structure of $\hat{P}^{ss'}_{f_1\dots f_m}$ is necessary. The tensor $\hat{P}^{ss'}_{f_1\dots f_m}$ is the (polarised) splitting function for the squared amplitude and depends on the transverse momenta $\tilde{k}_i$, the momentum fractions z_i, and the sub-energies s_{ij} of the collinear particles as well as the spin indices of the parent parton. As no confusion arises in general, we refer to both $\mathbf{Sp}^{c,c_1\dots c_m;s,s_1\dots s_m}_{f,f_1\dots f_m}$ and $\hat{P}^{ss'}_{f_1\dots f_m}$ as splitting functions, and they are related by

$$\left(\frac{2\mu^{2\epsilon}\,g_s^2}{s_{1\dots m}}\right)^{m-1} \hat{P}^{ss'}_{f_1\dots f_m} = \frac{1}{\mathcal{C}_f} \sum_{\substack{(s_1,\dots,s_m)\\(c,c_1,\dots,c_m)}} \mathbf{Sp}^{c,c_1\dots c_m;s,s_1\dots s_m}_{ff_1\dots f_m} \left[\mathbf{Sp}^{c,c_1\dots c_m;s',s_1\dots s_m}_{ff_1\dots f_m}\right]^*, \tag{2.18}$$

where $\mathcal{C}_f$ is the number of colour degrees of freedom of the parent parton with flavour f, i.e. $\mathcal{C}_g = N^2-1$ for a gluon and $\mathcal{C}_q = N$ for a quark.

It is sometimes useful to define the unpolarised splitting amplitude by averaging over the spins of the parent parton,

$$\langle \hat{P}_{f_1\dots f_m}\rangle \equiv \frac{1}{N_{\rm pol}}\,\delta_{ss'}\,\hat{P}^{ss'}_{f_1\dots f_m}\,, \tag{2.19}$$

where $N_{\rm pol}$ denotes the number of physical polarisation states for the parent parton, i.e. $N_{\rm pol} = 2$ for quarks and $N_{\rm pol} = D-2$ for gluons. When the parent parton is a quark, Lorentz invariance implies that the fermion number and the helicity must be conserved. Then it is easy to see that the tensorial structure of the splitting amplitude is trivial,

$$\hat{P}^{ss'}_{f_1\ldots,f_m} = \delta^{ss'} \langle \hat{P}_{f_1\ldots f_m} \rangle \,, \tag{2.20}$$

as we prove in the next section.

2.4. Proof of the factorisation of the splitting functions

We now focus the discussion on tree-level squared amplitudes and investigate the properties of their corresponding splitting functions. We aim in this section to prove eq. (2.16) in the tree-level case, and at the same time derive the general tensor structure of splitting functions. As we explained in the previous section, the only structure that can be non-trivial is spin, so we distinguish two cases, depending whether the parent parton is a quark or a gluon. Before specialising to these two cases, let us make a huge simplification valid in both cases.

We want to show that in the collinear limit, the squared amplitude at tree-level factorises. The point we are about to prove here is that this factorisation actually already happens at diagram level, when working in a physical gauge, thus largely simplifying the computation of splitting functions in said gauges. This proof is an adaptation of similar ideas in [85]. In this thesis, we work in the (light-like) axial gauge, whose gluon spin-polarisation is given by eq. (1.25). Notice that we chose to work with $d^{\mu\nu}(q,n)$ for a gluon of momentum q, that is that the auxiliary vector in the spin-polarisation tensor is chosen to be the same vector as the one appearing in the parametrisation of the collinear limit in eq. (2.5), for simplicity. As this auxiliary vector is the same for all spin-polarisation tensors, we often omit to reference it and write $d^{\mu\nu}(q)$. The first step in our proof consists in defining effective propagators and vertices in place of the normal ones, which have the advantage of showing explicitly their order in the collinear limit. We consider the partons with momenta q_i

which are sums of subsets S_i of the collinear momenta p_i:

$$\begin{aligned} q_i &= \sum_{j\in S_i} p_j \\ &= \sum_{j\in S_i} x_j p + \sum_{j\in S_i} k_j - \sum_{j\in S_i} \frac{k_j^2}{2x_j n\cdot p} n \\ &= \beta_i p + K_i - \alpha_i n, \end{aligned} \tag{2.21}$$

which we call collinear cluster partons. These include the collinear momenta and, apart from them, the most important of these partons is the parent parton, with $S_i = \{1, \ldots, m\}$, and its momentum $P = \sum_{i=1}^{m} p_i$. Notice that in eq. (2.21), α_i is of order $\mathcal{O}(\lambda^2)$ and K_i of order $\mathcal{O}(\lambda)$. For all the collinear cluster partons, we define an effective quark propagator by changing $\not{q}_i$ to

$$S(q_i) = \frac{1}{n\cdot p}\left(-\not{p} + \beta \not{n} - \frac{\not{K}_i}{\sqrt{|\alpha_i|}}\right), \tag{2.22}$$

as well as the following function:

$$U(q_i) = \sqrt{|\alpha_i|}\not{n} + \not{p}. \tag{2.23}$$

By acting on each side of the effective propagator with this new function $U(q_i)$, we retrieve the numerator of the propagator introduced in fig 1.2:

$$U(q_i)S(q_i)U(q_i) = \not{q}_i. \tag{2.24}$$

For the gluon propagator of a collinear cluster parton, we simply realise that we can act on each side of it with a spin-polarisation tensor in the collinear direction without changing anything at leading order:

$$d^{\mu\rho}(p,n)\, d_{\rho\sigma}(q_i,n)\, d^{\sigma\nu}(p,n) = d^{\mu\nu}(q_i,n) + \mathcal{O}(\lambda), \tag{2.25}$$

where the spin-polarisation tensors are those of axial gauge (c.f. eq. (1.25)). These two changes to the quark and gluon propagators imply that we can define effective vertices by attaching a $U(q_i)$ or a $d^{\mu\nu}(p,n)$ for the collinear cluster partons, up to higher order corrections.

For example, we consider the case of a process where a gluon produces a pair of quarks and a gluon ($g \to q_1\bar{q}_2 g_3$), and the anti-quark is collinear to the outgoing gluon. Amongst all diagrams contributing to the amplitude of this process, there is the one of fig 2.3.

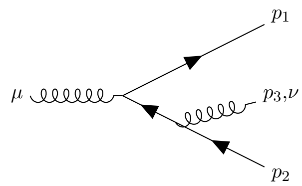

Figure 2.3: Illustration of a simple example

This diagram has an expression which is, up to some irrelevant pre-factor,

$$\frac{1}{s_{23}}\bar{u}(p_1)\gamma^\mu(\not{p}_2+\not{p}_3)\gamma^\nu v(p_2)\varepsilon_\mu(p_1+p_2+p_3)\varepsilon_\nu(p_3). \tag{2.26}$$

We change the initial states of the collinear partons in the amplitude as well. Indeed, when squaring the amplitude and summing over all external states, one encounters

$$\varepsilon_h^\mu(q)\ \varepsilon_h^\nu(q) = d^{\mu\nu}(q), \tag{2.27}$$

$$u(q)\ \bar{u}(q) = \not{q} = v(q)\ \bar{v}(q), \tag{2.28}$$

which suggest to change the external states for the collinear partons as

$$\varepsilon_h^\mu(q) = d^\mu_\nu(p)\ \tilde{\varepsilon}_h^\nu(q), \tag{2.29}$$

$$u(q) = U(q)\ \tilde{u}(q), \tag{2.30}$$

$$v(q) = U(q)\ \tilde{v}(q), \tag{2.31}$$

where $\tilde{\varepsilon}_h^\nu(q)$, $\tilde{u}(q)$, and $\tilde{v}(q)$ are effective external states. This means that we can rewrite the expression in eq. (2.26) as

$$\begin{aligned}
&\frac{1}{s_{23}}\bar{u}(p_1)\gamma^\mu\left[U(p_2+p_3)S(p_2+p_3)U(p_2+p_3)\right]\gamma^\nu\left[U(p_2)\tilde{v}(p_2)\right] \\
&\qquad\qquad\qquad\varepsilon_\mu(p_1+p_2+p_3)d^\rho_\nu(p)\tilde{\varepsilon}_\rho(p_3)+\dots \\
&= \frac{1}{s_{23}}\bar{u}(p_1)\left[\gamma^\mu U(p_2+p_3)\right]S(p_2+p_3)\left[U(p_2+p_3)\gamma^\nu d^\rho_\nu(p)U(p_2)\right] \\
&\qquad\qquad\qquad\tilde{v}(p_2)\varepsilon_\mu(p_1+p_2+p_3)\tilde{\varepsilon}_\rho(p_3)+\dots,
\end{aligned} \tag{2.32}$$

where the dots stand for higher order terms in λ. In this development, we first grouped with squared parenthesis the newly defined propagator for the collinear cluster parton carrying momentum $p_2 + p_3$, as well as the new initial states for the two collinear partons. Then, we gathered the new effective vertices. As we now demonstrate, this allows us to keep track of the order of the diagram quite easily.

In general, following this program, the γ^μ in the gluon-quark-quark vertex can become either

$$U(q_i)\gamma^\mu U(q_j) d_{\mu\nu}(p,n) = -2\sqrt{|\alpha_i|}n\cdot p\left(-\gamma^\nu + \frac{\not{p}n^\nu + \not{n}p^\nu}{n\cdot p}\right) - \left(\sqrt{|\alpha_i|} + \sqrt{|\alpha_j|}\right)\not{p}\gamma^\nu\not{n}, \quad (2.33)$$

if the three partons involved are collinear cluster partons,

$$\gamma^\mu d_{\mu\nu}(p,n) = -\gamma^\nu + \frac{\not{p}n^\nu + \not{n}p^\nu}{n\cdot p}, \quad (2.34)$$

if only the gluon is a collinear cluster parton, and

$$U(q_i)\gamma^\mu = \left(\sqrt{|\alpha_i|}\not{n} + \not{p}\right)\gamma^\mu, \quad (2.35)$$

if only one quark is a collinear cluster parton. If two partons are collinear cluster partons, then the third is too, by momentum conservation. The important observation here is that the gluon-quark-quark vertex is of order $\mathcal{O}(\lambda)$ if the three partons are collinear cluster partons, while this vertex is of order $\mathcal{O}(\lambda^0)$ in all other cases. For the three-gluon vertex, we have the same type of result, since $d_{\mu\nu}(p,n)q_i^\mu = -K_{i,\nu}$. Thus, if we attach to the triple gluon vertex spin-polarisation tensors on all three gluons, meaning we consider the case where all three gluons are collinear cluster partons, the vertex is of order $\mathcal{O}(\lambda)$, while in all other cases the order will be $\mathcal{O}(\lambda^0)$. Notice that this result is clearly linked to our choice of gauge, since the action of the spin-polarisation tensor with momentum in the collinear direction precisely cancels the order 0 which is in the collinear direction. Finally, the four-gluon vertex will always be of order $\mathcal{O}(\lambda^0)$, irrespectively of the number of its gluons being collinear cluster partons. To conclude, with this redefinition of vertices and propagators, we now see that the numerators of the effective propagators $S(q_i)$ as well as $d^{\mu\nu}(q_i, n)$ are of order zero for collinear cluster partons as well as all other partons (at leading order), while the only vertices to have non-zero order in λ are the triple vertices with three collinear cluster partons, and they are all of order one. Of course, the denominator of the propagators are of order $\mathcal{O}(\lambda^{-2})$ for collinear cluster partons and zero for the other ones.

In our simple example of eq. (2.26), the first factor $\frac{1}{s_{23}}$ is of order $\mathcal{O}(\lambda^{-2})$, since partons 2 and 3 are collinear. The first squared parenthesis is of order 0, since this vertex involves only one collinear cluster parton, as well as $S(p_2 + p_3)$, which is always of that order. The second parenthesis, on the other hand, is a gluon-quark-quark vertex where all three partons are collinear cluster partons, so it is of order 1. Note that we are not interested in the order in λ of the external states (being effective or not). Indeed, we are trying to find a hierarchy amongst diagrams for the same process, and all diagrams of a process have the same external states, which hence factor out. That being said, evaluating the order of a diagram (with factored out external states) is now as easy as counting the number of propagators carrying a collinear cluster momentum and 3-vertices connecting only collinear cluster partons.

Now that the order in λ of our building blocks is established, we turn to the actual proof. We start by reminding that for tree-level Feynman diagrams, which are simply connected trees in the language of graph theory, we have

$$p = v - 1, \tag{2.36}$$

where p is the number of propagators and v the number of vertices. We add another equation by counting the number of particles entering vertices, using either the number of propagators or vertices as input: on the one hand, there is one particle entering a vertex on each end of a propagator, to which we need to add all the external particles, of which there is n; on the other hand, there are 3 particles entering each three-particle vertex and 4 entering each four-particle vertex. We note a the number of four-particle vertices. Thus, we write

$$2p + n = 3(v - a) + 4a. \tag{2.37}$$

From these two equations, we deduce that the number of propagators and vertices in a n-parton QCD amplitude with a four-gluon vertices is

$$\begin{aligned} p &= n - a - 3, \\ v &= n - a - 2. \end{aligned} \tag{2.38}$$

For each of the Feynman diagrams contributing to the process of interest in eq. (2.14), the next step is to cut some propagators. The propagators we cut are the ones of collinear cluster partons which are connected to vertices which are not connections of only collinear cluster partons. In other words, we cut all collinear cluster parton propagators, except the ones that link vertices that connect only collinear cluster partons (see fig 2.4).

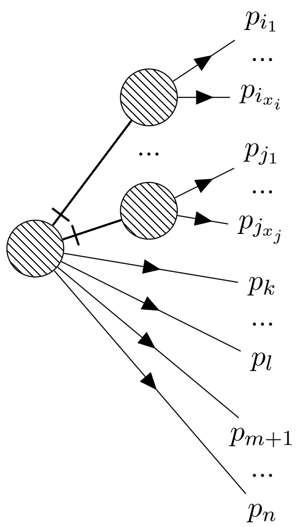

Figure 2.4: Representation of the cuts that factorise all the collinear information (all the momenta starting from the top to p_l are collinear momenta)

By momentum conservation, each of the sub-diagrams that we cut that way involves only collinear cluster partons for each of its vertices and propagators. Each of these sub-diagrams can then be seen as the Feynman diagram of one parton splitting into x_i collinear partons, hence a diagrams with $x_i + 1$ external particles. By virtue of eq. (2.38), it implies that we have $x_i - a_i - 2$ propagators and $x_i - a_i - 1$ vertices in this sub-diagram, a_i being the number of four-gluon vertices for this sub-diagram. Obviously, it immediately implies that we have $x_i - 2a_i - 1$ three-parton vertices. A small subtlety is that we add to this count the propagator of the collinear cluster parton that we cut, for a total of $x_i - a_i - 1$ propagators, as we keep this propagator in the sub-diagram. In each of these sub-diagrams, every three-parton vertex connects only collinear cluster partons so is of order 1 in λ, and every propagator is the propagator of a collinear cluster parton, hence is of order -2 in λ. The total degree of divergence, which we simply define as the number of negative power of λ at leading order, is then

$$2\,(x_i - a_i - 1) - (x_i - 2a_i - 1) = x_i - 1. \tag{2.39}$$

We remind that the four-gluon vertices are of order zero, hence why we did not count any degree of divergence for them. Let us now suppose that, having cut all the pieces as we explained before, we end up with n_x such sub-diagrams, each splitting one parton into x_i collinear partons, and x_0 collinear partons which are not part of these sub-diagrams. These lonely partons connect directly to vertices with non-collinear cluster partons. Since we have m collinear partons, this means that

$$\sum_{i=0}^{n_x} x_i = m. \tag{2.40}$$

In other words, these cuts made a partition of the set of collinear partons with n_x sets of cardinality x_i (for $i = 1, \ldots, n_x$) and x_0 sets of cardinality 1. Finally, we collect all the degrees of divergence: the separated sub-diagrams that split one parton into x_i collinear partons account for $(x_i - 1)$ degrees of divergence each, while what remains of the diagram after we removed these sub-diagrams is of order zero, since it has only vertices with one or no collinear cluster parton (which are of order zero). This means that the total degree of divergence for the whole diagram is the sum of the degrees of divergences of the sub-diagrams we cut:

$$\sum_{i=1}^{n_x}(x_i - 1) = \left(\sum_{i=0}^{n_x} x_i\right) - x_0 - n_x = m - x_0 - n_x. \tag{2.41}$$

It is now trivial to conclude that the diagrams that maximises this degree of divergence, hence those which are leading in the Laurent series in λ, are the ones with $n_x = 1$ and $x_0 = 0$. This means that amongst all diagrams contributing to a n-parton QCD amplitude, we can discard, in the limit where the m first partons are collinear, all the diagrams which do not connect all the collinear partons (and only those) in a sub-diagram, as they are sub-leading. In other words, we can keep only the diagrams that have a propagator with momentum P. A simple diagrammatic representation of the type of diagrams we are interested in is shown in figure 2.5, where the red propagator carries the parent parton momentum P. Once again, we insist on the fact that this is only true when working in a physical gauge.

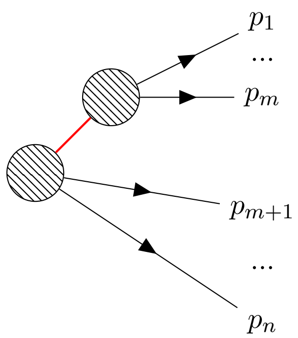

Figure 2.5: Representation of the type of diagrams that contributes to the collinear limit

With the property we just proved, it is obvious to realise that the amplitude, as well as the squared amplitude now factorises if we drop the diagrams that do not contribute in the end anyway. We can hence write

$$\begin{aligned}\mathscr{C}_{1\ldots m}|\mathcal{M}_{f_1\ldots f_m\ldots f_n}(p_1,\ldots,p_m,\ldots,p_n)|^2 = \\ \mathscr{C}_{1\ldots m}\Big(\left[\mathcal{M}^{(n)}_{f,f_{m+1}\cdots f_n}(P,p_{m+1},\ldots,p_n)\right]^* \mathcal{V}^{(n)}_{f_1\cdots f_m}(p_1,\ldots,p_m) \\ .\,\mathcal{M}^{(n)}_{f,f_{m+1}\cdots f_n}(P,p_{m+1},\ldots,p_n)\Big),\end{aligned} \tag{2.42}$$

where the superscript (n) is there to remind that these functions depend on the vector n. The function $\mathcal{V}^{(n)}_{f_1 \cdots f_m}$ is simply the sum of the interferences of all diagrams that split the parent parton into m particles with corresponding flavours. Note that this function still includes two propagators for the parent parton. The summation over colour and spin indices is understood on the right hand of this equation.

The function $\mathcal{V}^{(n)}_{f_1 \cdots f_m}$ must be proportional to the unit matrix in the colour indices of the parent parton by colour conservation, so that we can sum over colour in eq. (2.42) and use the definition of eq. (2.17) to write

$$\mathscr{C}_{1\ldots m}|\mathcal{M}_{f_1\ldots f_m \ldots f_n}(p_1,\ldots,p_m,\ldots,p_n)|^2 = \\ \left(\frac{2\mu^{2\epsilon}g_s^2}{s_{\ldots m}}\right)^{m-1} \mathscr{C}_{1\ldots m}\Big(V^{(n)}_{f_1\cdots f_m}(p_1,\ldots,p_m)\Big)\mathcal{T}_{f,f_{m+1}\ldots f_n}(Xp,p_{m+1},\ldots,p_n). \tag{2.43}$$

In eq. (2.43), we took $\mathcal{T}_{f,f_{m+1}\ldots f_n}$ out of the limit as the only dependence this function exhibits is on the parent parton momentum $P = \sum_{i=1}^m p_i$, which simply becomes $\sum_{i=1}^m x_i\, p$ in the collinear limit. In addition, we extracted a factor of $\left(\frac{2\mu^{2\epsilon}g_s^2}{s_{\ldots m}}\right)^{m-1}$ to factorise the leading pole as well as to get rid of the coupling constant in the splitting function. The function $V^{(n)}_{f_1\cdots f_m}$ is obtained by factorising this quantity from $\mathcal{V}^{(n)}_{f_1\cdots f_m}$ and averaging over the parent parton colour indices. In the continuation of this section, we consider separately the quark parent case from the gluon one.

2.4.1. Quark parent splitting functions

It is easier in this discussion to directly include the factors $\not{P} = \not{p}_1 + \ldots + \not{p}_m$ from the propagators of the parent parton in $V^{(n)}_{f_1\cdots f_m}$. Its general tensor structure is of the form

$$V^{(n)}_{f_1\ldots f_m} = \sum (\text{scalar factor})\,(\text{string of gamma matrices})\,. \tag{2.44}$$

The strings of gamma matrices are composed of either $\not{p}_i$ or $\not{n}\frac{s_{1\ldots m}}{n\cdot(p_1+\ldots+p_m)}$. Each of these building blocks can appear in a string only once, otherwise this string can be reduced to a linear combination of smaller length strings, since p_i as well as n square to zero. Note that these gamma matrices are homogeneous functions of n with vanishing homogeneity degree. As the function $V^{(n)}_{f_1\cdots f_m}$ must also be of homogeneity degree zero (for the very simple reason that in all definitions n appears, eq. (2.5) and eq. (1.25), the definition is of homogeneity degree zero), so does the scalar factors multiplying the Dirac strings. This in turn implies that these factors only depend on the variables $z_i = \frac{n\cdot p_i}{n\cdot P}$ and s_{ij}.

We now focus our attention on the type of string of gamma matrices that can appear. Our function $V^{(n)}_{f_1\ldots f_m}$ is composed of a sum of products of two diagrams. In each of these diagrams, the string of gamma matrices starting from the parent parton always has an even number of gamma matrices; indeed, each propagator has one gamma matrix as well as each vertex, and each propagator is followed by a vertex so that they come by pairs. So the two diagrams whose product we are interested in have an even number of gamma matrices, and an additional one that comes from the summation over all spin states of the parton that links the two strings together. This means that all the strings have an odd number of gamma matrices. We can now exploit the hermiticity of $V^{(n)}_{f_1\cdots f_m}$, as the scalar factors are real, to show that the strings of gamma matrices actually come in the form

$$\left(\frac{1}{s_{1\ldots m}}\right)^{\frac{a-1}{2}} \left(\not{p}_{i_1}\ldots\not{p}_{i_a} + \not{p}_{i_a}\ldots\not{p}_{i_1}\right), \tag{2.45}$$

where the normalisation factor $\left(\frac{1}{s_{1\ldots m}}\right)^{\frac{a-1}{2}}$ has been introduced to make the scalar factors in eq. (2.44) dimensionless. One could try to reduce this form by anti-commuting the matrices in the second term until we get a similar result as the first term in addition to terms of lesser length. A simple calculation shows that it takes $\frac{a(a-1)}{2}$ permutations to do so, meaning that we can reduce all terms of length $a = 3, 7, 11, \ldots$ to terms of length $a = 1, 5, 9, \ldots$. More generally, we can reduce terms of length such that a mod $4 = 3$ to terms of length such that a mod $4 = 1$.

According to all the properties we just established, the most general form for the function $V^{(n)}_{f_1\cdots f_m}$ is

$$V^{(n)}_{f_1\cdots f_m} = A^{(q)}_i \not{p}_i + B^{(q)} \frac{s_{1\ldots m}}{n\cdot P} \not{n} + \sum_{a=5,9,13,\ldots} C^{(q)}_a \frac{\not{p}_1 \cdots \not{p}_{a-1} \not{n} + \not{n} \not{p}_{a-1} \cdots \not{p}_1}{(n\cdot P)\ s_{1\ldots m}^{\frac{a-3}{2}}}, \tag{2.46}$$

where the coefficients $A^{(q)}_i$, $B^{(q)}$, and $C^{(q)}_a$ only depend on the variables z_i and s_{ij}, and a summation over the index i is understood. It should also be noted that the terms with coefficient $C^{(q)}_a$ only exist if $a - 1 \leq m$. Since we can write (cf. eq. (2.11))

$$p_i = z_i P + \tilde{k}_i + \mathcal{O}(\lambda^2), \tag{2.47}$$

we can just insert this relation in eq. (2.46), rescale $k_i \to \lambda k_i$ and take the leading order. Note that since they are dimensionless, the coefficients $A^{(q)}_i$, $B^{(q)}$, and $C^{(q)}_a$ are invariant under this rescaling. As we have already factorised the leading pole, the leading order in λ is the order 0. The terms with coefficient $B^{(q)}$ and $C^{(q)}_a$ scale like λ^2 and λ respectively and hence do not contribute to the leading term, while the terms with coefficient $A^{(q)}_i$ scale like λ^0 and are the only surviving terms. We are then left with

$$V^{(n)}_{f_1\cdots f_m} = \not{P} z_i A^{(q)}_i + \mathcal{O}(\lambda). \tag{2.48}$$

From here, we take back the $\not{P}$ in eq. (2.42) to reconstruct the squared amplitude $|\mathcal{M}_{f_1\cdots f_m}|^2$, and we get eq. (2.43) with an explicit expression for the quark splitting function in terms of the coefficients $A^{(q)}_i$:

$$\hat{P}^{ss'}_{f_1\ldots,f_m} = \mathscr{C}_{1\ldots m} V^{(n)}_{f_1\cdots f_m} = \delta^{ss'} z_i A^{(q)}_i. \tag{2.49}$$

As expected, by spin conservation, the splitting function for quark parents has trivial spin correlations. This means that these splitting functions can be expressed in terms of their unpolarised counterparts:

$$\hat{P}^{ss'}_{f_1\ldots,f_m} = \delta^{ss'} \langle \hat{P}_{f_1\ldots,f_m} \rangle. \tag{2.50}$$

It is also worth noticing from the final result in eq. (2.49) by comparison to the tensor structure of $V^{(n)}_{f_1\cdots f_m}$ in eq. (2.46) that we can obtain the quark splitting amplitude as

$$\langle \hat{P}_{f_1\ldots,f_m}\rangle = \mathscr{C}_{1\ldots m}\left[\mathrm{Tr}\left(\frac{V^{(n)}_{f_1\cdots f_m}\,\not{n}}{4n\cdot P}\right)\right]. \tag{2.51}$$

Since $V^{(n)}_{f_1\cdots f_m}$ is simply defined as the sum of all interferences of diagrams that split the parent parton into the m collinear ones, this equation is a direct and very convenient way of computing quark splitting functions.

2.4.2. Gluon parent splitting functions

Unlike the quark case, we keep for the gluon case the spin-polarisation tensors $d^{\mu\nu}(P)$ apart and only after add them. Because of Lorentz invariance and the vanishing degree of homogeneity of $V^{(n),\rho\sigma}_{f_1\cdots f_m}$ with respect to n, it can be written as

$$V^{(n),\rho\sigma}_{f_1\cdots f_m} = A^{(g)}g^{\rho\sigma} + B^{(g)}_{ij}\frac{p_i^\rho p_j^\sigma}{s_{1\ldots m}} + C^{(g)}_i\frac{p_i^\rho n^\sigma + n^\sigma p_i^\rho}{n\cdot P} + D^{(g)}\frac{s_{1\ldots m}n^\rho n^\sigma}{(n\cdot P)^2}, \tag{2.52}$$

where once again the coefficients $A^{(g)}$, $B^{(g)}_{ij}$, $C^{(g)}_i$, and $D^{(g)}$ are dimensionless functions of the variables z_i and s_{ij}, and a summation over the indices i and j is understood. Note that $B^{(g)}_{ij}$ is symmetric in $i \leftrightarrow j$ in order for the whole term to be symmetric in $\rho \leftrightarrow \sigma$.

We now take back the spin-polarisation tensors to obtain

$$d^\mu_\rho(P)\;V^{(n),\rho\sigma}_{f_1\cdots f_m}\;d^\nu_\sigma(P). \tag{2.53}$$

The terms with coefficients $C^{(g)}_i$ and $D^{(g)}$ immediately drop as $d^\mu_\nu(P)n^\nu = 0$. For the terms with coefficients $B^{(g)}_{ij}$ we notice that

$$d^\mu_\nu(P)p_i^\nu = -\tilde{k}_i^\mu + \mathcal{O}(\lambda^2). \tag{2.54}$$

Finally, for the term in $g^{\rho\sigma}$, we have

$$d^\mu_\rho(P)g^{\rho\sigma}d^\nu_\sigma(P) = -d^{\mu\nu}(p) + \mathcal{O}(\lambda). \tag{2.55}$$

With these expressions at hand, we have shown eq. (2.43) for the case of a gluon parent as well as provided an explicit expression for the tensor structure of the splitting function:

$$\hat{P}^{\mu\nu}_{f_1\dots,f_m} = -A^{(g)} d^{\mu\nu}(p) + B^{(g)}_{ij} \frac{\tilde{k}^{\mu}_i \tilde{k}^{\nu}_j}{s_{1\dots m}}. \tag{2.56}$$

Note that the definition of the splitting function in the gluon parent case is arbitrary since we can add any additional quantity proportional to either p^μ or p^ν, since $\mathcal{T}^{\mu\nu}$ is transverse: $\mathcal{T}^{\mu\nu} p_\mu = 0$ and $\mathcal{T}^{\mu\nu} p_\nu = 0$. This means that our expression in eq. (2.56) is not the simplest possible and could without loss of generality be written as

$$\hat{P}^{\mu\nu}_{f_1\dots,f_m} = A^{(g)} g^{\mu\nu} + B^{(g)}_{ij} \frac{\tilde{k}^{\mu}_i \tilde{k}^{\nu}_j}{s_{1\dots m}}, \tag{2.57}$$

as long as it is understood that this function is to be contracted with a transverse quantity.

3 | Quadruple Collinear Limit

In this chapter, we present the main results of this thesis, namely the computation of the quadruple splitting functions, which encompass the collinear behaviour of QCD squared amplitudes for 4 collinear partons. Our method follows the same lines as ref [58, 81] and is presented in Chapter 2. Using this technique we were able to reproduce all known results for double and triple collinear splitting functions [58, 86] as well as extend this knowledge to the realm of quadruple collinear splitting functions [78, 79]. Our results being quite lengthy are not directly available anywhere in printed form but rather in computer-readable form [77].

In this chapter, we first review the list of all independent quadruple collinear splitting functions we have to compute as well as their behaviour under the exchange of collinear partons. Afterwards we detail case by case the Feynman diagrams contributing to each splitting function. We also look how these functions depend on the Casimirs of *SU(N)*.

3.1. Quadruple splitting functions

In order to obtain all the possible quadruple splitting functions, we need to consider any parton, either a quark or a gluon, producing any four partons. However, we must do so and at the same time respect flavour conservation. In other words, if the parent parton is a quark, then the four final partons must be a quark of the same flavour as the initial one and a combination of gluons and pairs of quarks of any flavour. If the parent parton is a gluon, then the four final partons can only be a combination of gluons and pairs of quarks. All other possibilities are automatically zero. With that in mind, the set of splitting processes we have to focus on is the following:

- $q \to \bar{q}'\, q'\, q\, g$,
- $q \to \bar{q}\, q\, q\, g$,
- $q \to q\, g\, g\, g$,
- $g \to \bar{q}'\, q'\, \bar{q}\, q$,
- $g \to \bar{q}\, q\, \bar{q}\, q$,
- $g \to \bar{q}\, q\, g\, g$,
- $g \to g\, g\, g\, g$.

In this table, q' is simply a quark of a different flavour than the one of q. It can be noted that we did not include splitting processes for an anti-quark as a parent. This is because these splitting functions can be obtained by charge-conjugation invariance, for example $\hat{P}_{q'_1\bar{q}'_2\bar{q}_3g_4} = \hat{P}_{\bar{q}'_1q'_2q_3g_4}$. Similarly, we can change all quarks to anti-quarks and vice-versa in a splitting function with a gluon as a parent, for example $\hat{P}_{\bar{q}_1q_2\bar{q}_3q_4} = \hat{P}_{q_1\bar{q}_2q_3\bar{q}_4}$. In summary, we have seven independent quadruple collinear splitting functions to compute.

In the rest of this chapter, we will not explicitly indicate the spin indices of the splitting functions as we are interested in their symmetries and their colour structure. This means that implicitly each quark-parent splitting function has indices s and s' (and is proportional to $\delta^{ss'}$), while gluon-parent ones have Lorentz indices μ and ν.

3.2. Exchange symmetries

Symmetry is a very useful tool when it comes to simplify computations or to make explicit some physical properties. In the case of splitting functions, the symmetry we are looking for is exchange symmetry. Indeed, whether they follow the laws of Bose-Einstein or Fermi-Dirac statistics, the exchange of two indistinguishable partons will not change the result of any squared amplitude, or for what matters of any splitting function. This implies that if a splitting function has two identical partons (two quarks, two anti-quarks or two gluons), it will be symmetric in the variables that involve these two partons. To be more concrete, if parton i and j are identical, then the symmetry of interest involves these operations (remember that splitting functions only depend on sub-energies s_{kl}, momentum fractions z_k and orthogonal momenta $\tilde{k}_l$):

$$\begin{aligned} s_{ik} &\leftrightarrow s_{jk}, \qquad \forall k = 1, \ldots, m \\ z_i &\leftrightarrow z_j, \\ \tilde{k}_i &\leftrightarrow \tilde{k}_j, \end{aligned} \tag{3.1}$$

and such a splitting function will have the following form:

$$\hat{P}_{f_1 \ldots, f_m}(\{z_k, s_{kl}, \tilde{k}_l\}) = \hat{P}^{(\mathrm{symm})}_{f_1 \ldots, f_m}(\{z_k, s_{kl}, \tilde{k}_l\}) + (i \leftrightarrow j), \tag{3.2}$$

where the second term is a notation for the previous term with the exchange of variables described in eq. (3.1). Obviously, this fully generalises to more than just two identical partons. If there are α identical partons, then the splitting amplitude is invariant under any permutation of the α identical partons, which are just combinations of simpler permutations of two partons (as described in eq. (3.1)). In this case, we can rearrange the splitting function into $\alpha!$ terms as

$$\hat{P}_{f_1 \ldots, f_m}(\{z_k, s_{kl}, \tilde{k}_l\}) = \hat{P}^{(\mathrm{symm})}_{f_1 \cdots, f_m}(\{z_k, s_{kl}, \tilde{k}_l\}) + ((\alpha! - 1) \text{ perm}), \tag{3.3}$$

where the second term stands for the other $\alpha! - 1$ possible permutations of $\hat{P}^{(\mathrm{symm})}_{f_1 \cdots, f_m}(\{z_k, s_{kl}, \tilde{k}_l\})$. The *a priori* knowledge of this structure comes in handy in two ways. First, it means that we only really have to compute the function $\hat{P}^{(\mathrm{symm})}_{f_1 \cdots, f_m}(\{z_k, s_{kl}, \tilde{k}_l\})$ in order to have the full splitting function basically for free, which could be a more efficient way of computing these functions: using their symmetries to make them faster to compute. Second, if we manage to compute this function $\hat{P}^{(\text{symm})}_{f_1\cdots,f_m}(\{z_k, s_{kl}, \tilde{k}_l\})$, this structure makes the symmetry of the function explicit.

The only question left unanswered to conclude this section is how to compute the part that once symmetrised provides the whole splitting function, the function $\hat{P}^{(\text{symm})}_{f_1\cdots,f_m}(\{z_k, s_{kl}, \tilde{k}_l\}))$ in eq. (3.3). To tackle it, let us focus on an example. Suppose the splitting function we want to compute depends on three Feynman diagrams, that we call d_1, d_2 and d_3, and that under the exchange of partons 1 and 2, diagram d_1 becomes d_2 (and vice-versa), while diagram d_3 stays the same. The quantity we want to compute is the limit of the modulus square of the sum of these diagrams, so

$$|d_1 + d_2 + d_3|^2 = |d_1|^2 + |d_2|^2 + |d_3|^2 + (d_1^* d_2 + d_1^* d_3 + d_2^* d_3 + \text{cc})\,, \quad (3.4)$$

where cc is the complex conjugate of all that is inside the parenthesis. The next thing we need to know is how each of these terms will transform under the symmetry $1 \leftrightarrow 2$, for example, d_1 becomes d_2 while d_3 stays the same, which implies that if we put $|d_1|^2$ as a term in the function $\hat{P}^{(\text{symm})}_{f_1\cdots,f_m}(\{z_k, s_{kl}, \tilde{k}_l\})$ for this splitting function it will produce $|d_2|^2$ after symmetry, which is what we want, but $|d_3|^2$ on the other hand will produce a second $|d_3|^2$ so that we have to multiply it by $1/2$ in the function $\hat{P}^{(\text{symm})}_{f_1\cdots,f_m}(\{z_k, s_{kl}, \tilde{k}_l\})$. In the end, we could have for example (bear in mind that the choice of $\hat{P}^{(\text{symm})}_{f_1\cdots,f_m}(\{z_k, s_{kl}, \tilde{k}_l\}))$ is not unique):

$$\hat{P}^{(\text{symm})}_{f_1\cdots,f_m}(\{z_k, s_{kl}, \tilde{k}_l\}) = |d_1|^2 + \frac{1}{2}|d_3|^2 + \left(\frac{1}{2}d_1^* d_2 + d_1^* d_3 + \text{cc}\right). \quad (3.5)$$

We need to emphasise on the symmetry factors that we added. Here, there is only factors of 1/2 but for more than two identical partons, one could have different factors. These factors allow us to keep terms that are invariant under (at least) some permutations of the identical partons without having to keep them separate.

In this simple example, it does not seem like we gained so much simplification. After all, we only lost a third of the terms to compute. However, this mitigation becomes more and more important with the number of diagrams and the number of identical partons. The most extreme example in this thesis come from the splitting functions of one gluon to four gluons $\hat{P}_{gggg}$. We have in that case 25 Feynman diagrams contributing, which is the highest number of Feynman diagrams for quadruple splitting functions, and of course all partons are identical, allowing $4! = 24$ possible permutations. The 25 diagrams would normally lead to the computation of 325 terms for the splitting functions (and their complex conjugate), but the use of the symmetries makes it possible to compute the whole splitting function having computed only 27 of these terms, i.e. less than a tenth of the total.

3.3. Presentation of the results

In this section, we present each one of the quadruple QCD splitting functions in turn, going from the Feynman diagrams that contribute to the splitting function of interest to the symmetries that they might have and the different colour structures of the result. By colour structure, we mean that these functions will appear as polynomials of T_R, $\mathcal{C}_F$, and $\mathcal{C}_A$, the Casimirs of *SU(N)* (or more specifically *SU(3)* in the case of QCD) as defined in Chapter 1 and we sort the different terms according to which powers of which Casimir they have. Usually, we call terms *abelian* when they do not have any power of $\mathcal{C}_A$. Indeed, $\mathcal{C}_A$ comes from the self-couplings of gluons which do not appear in abelian theory such as QED (for Quantum Electrodynamics) which is a *U(1)* gauge theory. Conversely, we call terms with any power of $\mathcal{C}_A$ *non-abelian*. Note that certain terms come with a coefficient of $\mathcal{C}_A - 2\ \mathcal{C}_F$ which is equal to $\frac{1}{N}$. This means that if one considers the limit where N goes to infinity (called $1/N$-expansion), such terms are sub-leading.

3.3.1. $q \to \bar{q}'\, q'\, q\, g$

The first quadruple splitting function we focus on is $\hat{P}_{\bar{q}'q'qg}$. The function $V^{(n)}_{\bar{q}'q'qg}$ from eq. (2.43) for this case depends on 5 Feynman diagrams displayed in figure 3.1. Being the simplest of the seven quadruple splitting functions unfortunately comes with a price: it has no identical partons, and hence no symmetries we can exploit. Going through all the steps described in Chapter 2, we find that the result can be decomposed into an abelian and a non-abelian part:

$$\hat{P}_{\bar{q}'_1 q'_2 q_3 g_4} = T_R\, \mathcal{C}_F^2\, \hat{P}^{(\mathrm{ab})}_{\bar{q}'_1 q'_2 q_3 g_4} + T_R\, \mathcal{C}_A\, \mathcal{C}_F\, \hat{P}^{(\mathrm{nab})}_{\bar{q}'_1 q'_2 q_3 g_4}. \tag{3.6}$$

The indices carried by the partons label refer to the indices of their momenta.

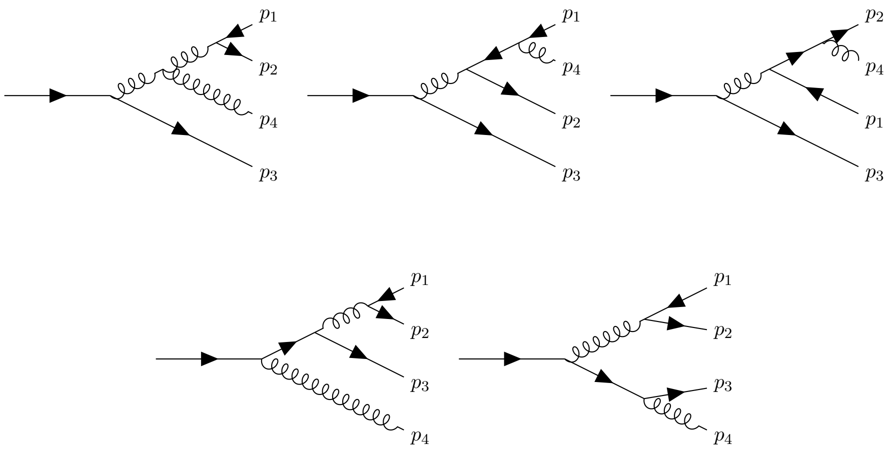

Figure 3.1: Diagrams contributing to the splitting function $q \to \bar{q}'_1 q'_2 q_3 g_4$

3.3.2. $q \to \bar{q}\, q\, q\, g$

The next splitting function we are interested in is $\hat{P}_{\bar{q}qqg}$, which is essentially the same as the previous one, except that now the quarks all have identical flavour. The diagrams are the exact same as the ones for the previous case (see again figure 3.1), with the addition of an extra copy of those diagrams with quarks 2 and 3 exchanged. This implies that we can write this splitting function as the one with different flavours of quarks, with the addition of an extra copy of the different flavours of quarks splitting function where quarks 2 and 3 have been exchanged, and finally the interference term coming from the products of diagrams from figure 3.1 and those with quarks 2 and 3 exchanged:

$$\hat{P}_{\bar{q}_1 q_2 q_3 g_4} = \Big(\hat{P}_{\bar{q}'_1 q'_2 q_3 g_4} + (2 \leftrightarrow 3)\Big) + \hat{P}^{(\mathrm{id})}_{\bar{q}_1 q_2 q_3 g_4}, \tag{3.7}$$

where $\hat{P}^{(\mathrm{id})}_{\bar{q}_1 q_2 q_3 g_4}$ is the interference term. Again, using the method exposed in Chapter 2, this new additional part can be computed and found to be decomposable into an abelian and a non-abelian part:

$$\hat{P}^{(\mathrm{id})}_{\bar{q}_1 q_2 q_3 g_4} = \mathcal{C}_F^2\,(\mathcal{C}_A - 2\mathcal{C}_F)\,\hat{P}^{(\mathrm{id})(\mathrm{ab})}_{\bar{q}_1 q_2 q_3 g_4} + \mathcal{C}_A\,\mathcal{C}_F\,(\mathcal{C}_A - 2\mathcal{C}_F)\,\hat{P}^{(\mathrm{id})(\mathrm{nab})}_{\bar{q}_1 q_2 q_3 g_4}. \tag{3.8}$$

3.3.3. $q \to q\,g\,g\,g$

We now turn to the last quark-initiated quadruple splitting function, $\hat{P}_{qggg}$, which depends on the 16 diagrams whose different possible topologies are depicted in figure 3.2. Unlike the two previous cases, this function has a lot of symmetries we can use. Indeed, all three gluons are fully interchangeable, which makes up for a total of $3! = 6$ possible permutations. According to eq. (3.3), we can then write this splitting function as

$$\hat{P}_{q_1 g_2 g_3 g_4} = \hat{P}^{(\mathrm{symm})}_{q_1 g_2 g_3 g_4} + 5 \text{ perm.} \tag{3.9}$$

We are again emphasising on the improvement in the efficiency of the calculation this little trick of using symmetries allows. In this case, the number of terms to compute went down from 136 to only 31.

In a similar fashion than previously, we can decompose the "seed" of this splitting function into its different colour structures:

$$\hat{P}^{(\mathrm{symm})}_{q_1 g_2 g_3 g_4} = \mathcal{C}_F^3\,\hat{P}^{(\mathrm{symm})(\mathrm{ab})}_{q_1 g_2 g_3 g_4} + \mathcal{C}_A\,\mathcal{C}_F^2\,\hat{P}^{(\mathrm{symm})(\mathrm{nab})_1}_{q_1 g_2 g_3 g_4} + \mathcal{C}_A^2\,\mathcal{C}_F\,\hat{P}^{(\mathrm{symm})(\mathrm{nab})_2}_{q_1 g_2 g_3 g_4}. \tag{3.10}$$

Note that here we have two different non-abelian structures.

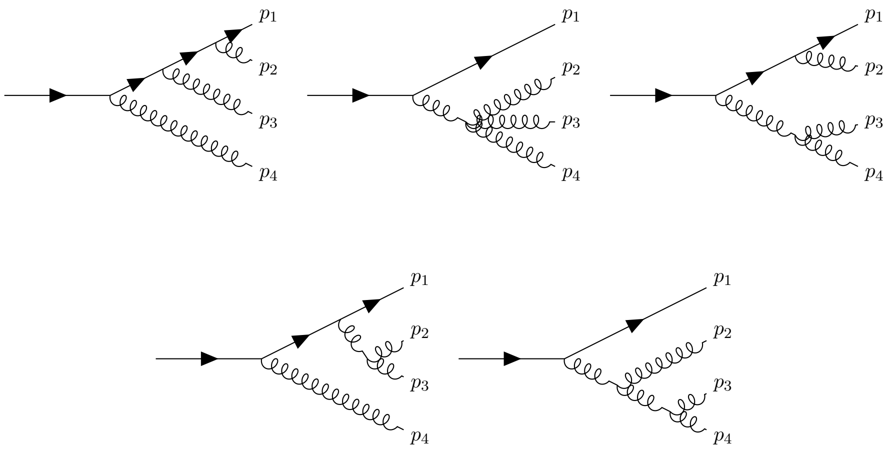

Figure 3.2: Diagrams contributing to the splitting function $q \to q_1 g_2 g_3 g_4$ (note that you must add all the possible permutations of the gluons as well, which add 5 diagrams to the first topology, none to the second, and two to each of the third, fourth and fifth ones)

3.3.4. $g \to \bar{q}'\, q'\, \bar{q}\, q$

We then turn to the first of the gluon-initiated splitting functions, $\hat{P}_{\bar{q}'q'\bar{q}q}$, which depends on the 5 diagrams depicted in figure 3.3. This function is a little bit special as the symmetry it exhibits is not under the exchange of two partons but under the exchange of two pairs of partons. Indeed, we can switch the pair of partons 1 and 2 with the pair 3 and 4 without changing the expression of the splitting function. This can be understood by the fact that the different flavours all behave exactly the same way in (massless) QCD; the only consequence of having different flavours here is that we can not interchange them, they are not indistinguishable. As a result, we can change the name (or label) of the flavours, by calling q as q' and vice-versa, without changing anything. The only information the naming of the two different flavours carries is that they are different. Hence, we can write

$$\hat{P}_{\bar{q}'_1 q'_1 \bar{q}_3 q_4} = \hat{P}^{(symm)}_{\bar{q}'_1 q'_1 \bar{q}_3 q_4} + \left(\binom{1}{2} \leftrightarrow \binom{3}{4}\right) . \tag{3.11}$$

Finally, as we did for the cases beforehand, we can explore the colour structure of $\hat{P}^{(symm)}_{\bar{q}'_1 q'_1 \bar{q}_3 q_4}$ and find

$$\hat{P}^{(symm)}_{\bar{q}'_1 q'_1 \bar{q}_3 q_4} = T_R^2\, \mathcal{C}_F\, \hat{P}^{(symm)(\mathrm{ab})}_{\bar{q}'_1 q'_1 \bar{q}_3 q_4} + T_R^2\, \mathcal{C}_A\, \hat{P}^{(symm)(\mathrm{nab})}_{\bar{q}'_1 q'_1 \bar{q}_3 q_4}. \tag{3.12}$$

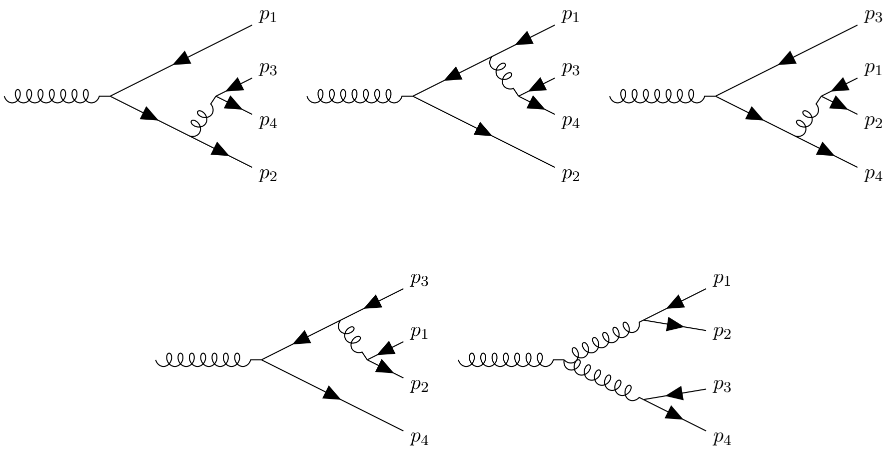

Figure 3.3: Diagrams contributing to the splitting function $g \to \bar{q}'_1 q'_2 \bar{q}_3 q_4$

3.3.5. $g \to \bar{q}\, q\, \bar{q}\, q$

The next splitting function is $\hat{P}_{\bar{q}q\bar{q}q}$ and the diagrams for this one are the same as the previous one (see figure 3.3) with the addition of a copy where the two quarks are exchanged. As it was the case for $\hat{P}_{\bar{q}qqg}$, it means we can write this splitting function as

$$\hat{P}_{\bar{q}_1 q_2 \bar{q}_3 q_4} = \Big(\hat{P}_{\bar{q}'_1 q'_2 \bar{q}_3 q_4} + (1 \leftrightarrow 3)\Big) + \hat{P}^{(\mathrm{id})}_{\bar{q}_1 q_2 \bar{q}_3 q_4}, \tag{3.13}$$

where once again $\hat{P}^{(\mathrm{id})}_{\bar{q}_1 q_2 \bar{q}_3 q_4}$ contains all interferences between the diagram for non-identical flavours and the ones with the quarks exchanged. It turns out that this interference term has three symmetries: one can either exchange the two quarks, or the two anti-quarks, or the pairs of a quark and an anti-quark without changing the expression of this term. Consequently, it admits the following expression:

$$\hat{P}^{(\mathrm{id})}_{\bar{q}_1 q_2 \bar{q}_3 q_4} = \hat{P}^{(\mathrm{id})(\mathrm{symm})}_{\bar{q}_1 q_2 \bar{q}_3 q_4} + (1 \leftrightarrow 3) + (2 \leftrightarrow 4) + \left(\binom{1}{2} \leftrightarrow \binom{3}{4}\right). \tag{3.14}$$

Finally, we can specify the colour structure of $\hat{P}^{(\mathrm{id})(\mathrm{symm})}_{\bar{q}_1 q_2 \bar{q}_3 q_4}$ as

$$\begin{aligned}\hat{P}^{(\mathrm{id})(\mathrm{symm})}_{\bar{q}_1 q_2 \bar{q}_3 q_4} = T_R\, \mathcal{C}_F\, (\mathcal{C}_A - 2\mathcal{C}_F)\, \hat{P}^{(\mathrm{id})(\mathrm{symm})(\mathrm{ab})}_{\bar{q}_1 q_2 \bar{q}_3 q_4} \\ + T_R\, \mathcal{C}_A\, (\mathcal{C}_A - 2\mathcal{C}_F)\, \hat{P}^{(\mathrm{id})(\mathrm{symm})(\mathrm{nab})}_{\bar{q}_1 q_2 \bar{q}_3 q_4}\end{aligned} \quad (3.15)$$

3.3.6. $g \to \bar{q}\, q\, g\, g$

We now turn to the splitting function $\hat{P}_{\bar{q}qgg}$, which depends on the 16 diagrams whose topologies are depicted in figure 3.4. There is two symmetries that we can exploit here: the exchange of the two gluons and the exchange of the quark and the anti-quark (indeed, due to charge conjugation invariance, the exchange of the quark pair is a symmetry). Having these symmetries at hand, we go down from 136 terms to compute to only 76. Following eq. (3.3) as before, we write this splitting function as

$$\hat{P}_{\bar{q}_1 q_2 g_3 g_4} = \hat{P}^{(\mathrm{symm})}_{\bar{q}_1 q_2 g_3 g_4} + (1 \leftrightarrow 2) + (3 \leftrightarrow 4) + \left(\binom{1}{3} \leftrightarrow \binom{2}{4}\right). \quad (3.16)$$

For what concerns the colour structure of $\hat{P}^{(\mathrm{symm})}_{\bar{q}_1 q_2 g_3 g_4}$, we can write

$$\begin{aligned}\hat{P}^{(\mathrm{symm})}_{\bar{q}_1 q_2 g_3 g_4} = T_R\, \mathcal{C}_F^2\, \hat{P}^{(\mathrm{symm})(\mathrm{ab})}_{\bar{q}_1 q_2 g_3 g_4} + T_R\, \mathcal{C}_A\, \mathcal{C}_F\, \hat{P}^{(\mathrm{symm})(\mathrm{nab})_1}_{\bar{q}_1 q_2 g_3 g_4} \\ + T_R\, \mathcal{C}_A^2\, \hat{P}^{(\mathrm{symm})(\mathrm{nab})_2}_{\bar{q}_1 q_2 g_3 g_4}.\end{aligned} \quad (3.17)$$

3.3.7. $g \to g\, g\, g\, g$

Finally we focus on the last of the quadruple splitting function, $\hat{P}_{gggg}$. This splitting function is by far the most complex of all the quadruple splitting functions for at least two reasons. First of all, it contains only gluon couplings which have more than one term each as opposed to the quark-gluon coupling (see figure 1.3), so that the number of terms to compute for each diagrams is bigger than in any of the previous cases. In addition, the number of diagrams involved in the computation of this splitting function is 25, which is more than the number of diagrams for any other quadruple splitting function. The different topologies for

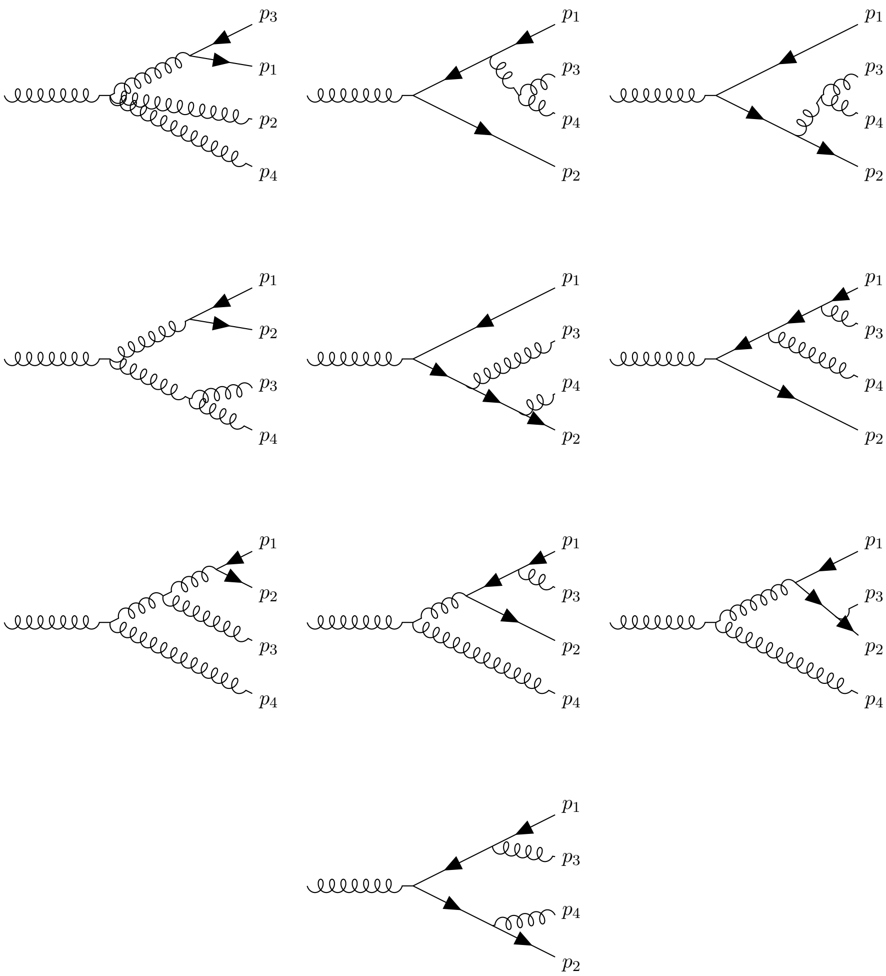

Figure 3.4: Diagrams contributing to the splitting function $g \to \bar{q}_1 q_2 g_3 g_4$ (note that, except for the four first ones, one must add to each diagram the same one with gluons exchanged)

these diagrams are represented in figure 3.5. Since we are computing all possible products of these diagrams, the number of products of diagrams grows like the square of the number of diagrams, which makes this last fact even worse. Despite these two factors against us, we can still have some hope because this is the place where symmetries are the most powerful for quadruple splitting functions. Indeed, our result has to be invariant under any of the 24 permutations of the 4 gluons. As a consequence, we are able to compute only 27 terms instead of 325 and we write

$$\hat{P}_{g_1 g_2 g_3 g_4} = \hat{P}^{(\text{symm})}_{g_1 g_2 g_3 g_4} + (23 \text{ perm}). \tag{3.18}$$

Being a purely non-abelian process, in the sense that it would simply be zero if there was no gluon self-coupling, this splitting function has only one colour structure proportional $\mathcal{C}_A^3$:

$$\hat{P}^{(\text{symm})}_{g_1 g_2 g_3 g_4} = \mathcal{C}_A^3 \, \hat{P}^{(\text{symm})(\text{nab})}_{g_1 g_2 g_3 g_4}. \tag{3.19}$$

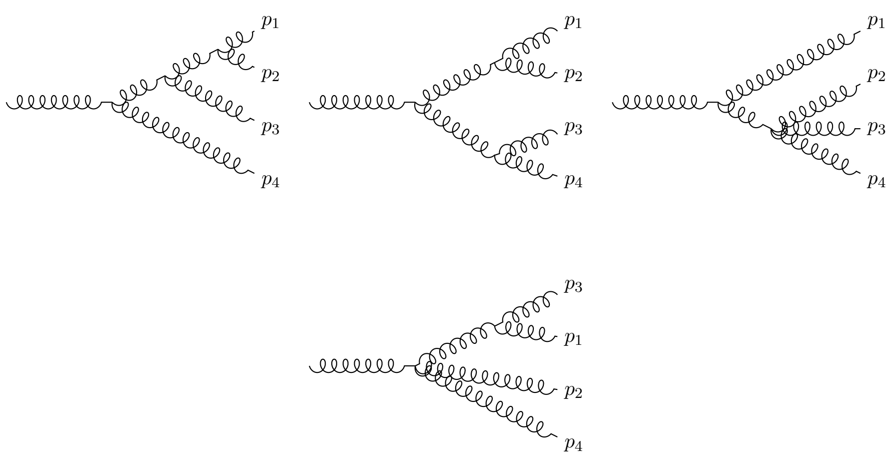

Figure 3.5: Diagrams contributing to the splitting function $g \to g_1 g_2 g_3 g_4$ (note that one must add to these diagrams all the possible permutations of gluons, which gives 11 additional diagrams of the first topology, 2 of the second, 3 of the third and 5 of the fourth, for a total of 25 diagrams)

3.4. Summary

We presented in this chapter the quadruple collinear splitting functions. There is seven independent of these:

- $q \to \bar{q}' \, q' \, q \, g$,
- $q \to \bar{q} \, q \, q \, g$,
- $q \to q \, g \, g \, g$,
- $g \to \bar{q}' \, q' \, \bar{q} \, q$,
- $g \to \bar{q} \, q \, \bar{q} \, q$,
- $g \to \bar{q} \, q \, g \, g$,
- $g \to g \, g \, g \, g$.

We presented our results by showcasing the symmetries they exhibit, as well as their colour structure. These functions were computed for the very first time in our papers [78, 79] and can be found online [77].

4 | Sub-Collinear Limit

After the computation of the splitting functions presented in the previous chapter, we now explore the mathematical properties of these functions. In this chapter, we look at the sub-collinear limit, meaning that amongst the collinear partons we choose a subset of these to undergo a second collinear limit. Since collinear splitting functions are built as some limit of a squared amplitude (more precisely it is built as the collinear limit of the amplitude squared of the parent parton splitting into the collinear partons, keeping the spin indices of the parent parton open), it is not unreasonable to expect the splitting functions themselves to factorise in this new sub-collinear limit.

The reasons to look at such a limit are twofold. First, confirming that the splitting functions presented in Chapter 3 do have the correct limits is a strong sanity check of our results. Secondly, the knowledge of these limits is an important ingredient when it comes to building counter-terms to subtract infrared divergences in higher-order computations.

This chapter first makes a clear distinction between two different ways to look at this limit before concluding that the two points of view are the same. Afterwards, we prove the factorisation formula for the sub-collinear limit. Then, we discuss the tensor structure of the splitting tensor and distinguish between two cases: the sub-parent parton, which is the parton whose momenta is the sum of all the partons going into the sub-collinear limit, can either be a quark or a gluon. If the sub-parent is a quark, then the splitting function factorises as the product of two splitting functions. However, if the sub-parent parton is a gluon, the splitting function factorises as the tensor product of a splitting function and a new object that we call a *splitting tensor*. A second distinction can then be made according to whether the parent parton is a quark or a gluon. Finally, we move to the parametrisation of the sub-collinear limit and most importantly we show how one can relate the two different collinear limits at play: the one that defines the splitting function and the sub-collinear one.

4.1. Strongly-ordered versus iterated collinear limits

In this chapter, we consider a QCD process involving n partons amongst which partons 1 to m are collinear. But this time we add a twist as the first m' partons (with $m' < m$) amongst the m collinear ones will undergo another collinear limit. Note that we do not lose any generality by considering the sub-collinear partons to be the firsts in the collinear set. The problem we are facing right now is that there is two ways to approach this kinematic region, depending on which order the limits are taken. The two scenarios are the following, supposing that the m partons go in the direction p and the m' sub-collinear in the direction $\bar{p}$:

1. The parent parton (with momentum P) splits into m partons collinear to p first, and then the m' sub-collinear partons become collinear to the sub-collinear direction $\bar{p}$. We call this limit the *iterated collinear limit* and we define it by (see figure 4.1)

$$\mathscr{C}_{1\ldots m'}\mathscr{C}_{1\ldots m}|\mathcal{M}_{f_1\ldots f_n}(p_1,\ldots,p_n)|^2. \tag{4.1}$$

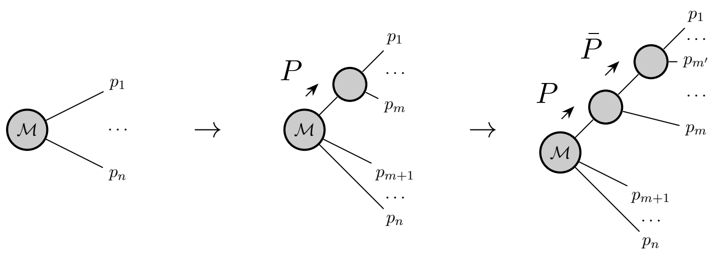

Figure 4.1: Diagrammatic representation of iterated collinear limit: the collinear partons first go all collinear, then the sub-collinear set goes through a second collinear limit.

2. The sub-collinear partons first become collinear to the direction $\bar{p}$, then the sub-parent parton, with momentum $\bar{P} = \sum_{i=1}^{m'} p_i$, and the rest of the collinear partons (hence those with indices from $m'+1$ to m) become collinear to the direction p. We call this limit the

strongly-ordered collinear limit and we define it as

$$\mathscr{C}_{(1\ldots m')\ldots m}\mathscr{C}_{1\ldots m'}|\mathcal{M}_{f_1\ldots f_n}(p_1,\ldots,p_n)|^2, \tag{4.2}$$

where in the first $\mathscr{C}$ symbol, the parenthesis stands for the sub-parent parton (see figure 4.2).

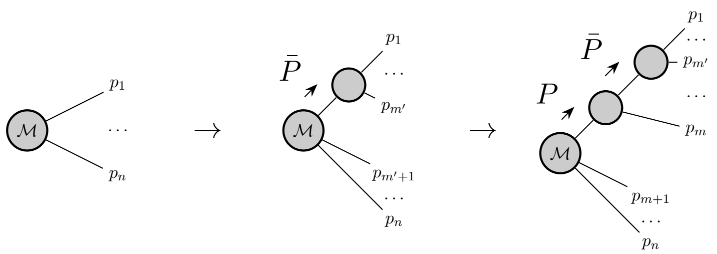

Figure 4.2: Diagrammatic representation of strongly-ordered collinear limit: the sub-collinear partons first go collinear, then the sub-collinear parent parton and the rest of the collinear partons become collinear.

It is clear that these two limits describe the same region of phase space. It is even trivial to prove at tree-level, since at that order squared amplitudes are simply rational functions of the Mandelstam invariants. Thus, the Laurent series obtained in the two limits must be the same. Consequently, the behaviour of the squared amplitudes in the two limits must agree as the value of the amplitude in any given point of phase space cannot depend on how this point was approached. This directly implies that the strongly-ordered collinear limit and the iterated collinear one are the same:

$$\begin{aligned}\mathscr{C}_{1\ldots m'}\mathscr{C}_{1\ldots m}&|\mathcal{M}_{f_1\ldots f_n}(p_1,\ldots,p_n)|^2\\ &= \mathscr{C}_{(1\ldots m')\ldots m}\mathscr{C}_{1\ldots m'}|\mathcal{M}_{f_1\ldots f_n}(p_1,\ldots,p_n)|^2\end{aligned} \tag{4.3}$$

From now on we will not distinguish further between the two limits. However, this commutativity property is used in section 4.2 to prove that splitting functions factorise in this limit.

4.2. Factorisation in the sub-collinear limit

In order to prove the factorisation of splitting functions in the sub-collinear limit, we start from the equivalence of its two possible approaches in eq. (4.3). The left hand side of this equation can be developed quite simply using the factorisation formula for squared amplitudes in eq. (2.16):

$$
\begin{aligned}
&\mathscr{C}_{1\ldots m'}\mathscr{C}_{1\ldots m}|\mathcal{M}_{f_1\ldots f_n}|^2 \\
&= \mathscr{C}_{1\ldots m'}\left(\frac{2\mu^{2\epsilon}\,g_s^2}{s_{1\ldots m}}\right)^{m-1} \hat{P}^{ss'}_{f_1\cdots f_m}\,\mathcal{T}^{ss'}_{ff_{m+1}\cdots f_n} \\
&= \left(\frac{2\mu^{2\epsilon}\,g_s^2}{s_{(1\ldots m')\ldots m}}\right)^{m-1} \left(\mathscr{C}_{1\ldots m'}\hat{P}^{ss'}_{f_1\cdots f_m}\right)\mathcal{T}^{ss'}_{ff_{m+1}\cdots f_n},
\end{aligned}
\tag{4.4}
$$

where the dependences on momenta have not been indicated for more clarity. In this last equation, $s_{(1\ldots m')\ldots m}$ is simply $s_{1\ldots m}$ in the sub-collinear limit. Notice that to go from the second to the third line we use the fact that $\mathcal{T}^{ss'}_{ff_{m+1}\cdots f_n}$ does not depend on any of the collinear nor sub-collinear variables anymore. If we now look at the right hand side of eq. (4.3), we can write:

$$
\begin{aligned}
&\mathscr{C}_{(1\ldots m')\ldots m}\mathscr{C}_{1\ldots m'}|\mathcal{M}_{f_1\ldots f_n}|^2 \\
&= \mathscr{C}_{(1\ldots m')\ldots m}\left(\frac{2\mu^{2\epsilon}\,g_s^2}{s_{1\ldots m'}}\right)^{m'-1} \hat{P}^{hh'}_{f_1\cdots f_{m'}}\,\mathcal{T}^{hh'}_{ff_{m'+1}\cdots f_n} \\
&= \left(\frac{2\mu^{2\epsilon}\,g_s^2}{s_{1\ldots m'}}\right)^{m'-1} \hat{P}^{hh'}_{f_1\cdots f_{m'}}\left(\mathscr{C}_{(1\ldots m')\ldots m}\mathcal{T}^{hh'}_{f'f_{m'+1}\cdots f_n}\right) \\
&= \left(\frac{2\mu^{2\epsilon}\,g_s^2}{s_{1\ldots m'}}\right)^{m'-1} \hat{P}^{hh'}_{f_1\cdots f_{m'}}\left(\left(\frac{2\mu^{2\epsilon}\,g_s^2}{s_{(1\ldots m')\ldots m}}\right)^{m-m'} H^{hh';ss'}_{f'f_{m'+1}\cdots f_m}\,\mathcal{T}^{ss'}_{ff_{m+1}\cdots f_n}\right) \\
&= \left(\frac{2\mu^{2\epsilon}\,g_s^2}{s_{1\ldots m'}}\right)^{m'-1}\left(\frac{2\mu^{2\epsilon}\,g_s^2}{s_{(1\ldots m')\ldots m}}\right)^{m-m'} \hat{P}^{hh'}_{f_1\cdots f_{m'}}\,H^{hh';ss'}_{f'f_{m'+1}\cdots f_m}\,\mathcal{T}^{ss'}_{ff_{m+1}\cdots f_n},
\end{aligned}
\tag{4.5}
$$

where f' is the flavour of the sub-parent parton and once again we removed the dependence on momenta for the sake of clarity. Note that between the third and the fourth lines we factorised the tensor $H^{hh';ss'}_{f' f_{m'+1} \cdots f_m}$, which becomes a squared amplitude if we sum over all possible states of the sub-parent parton. We call this tensor the splitting tensor and give more information about it in section 4.3.

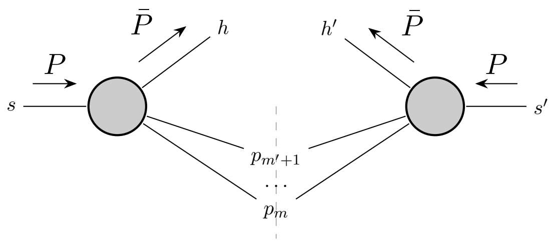

Figure 4.3: Diagrammatic representation of the splitting tensor (the dotted line indicates that we sum over all states

Putting together the developments of both sides of eq. (4.3), we finally get

$$\mathscr{C}_{1\ldots m'} \hat{P}^{ss'}_{f_1 \cdots f_m} = \left(\frac{s_{(1\ldots m')\ldots m}}{s_{1\ldots m'}} \right)^{m'-1} \hat{P}^{hh'}_{f_1 \cdots f_{m'}} \, H^{hh';ss'}_{f' f_{m'+1} \cdots f_m}. \tag{4.6}$$

This formula directly gives the collinear limit of a collinear splitting function, hence what we called the sub-collinear limit.

4.3. Splitting tensor

In this section, we give some more details on the new function appearing in eq. (4.6), the splitting tensor $H^{hh' ss'}_{f' f_{m'+1} \cdots f_m}$. We hence aim at proving the following identity:

$$\mathscr{C}_{(1\ldots m')\ldots m} \mathcal{T}^{hh'}_{f' f_{m'+1} \cdots f_n} = \left(\frac{2\mu^{2\epsilon} g_s^2}{s_{(1\ldots m')\ldots m}} \right)^{m-m'} H^{hh';ss'}_{f' f_{m'+1} \cdots f_m} \, \mathcal{T}^{ss'}_{f f_{m+1} \cdots f_n}, \tag{4.7}$$

as well as providing more context for the splitting tensor. Note that once again, we removed the dependence on the momenta of the partons in order to not overload the notations. Actually, we will rather prove a more general version of eq. (4.7):

$$\mathscr{C}_{1\ldots m}\mathcal{T}^{hh'}_{f_1\cdots f_n} = \left(\frac{2\mu^{2\epsilon}\,g_s^2}{s_{1\ldots m}}\right)^{m-1} H^{hh';ss'}_{f_1\cdots f_m}\,\mathcal{T}^{ss'}_{ff_{m+1}\cdots f_n}, \tag{4.8}$$

giving the collinear limit (for partons 1 to m being collinear) of the helicity tensor $\mathcal{T}^{hh'}_{f_1\cdots f_n}$, which is just the squared amplitude on an n-parton QCD process with the spin indices of parton 1, h and h', open. The indices s and s' are then the spin indices of the parent parton. Since we can obtain a squared amplitude from the tensor $\mathcal{T}^{hh'}_{f_1\cdots f_n}$ just by summing over the indices of parton 1, we get from eq. (4.8) and eq. (2.16) that the splitting tensor is simply a splitting function with one extra open leg (the one of parton 1):

$$\delta^{hh'} H^{hh';ss'}_{f_1\cdots f_m} = \hat{P}^{ss'}_{f_1\cdots f_m}. \tag{4.9}$$

We start the proof in the same fashion as the proof of the factorisation of squared amplitudes (see section 2.4). For the same reason as in that case, in a physical gauge, only diagrams with a propagator carrying the momentum of the parent parton will contribute at leading order. Indeed, the non-contraction of the spin indices of parton 1 does not invalidate any of the arguments used in the proof. This immediately leads to the following result:

$$\begin{aligned}
&\mathscr{C}_{1\ldots m}\mathcal{T}^{hh'}_{f_1\cdots f_n} \\
&\quad = \mathscr{C}_{1\ldots m}\left[\left(\frac{2\mu^{2\epsilon}g_s^2}{s_{1\ldots m}}\right)^{m-1}\left[\mathcal{M}^{(n)s}_{ff_{m+1}\cdots f_n}\right]^* H^{(n)hh';ss'}_{f_1\cdots f_m}\,\mathcal{M}^{(n)s'}_{ff_{m+1}\cdots f_n}\right] \\
&\quad = \left(\frac{2\mu^{2\epsilon}g_s^2}{s_{1\ldots m}}\right)^{m-1}\left(\mathscr{C}_{1\ldots m}\,H^{(n)hh';ss'}_{f_1\cdots f_m}\right)\mathcal{T}^{ss'}_{ff_{m+1}\cdots f_n} \\
&\quad = \left(\frac{2\mu^{2\epsilon}g_s^2}{s_{1\ldots m}}\right)^{m-1} H^{hh';ss'}_{f_1\cdots f_m}\,\mathcal{T}^{ss'}_{ff_{m+1}\cdots f_n},
\end{aligned} \tag{4.10}$$

where the function $H^{(n)hh';ss'}_{f_1\cdots f_m}$ is simply the sum of the interferences of all diagrams that split the parent parton into the m collinear ones, while keeping the spin indices of both parton 1 and the parent parton open (their respective spin indices being (h, h') and (s, s')). Equation (4.10) shows that $\mathcal{T}^{hh'}_{f_1 \cdots f_n}$ factorises in the collinear limit but does not give any information about $H^{(n)hh';ss'}_{f_1 \cdots f_m}$.

We now separate different cases according to the nature of parton 1 and the parent parton:

1. both the parent parton and parton 1 are quarks,
2. the parent parton is a gluon and parton 1 is a quark,
3. the parent parton is a quark and parton 1 is a gluon,
4. both the parent parton and parton 1 are gluons.

For cases 1 and 2, the sub-parent parton is a quark, i.e. $f' = q$, and we know that the splitting function has trivial spin correlations. Hence, we can further simplify eq. (4.6):

$$\begin{aligned}
\mathscr{C}_{1 \dots m'} \hat{P}^{ss'}_{f_1 \cdots f_m} &= \left(\frac{s_{(1 \dots m') \dots m}}{s_{1 \dots m'}} \right)^{m'-1} \hat{P}^{hh'}_{f_1 \cdots f_{m'}} \, H^{hh';ss'}_{q f_{m'+1} \cdots f_m} \\
&= \left(\frac{s_{(1 \dots m') \dots m}}{s_{1 \dots m'}} \right)^{m'-1} \langle \hat{P}_{f_1 \dots f_{m'}} \rangle \, \delta^{hh'} \, H^{hh';ss'}_{q f_{m'+1} \cdots f_m} \\
&= \left(\frac{s_{(1 \dots m') \dots m}}{s_{1 \dots m'}} \right)^{m'-1} \langle \hat{P}_{f_1 \dots f_{m'}} \rangle \, \hat{P}^{ss'}_{q f_{m'+1} \cdots f_m} . \qquad (4.11)
\end{aligned}$$

This proves that quark-initiated splitting functions factorise as two splitting functions in the sub-collinear limit and we do not need any new function to describe that limit. For case 1, as the parent parton is a quark (with trivial spin correlations), eq. (4.6) can be written to involve only scalar quantities:

$$\mathscr{C}_{1 \dots m'} \langle \hat{P}_{f_1 \dots f_m} \rangle = \left(\frac{s_{(1 \dots m') \dots m}}{s_{1 \dots m'}} \right)^{m'-1} \langle \hat{P}_{f_1 \dots f_{m'}} \rangle \, \langle \hat{P}_{q f_{m'+1} \cdots f_m} \rangle , \qquad (4.12)$$

whereas in case 2, with a gluon as the parent parton, the factorisation involves a scalar quantity multiplying a rank two Lorentz tensor:

$$\mathscr{C}_{1\dots m'}\hat{P}^{\mu\nu}_{f_1\cdots f_m} = \left(\frac{s_{(1\dots m')\dots m}}{s_{1\dots m'}}\right)^{m'-1} \langle \hat{P}_{f_1\cdots f_{m'}}\rangle\,\hat{P}^{\mu\nu}_{qf_{m'+1}\cdots f_m}. \tag{4.13}$$

In cases 3 and 4, where parton 1 is a gluon, spin correlations are not so simple and the factorisation necessarily involves a tensor product. For case 3, as the parent parton is a quark (and there is as such no spin correlations), the splitting tensor is of rank 2 and its indices are contracted with those of the splitting function:

$$\mathscr{C}_{1\dots m'}\langle\hat{P}_{f_1\dots f_m}\rangle = \left(\frac{s_{(1\dots m')\dots m}}{s_{1\dots m'}}\right)^{m'-1} \hat{P}^{\mu\nu}_{f_1\cdots f_{m'}}\;H^{\mu\nu}_{gf_{m'+1}\cdots f_m}, \tag{4.14}$$

where $H^{\mu\nu}_{gf_{m'+1}\cdots f_m}$ is defined by $H^{\mu\nu;ss'}_{gf_{m'+1}\cdots f_m} = \delta^{ss'}H^{\mu\nu}_{gf_{m'+1}\cdots f_m}$. Finally, in case 4, with both the parent and parton 1 being gluons, the splitting tensor is of rank 4:

$$\mathscr{C}_{1\dots m'}\hat{P}^{\mu\nu}_{f_1\cdots f_m} = \left(\frac{s_{(1\dots m')\dots m}}{s_{1\dots m'}}\right)^{m'-1} \hat{P}^{\rho\sigma}_{f_1\cdots f_{m'}}\;H^{\rho\sigma;\mu\nu}_{gf_{m'+1}\cdots f_m}. \tag{4.15}$$

Hence, the only cases that involve new objects are cases 3 and 4, and we are left to detail the tensor structure of $H^{\mu\nu}_{gf_{m'+1}\cdots f_m}$ and $H^{\rho\sigma;\mu\nu}_{gf_{m'+1}\cdots f_m}$.

To describe the tensor structure of the splitting tensors, we go back to eq. (4.10) and start by showing the structure of $H^{(n)hh';ss'}_{gf_2\cdots f_m}$. The first thing to notice for both case 3 and 4 is that, because splitting functions have no dimension (in units of energy), eq. (4.6) immediately show that neither do splitting tensors (and thus neither do the function $H^{(n)hh';ss'}_{gf_2\cdots f_m}$). In addition, due to the factorised pre-factor, and the fact that splitting functions are of order zero in the scaling parameter λ, $H^{(n)hh';ss'}_{gf_2\cdots f_m}$ must be of order zero in both λ and $\bar{\lambda}$.

Hence, in a very similar way to the way we computed splitting functions, we will square the sum of all diagrams splitting the parent parton into m

partons, with the difference that we do not sum over all possible states for parton 1. In case 3, the generic expression for the tensor $H^{(n)hh';ss'}_{gf_2\cdots f_m}$ has two Lorentz indices and can only depend on the momenta of the collinear partons:

$$H^{(n)\mu\nu}_{gf_2\cdots f_m} = \bar{A}\; g^{\mu\nu} \;+\; \bar{B}_{ij}\; \frac{p_i^\mu p_j^\nu}{s_{1\ldots m}} \;+\; \text{n-terms}, \tag{4.16}$$

where n-terms stand for terms that are proportional either to n^μ or n^ν and the p_i stand for the collinear momenta. As for the splitting functions, we add some sub-energies in the denominator such that the scalar factors $\bar{A}$ and $\bar{B}_{ij}$ are scaleless and so, by the same argument, they are of order zero in the limit. Note that we also used the fact that this tensor must be symmetric under the exchange $\mu \leftrightarrow \nu$ (which means that $\bar{B}_{ij}$ is symmetric under $i \leftrightarrow j$). We now add a spin-polarisation tensor on each side to project the tensor to the transverse space:

$$d_{\mu\rho}(p_1,n)\; H^{(n)\rho\sigma}_{gf_2\cdots f_m}\; d_{\sigma\nu}(p_1,n). \tag{4.17}$$

Because n is orthogonal to the spin-polarisation tensor, all n-terms disappear, while the other tensor structures become

$$\begin{aligned} d^{\mu\rho}(p_1,n) g_{\rho\sigma} d^{\sigma\nu}(p_1,n) &= -d^{\mu\nu}(p,n) + \mathcal{O}(\lambda^2), \\ d_{\mu\rho}(p_1,n) p_{i,\rho} &= -\tilde{k}_i^\mu + \frac{z_i}{z_1}\; \tilde{k}_1^\mu + \mathcal{O}(\lambda^2). \end{aligned} \tag{4.18}$$

With that at hand, we know that, in the limit, $H^{\mu\nu}_{gf_2\cdots f_m}$ can be build from two tensor structures: $d^{\mu\nu}(p,n)$ and $\tilde{k}_i^\mu \tilde{k}_j^\nu$, with i and j in $\{1,\ldots,m\}$. In the end, the general structure of the splitting tensor for a quark parent (case 3) is

$$H^{\mu\nu}_{gf_2\cdots f_m} = A\; d^{\mu\nu}(p,n) \;+\; B_{ij}\; \frac{\tilde{k}_i^\mu \tilde{k}_j^\nu}{s_{1\ldots m}}. \tag{4.19}$$

The exact same argument can be repeated for case 4 (gluon parent) only with 4 Lorentz indices. We then get the most general tensor structure before the limit is taken:

$$\begin{aligned} H^{(n)\rho\sigma;\mu\nu}_{gf_2\cdots f_m} = \bar{A}\; g^{\rho\sigma} g^{\mu\nu} &+ \bar{B}_{ij}\; \frac{p_i^\mu p_j^\nu}{s_{1\ldots m}}\, g^{\rho\sigma} + \bar{C}_{ij}\; \frac{p_i^\rho p_j^\sigma}{s_{1\ldots m}}\, g^{\mu\nu} + \bar{D}_{ijkl}\; \frac{p_i^\mu p_j^\nu p_k^\rho p_l^\sigma}{s^2_{1\ldots m}} \\ &+ \bar{E}_{1\,ij}\; \frac{g^{\mu\rho}\, p_i^\nu p_j^\sigma + g^{\nu\sigma}\, p_i^\mu p_j^\rho}{s_{1\ldots m}} + \bar{E}_{2\,ij}\; \frac{g^{\nu\rho}\, p_i^\mu p_j^\sigma + g^{\mu\sigma}\, p_i^\nu p_j^\rho}{s_{1\ldots m}} \\ &+ \bar{F}_1\; g^{\mu\rho} g^{\nu\sigma} + \bar{F}_2\; g^{\nu\rho} g^{\mu\sigma} + \text{n-terms}, \end{aligned} \tag{4.20}$$

where we used the fact that this tensor needs to be symmetric if we exchange at the same time the indices of the parent parton and parton 1 (i.e. $\mu \leftrightarrow \nu$ and $\rho \leftrightarrow \sigma$). By the same argument as before, the coefficients $\bar{A}$ through $\bar{F}_2$ in eq. (4.20) are dimensionless and of order zero in the collinear limit. In addition, we have the following symmetries, which follow directly from the symmetry of the tensor:

$$\begin{aligned} \bar{B}_{ij} &= \bar{B}_{ji}, \\ \bar{C}_{ij} &= \bar{C}_{ji}, \\ \bar{D}_{ijkl} &= \bar{D}_{jilk}. \end{aligned} \tag{4.21}$$

As for the previous case, since only the transverse part of this tensor carries physical information, we now multiply this tensor by spin-polarisation tensors for parton 1, as well as spin-polarisation tensors for the parent parton (as we did for splitting functions):

$$d_{\mu\tilde{\mu}}(P,n)\; d_{\nu\tilde{\nu}}(P,n)\; d_{\rho\tilde{\rho}}(p_1,n)\; d_{\sigma\tilde{\sigma}}(p_1,n)\; H^{(n)\tilde{\rho}\tilde{\sigma};\tilde{\mu}\tilde{\nu}}_{gf_2\cdots f_m}. \tag{4.22}$$

In addition to the previous identities, we note the following results:

$$\begin{aligned} d^{\mu\nu}(P,n)P_\nu &= \mathcal{O}(\lambda^2), \\ d^{\mu\nu}(p_1,n)P_\nu &= -\frac{1}{z_1}\,\tilde{k}_1^\mu + \mathcal{O}(\lambda^2), \\ d^\mu_\nu(P,n)p_i^\nu &= -\tilde{k}_i^\mu + \mathcal{O}(\lambda^2). \end{aligned} \tag{4.23}$$

Furthermore, we can take into account that in eq. (4.10) the splitting tensor is contracted with the symmetric tensor $\mathcal{T}^{\mu\nu}_{ff_{m+1}\cdots f_n}$, which allows us to discard terms in $H^{\rho\sigma;\mu\nu}_{gf_2\cdots f_m}$ that are anti-symmetric under the exchange $\mu \leftrightarrow \nu$. This leads to the following expression for the splitting tensor:

$$\begin{aligned} &H^{\rho\sigma;\mu\nu}_{gf_2\cdots f_m} \\ &\quad = -A\; d^{\rho\sigma}\, d^{\mu\nu} \;+ B_{ij}\;\frac{\tilde{k}_i^\mu\tilde{k}_j^\nu}{s_{1\ldots m}}\, d^{\rho\sigma} - C_{ij}\;\frac{\tilde{k}_i^\rho\tilde{k}_j^\sigma}{s_{1\ldots m}}\, d^{\mu\nu} + D_{ijkl}\;\frac{\tilde{k}_i^\mu\tilde{k}_j^\nu\tilde{k}_k^\rho\tilde{k}_l^\sigma}{s^2_{1\ldots m}} \\ &\qquad - E_{ij}\;\frac{d^{\mu\rho}\,\tilde{k}_i^\nu\tilde{k}_j^\sigma + d^{\nu\sigma}\,\tilde{k}_i^\mu\tilde{k}_j^\rho + d^{\nu\rho}\,\tilde{k}_i^\mu\tilde{k}_j^\sigma + d^{\mu\sigma}\,\tilde{k}_i^\nu\tilde{k}_j^\rho}{s_{1\ldots m}} \\ &\qquad + F\;\left(d^{\mu\rho}\, d^{\nu\sigma} + d^{\nu\rho}\, d^{\mu\sigma}\right), \end{aligned} \tag{4.24}$$

where we have suppressed the dependence of the spin-polarisation tensor on the vectors p and n. The scalar coefficients appearing in eq. (4.24) are linear combinations of the coefficients in eq. (4.20). To keep the symmetry of this expression, the coefficients now satisfy

$$\begin{aligned} \bar{B}_{ij} &= \bar{B}_{ji}, \\ \bar{C}_{ij} &= \bar{C}_{ji}, \\ \bar{D}_{ijkl} = \bar{D}_{jikl} &= \bar{D}_{ijlk} = \bar{D}_{jilk}. \end{aligned} \tag{4.25}$$

The tensor structure given in eq. (4.24) involves only polarisation tensors, which makes the splitting tensor explicitly transverse. However, similar to the case of the splitting amplitude discussed in Chapter 2, some of the gauge-dependent terms drop out in the contraction in eq. (4.5). In particular, we can perform the following replacements:

$$d^{\alpha\beta}(p,n) \leftrightarrow -g^{\alpha\beta}\,, \quad (\alpha,\beta) \in \{(\mu,\nu),(\mu,\rho),(\mu,\sigma),(\nu,\rho),(\nu,\sigma)\}. \tag{4.26}$$

For $(\alpha,\beta)=(\mu,\nu)$, the equivalence between the polarisation tensor and the metric tensor follows directly from the contraction with the transverse tensor $\mathcal{T}^{\mu\nu}_{ff_{m+1}\cdots f_n}$, while the other cases follow from relations like

$$\begin{aligned} \hat{P}^{\rho\sigma}_{f_1\cdots f_{m'}}\, d_{\mu\rho}(p,n)\, d_{\nu\sigma}(p,n)\, \mathcal{T}^{\mu\nu}_{ff_{m+1}\cdots f_n} &= \hat{P}^{\rho\sigma}_{f_1\cdots f_{m'}}\, g_{\mu\rho}\, g_{\nu\sigma}\, \mathcal{T}^{\mu\nu}_{ff_{m+1}\cdots f_n}\,, \\ \hat{P}^{\rho\sigma}_{f_1\cdots f_{m'}}\, d_{\mu\rho}(p,n)\, \tilde{k}_{i,\sigma}\tilde{k}_{j,\nu}\, \mathcal{T}^{\mu\nu}_{ff_{m+1}\cdots f_n} &= -\hat{P}^{\rho\sigma}_{f_1\cdots f_{m'}}\, g^{\mu\rho}\, \tilde{k}_{i,\sigma}\tilde{k}_{j,\nu}\, \mathcal{T}^{\mu\nu}_{ff_{m+1}\cdots f_n}. \end{aligned} \tag{4.27}$$

Finally, we end up with the most general tensor structure for the splitting tensor in case 4:

$$\begin{aligned} H^{\rho\sigma;\mu\nu}_{gf_2\dots f_m} &= A\ d^{\rho\sigma}\, g^{\mu\nu} \ + B_{ij}\ \frac{\tilde{k}_i^\mu \tilde{k}_j^\nu}{s_{1\dots m}}\, d^{\rho\sigma} + C_{ij}\ \frac{\tilde{k}_i^\rho \tilde{k}_j^\sigma}{s_{1\dots m}}\, g^{\mu\nu} + D_{ijkl}\ \frac{\tilde{k}_i^\mu \tilde{k}_j^\nu \tilde{k}_k^\rho \tilde{k}_l^\sigma}{s_{1\dots m}^2} \\ &\quad + E_{ij}\ \frac{g^{\mu\rho}\, \tilde{k}_i^\nu \tilde{k}_j^\sigma + g^{\nu\sigma}\, \tilde{k}_i^\mu \tilde{k}_j^\rho + g^{\nu\rho}\, \tilde{k}_i^\mu \tilde{k}_j^\sigma + g^{\mu\sigma}\, \tilde{k}_i^\nu \tilde{k}_j^\rho}{s_{1\dots m}} \\ &\quad + F\ \left(g^{\mu\rho}\, g^{\nu\sigma} + g^{\nu\rho}\, g^{\mu\sigma}\right)\,. \end{aligned} \tag{4.28}$$

4.4. Parametrisation of the sub-collinear limit

In the sub-collinear limit, each of the collinear momenta still follows the parametrisation of eq. (2.11), namely:

$$p_i = z_i P + \tilde{k}_i + \mathcal{O}(\tilde{k}^2) \qquad\qquad i = 1, \ldots, m. \tag{4.29}$$

Note that we use this parametrisation instead of eq. (2.5) as it uses directly the variables that appear in the splitting functions, and remember that the last term is proportional to n. As we now consider the first m' partons to undergo a second collinear limit, their momenta obey another parametrisation,

$$p_i = \bar{z}_i \bar{P} + \tilde{\kappa}_i + \mathcal{O}(\tilde{\kappa}^2) \qquad\qquad i = 1, \ldots, m'. \tag{4.30}$$

In eq. (4.30), the new variables are defined in a similar fashion as for the parametrisation of the collinear limit, only for this new limit with $\bar{P} = \sum_{i=1}^{m'} p_i$, the momentum of the sub-parent parton. One could worry that we need to introduce a new vector n (which appear in the last term that we did not mention here) for the sub-collinear limit, but it is not the case. Indeed, the only specification for this light-like vector was that it should not be orthogonal to p, the collinear direction, $n \cdot p \neq 0$. However, since n is orthogonal to k_i and itself, this inequality implies that any p_i is also not orthogonal to n ($n \cdot p_i = x_i \; n \cdot p$). Hence, n is not orthogonal to $\bar{P}$ and can be used in the sub-collinear limit as well.

In eq. (4.30), the only unknowns left are $\bar{z}_i$ and $\tilde{\kappa}_i$. To find an explicit expression for these variables, one simply writes $\tilde{\kappa}_i$ as a linear combination of the generating set $\{P, \tilde{k}_i, n\}$:

$$\tilde{\kappa}_i = \alpha_i P + \beta_{ij} \tilde{k}_j + \gamma_i n, \tag{4.31}$$

where we sum over $j = m' + 1, \ldots, m$. Immediately, from the fact that $\tilde{\kappa}_i$ should be orthogonal to n, one deduces that α_i is zero. Then, one can insert eq. (4.31) into eq. (4.30), and identify the factors to those in eq. (4.29). To do so, the only missing information is the expression of $\bar{P}$

in term of P:

$$\begin{aligned}
\bar{P} &= \sum_{j=1}^{m'} p_j \\
&= P - \sum_{j=m'+1}^{m} p_j \\
&= P - \sum_{j=m'+1}^{m} \left(z_j P + \tilde{k}_j + \mathcal{O}(\tilde{k}^2) \right) \\
&= \left(1 - \sum_{j=m'+1}^{m} z_j \right) P - \sum_{j=m'+1}^{m} \tilde{k}_j + \mathcal{O}(\tilde{k}^2). \qquad (4.32)
\end{aligned}$$

Following the procedure we just described, we find

$$\begin{aligned}
p_i &= \bar{z}_i \bar{P} + \tilde{\kappa}_i + \mathcal{O}(\tilde{\kappa}^2) \\
&= \bar{z}_i \left(\left(1 - \sum_{j=m'+1}^{m} z_j \right) P - \sum_{j=m'+1}^{m} \tilde{k}_j \right) + \beta_{ij} \tilde{k}_j + \gamma_i n + \mathcal{O}(\tilde{\kappa}^2) \\
&= z_i P + \tilde{k}_i + \mathcal{O}(\tilde{k}^2), \qquad (4.33)
\end{aligned}$$

from which we deduce

$$\bar{z}_i = \frac{z_i}{1 - \sum_{j=m'+1}^{m} z_j}, \qquad (4.34)$$

as well as

$$\beta_{ij} \tilde{k}_j = \tilde{k}_i + \bar{z}_i \sum_{j=m'+1}^{m} \tilde{k}_j. \qquad (4.35)$$

In principle, all we have do to now is to find the value of γ_i. Although it is actually quite feasible, for example by imposing $\tilde{\kappa}_i$ to be orthogonal to the sub-collinear direction, we will not even do it since, as it will be shown later on, it is not useful and the exact value of γ_i will never be of any relevance.

We now go back to eq. (4.6) and analyse both sides. On the left hand side, we have the sub-collinear limit of a m-parton splitting functions, which depends on variables z_i, s_{ij}, and $\tilde{k}_i$ for i and j from 1 to m. Once we use the parametrisation we just established, the z_i for $i = 1, \ldots, m'$ will transform according to eq. (4.34) to become

$$z_i = \bar{z}_i \left(1 - \sum_{i=m'+1}^{m} z_i \right), \tag{4.36}$$

while the other z_i (for $i = m'+1, \ldots, m$) remain as such. In a similar fashion, following eq. (4.35), we replace $\tilde{k}_i$ by

$$\tilde{k}_i = \tilde{\kappa} - \bar{z}_i \sum_{j=m'+1}^{m} \tilde{k}_j - \gamma_i n, \tag{4.37}$$

for $i = 1, \ldots, m'$ and we leave it as such for $i = m'+1, \ldots, m$. For the sub-energies s_{ij}, there are three cases to consider. First, if both i and j are not in the sub-collinear set $\{1, \ldots, m'\}$, we use the expression given by eq. (2.8):

$$s_{ij} = -z_i z_j \left(\frac{\tilde{k}_i}{z_i} - \frac{\tilde{k}_j}{z_j} \right)^2. \tag{4.38}$$

If both i and j are in the sub-collinear set $\{1, \ldots, m'\}$, the expression is simply the mirror of the last case with sub-collinear variables:

$$s_{ij} = -\bar{z}_i \bar{z}_j \left(\frac{\tilde{\kappa}_i}{\bar{z}_i} - \frac{\tilde{\kappa}_j}{\bar{z}_j} \right)^2 = -\frac{\bar{z}_j}{\bar{z}_i} \tilde{\kappa}_i^2 + 2\bar{\kappa}_i \cdot \bar{\kappa}_j - \frac{\bar{z}_i}{\bar{z}_j} \tilde{\kappa}_j^2. \tag{4.39}$$

Finally, if i is in the sub-collinear set but j is not, the result is less trivial. We start from eq. (2.8) and use the transformation rules for z_i and κ_i (eq. (4.34) and eq. (4.35)):

$$\begin{aligned}
s_{ij} &= -z_i z_j \left(\frac{\tilde{k}_i}{z_i} - \frac{\tilde{k}_j}{z_j} \right)^2 \\
&= -\bar{z}_i \left(1 - \sum_{l=m'+1}^{m} z_l \right) z_j \Bigg(\frac{\tilde{\kappa}_i}{\bar{z}_i \left(1 - \sum_{l=m'+1}^{m} z_l\right)} \\
&\qquad\qquad - \frac{\sum_{l=m'+1}^{m} \tilde{k}_l}{\left(1 - \sum_{l=m'+1}^{m} z_l\right)} - \frac{\tilde{k}_j}{z_j} - \frac{\gamma_i}{z_i} n \Bigg)^2 \\
&= -\frac{\bar{z}_i \left(1 - \sum_{l=m'+1}^{m} z_l\right)}{z_j} \tilde{k}_j^2 - 2\bar{z}_i \tilde{k}_j \cdot \left(\sum_{l=m'+1}^{m} \tilde{k}_l \right) \\
&\quad - \frac{\bar{z}_i z_j}{\left(1 - \sum_{l=m'+1}^{m} z_l\right)} \left(\sum_{l=m'+1}^{m} \tilde{k}_l \right)^2 + 2\tilde{\kappa}_i \cdot \tilde{k}_j \\
&\quad + 2 \frac{z_j}{\left(1 - \sum_{l=m'+1}^{m} z_l\right)} \tilde{\kappa}_i \cdot \left(\sum_{l=m'+1}^{m} \tilde{k}_l \right) - \frac{z_j}{\bar{z}_i \left(1 - \sum_{l=m'+1}^{m} z_l\right)} \tilde{\kappa}_i^2 .
\end{aligned} \tag{4.40}$$

Note that this expression does not depend on γ_i, since n is orthogonal to all the vectors involved in the square.

Taking the sub-collinear limit of the splitting function as in the left hand side of eq. (4.6) is now only a matter of making these replacements, rescaling $\tilde{\kappa}_i$ as $\bar{\lambda}\tilde{\kappa}_i$ and keeping only the leading term in $\bar{\lambda}$.

4.5. Summary and results

In this chapter, we introduced the sub-collinear limit which allowed us to consider collinear limits of splitting functions. Our results show that splitting functions factorise in this limit in a way that is highly reminiscent of the factorisation of squared amplitudes in the collinear limit. This should not come as a surprise since we showed in Chapter 2 that one can compute splitting functions as the limit of a squared amplitude, with open spin indices for the parent parton. In addition, we encountered new building blocks in these factorisations, that we called splitting tensors, and described their possible tensor structure, according to the nature of the parent and sub-parent partons. For this thesis, we computed all the triple collinear splitting tensors and then checked every possible sub-collinear limit for the quadruple collinear splitting functions and found all of them to match the expected results.

5 | Soft-Collinear Limit

After exploring the collinear limits of splitting functions, that we called sub-collinear limits, we now turn our attention to the soft collinear limits of splitting functions, dubbed soft-collinear limits. We remind that the soft limit is simply the limit in which one or more partons have vanishing energies. In the same stream of ideas as the sub-collinear limit, we expect the splitting functions to behave similarly to squared amplitudes in this limit.

Our interest in such a limit is exactly the same as it was for the sub-collinear limit too: to provide another sanity check of our results on the quadruple collinear splitting functions, as well as explore this corner of phase-space to allow the building of counter-terms to subtract the infrared divergences in higher-order computations.

This chapter first introduces formally the concept of soft limit, and especially the soft limit of squared amplitudes. In particular, we focus on the single and double soft limits, which are the only non trivial limits for quadruple splitting functions. Afterwards, we prove and formulate how splitting functions factorise in the single and double soft limits. Finally, we apply these formula to our specific results.

5.1. Colour algebra

In this chapter, we use a slightly different notation than what we introduced in Chapter 1, which is more convenient for the colour correlations that appear in soft limits. We introduce the colour charge of parton i with colour c, $\mathbf{T}_i^c$, which is the *SU(N)* generator in the representation of the parton i. This means that we have $(\mathbf{T}_i^c)_{ab} = \mathbf{T}^c_{a_i b_i} = T^c_{a_i b_i}$ if parton i is a quark, $(\mathbf{T}_i^c)_{ab} = -T^c_{b_i a_i}$ if parton i is an anti-quark, and $(\mathbf{T}_i^c)_{ab} = i f^{a_i c b_i}$ if parton i is a gluon. In these notations, we define a product of colour charges as

$$\mathbf{T}_i \cdot \mathbf{T}_j = \sum_c \mathbf{T}_i^c \cdot \mathbf{T}_j^c, \tag{5.1}$$

where the index c runs up to the number of colour degrees of freedom in the representation of partons i and j. This product of colour charges satisfy the following algebra:

$$\mathbf{T}_i \cdot \mathbf{T}_j = \mathbf{T}_j \cdot \mathbf{T}_i \qquad \text{if } i \neq j, \qquad \mathbf{T}_i \cdot \mathbf{T}_i = \mathbf{T}_i^2 = \mathcal{C}_i, \tag{5.2}$$

where $\mathcal{C}_i$ is the Casimir of representation i. With full indices, these relations read

$$\sum_c \mathbf{T}^c_{a_i b_i} \mathbf{T}^c_{a_j b_j} = \sum_c \mathbf{T}^c_{a_j b_j} \mathbf{T}^c_{a_i b_i} \qquad \text{if } i \neq j, \qquad \sum_c \mathbf{T}^c_{a_i b_i} \mathbf{T}^c_{b_i c_i} = \mathcal{C}_i \delta_{a_i c_i}. \tag{5.3}$$

5.2. Soft limit of amplitudes and squared amplitudes

Before turning to the main subject of this chapter, the soft-collinear limit, we first review the soft limit. We consider here a QCD process with n particles, amongst which m are soft ($m \leq n-2$), meaning they have vanishing energy. This limit is simply evaluated by rescaling all the soft momenta as

$$p_i \to \lambda p_i \qquad i = 1, \ldots, m, \tag{5.4}$$

and taking λ to zero, such that all soft momenta approach zero at the same rate. In these conditions, the amplitude for such a process is divergent and behaves in the soft limit as

$$\mathscr{S}_{1\dots m}\mathcal{M}^{c_1\dots c_n;s_1\dots s_n}_{f_1\dots f_n}(p_1,\dots,p_n) = \mathbf{J}^{c_1\dots c_m;s_1\dots s_m}\mathcal{M}^{c_{m+1}\dots c_n;s_{m+1}\dots s_n}_{f_{m+1}\dots f_n}(p_{m+1},\dots,p_n)\,, \quad (5.5)$$

where $\mathscr{S}_{1\dots m}$ denotes the operation of keeping only the leading pole in the Laurent series in λ, in a very similar way as $\mathscr{C}_{1\dots m}$ works for the collinear limit. The amplitude on the right hand side $\mathcal{M}^{c_{m+1}\dots c_n;s_{m+1}\dots s_n}_{f_{m+1}\dots f_n}$ is simply the same as the one the left hand side but stripped of all the soft partons and is called the hard amplitude. The soft current $\mathbf{J}^{c_1\dots c_m;s_1\dots s_m}$ is an operator in colour space that maps the colour space of the hard partons to the total colour space of both the soft and hard partons (note that we refer here to all the partons which are not soft as hard partons). This current is also depending on the spin of the soft partons, the momenta of both the soft and hard partons, and the flavours of the soft partons (though we do not show that dependence explicitly). The soft current has been computed at tree level for the emission of up to three soft partons [58, 68, 87, 88].

We can also consider the soft current with all the polarisation vectors of the external gluons removed, i.e.

$$\mathbf{J}^{c_1\dots c_m;s_1\dots s_m} \equiv \varepsilon^{s_1}_{\nu_1}(p_1,n)\dots\varepsilon^{s_m}_{\nu_m}(p_m,n)\,\mathbf{J}^{c_1\dots c_m;\nu_1\dots\nu_m}. \quad (5.6)$$

It is then expected that the soft current $\mathbf{J}^{c_1\dots c_m;\nu_1\dots\nu_m}$ is gauge invariant, in the sense that it is transverse to any soft gluon momentum, up to colour conservation in the hard amplitude:

$$p_k^{\nu_k}\,\mathbf{J}^{c_1\dots c_k\dots c_m}_{\nu_1\dots\nu_k\dots\nu_m} = 0 \mod \sum_{i=m+1}^{n}\mathbf{T}_i^c = 0\,. \quad (5.7)$$

Equation (5.7) is known to hold for $m = 2$ [58] and for $m = 3$ [68], and conjectured to hold for any m [68].

The soft current for the emission of a single soft gluon is

$$\mathbf{J}^{c;s}(p_1) = \mu^\epsilon g_s\,\varepsilon^s_\nu(p_1,n)\sum_{i=2}^{n}\mathbf{T}_i^c\,\frac{p_i^\nu}{p_i\cdot p_1}, \quad (5.8)$$

where the sum runs over the $n-1$ hard partons. Eq. (5.8) essentially is the emission of the soft gluon from any hard leg. This current is manifestly gauge invariant, up to colour conservation in the hard amplitude:

$$p_1^\nu \, \mathbf{J}_\nu^c = \mu^\epsilon g_s \sum_{i=2}^{n} \mathbf{T}_i^c = 0. \tag{5.9}$$

Since the soft current is transverse, we can drop all gauge-dependent terms when squaring the amplitude. Hence, we obtain for a single soft gluon in a squared amplitude (without loss of generality, the soft gluon is parton 1):

$$\mathscr{S}_1 |\mathcal{M}_{g_1 f_2 \dots f_n}|^2 = \mu^{2\epsilon} g_s^2 \sum_{j,k=2}^{n} \mathcal{S}_{jk}(p_1) \left[\mathcal{M}_{f_2 \dots f_n}^{c_2 \dots c_j' \dots c_k \dots c_n; s_2 \dots s_n} \right]^* \mathbf{T}_{c_j' c_j}^{c_1} \mathbf{T}_{c_k c_k'}^{c_1} \mathcal{M}_{f_2 \dots f_n}^{c_2 \dots c_j \dots c_k' \dots c_n; s_2 \dots s_n}, \tag{5.10}$$

where we introduced the so-called *eikonal factor*,

$$\mathcal{S}_{jk}(p_1) = -\frac{2\, s_{jk}}{s_{1j} s_{1k}}. \tag{5.11}$$

Eq. (5.10) shows that in the single soft gluon limit, each of the two amplitudes emits a soft gluon from an hard leg (the hard legs being respectively labeled j and k) and the two soft gluons are colour-correlated to each other. Then, one needs to sum over all possible pair $\{j, k\}$ of hard partons.

Next, we examine the double soft parton cases: a soft pair of quarks or two soft gluons. We first consider the case of a soft pair of a quark of momentum p_1 and an antiquark of momentum p_2. In this limit, the squared amplitude factorises as [58]

$$\mathscr{S}_{12}^{q\bar{q}} |\mathcal{M}_{q_1 \bar{q}_2 f_3 \dots f_n}|^2 = (\mu^{2\epsilon} g_s^2)^2 \sum_{j,k=3}^{n} \mathcal{S}_{jk}^{q\bar{q}}(p_1, p_2) \left[\mathcal{M}_{f_3 \dots f_n}^{c_3 \dots c_j' \dots c_k \dots c_n; s_3 \dots s_n} \right]^* \mathbf{T}_{c_j' c_j}^{c_{12}} \mathbf{T}_{c_k c_k'}^{c_{12}} \mathcal{M}_{f_3 \dots f_n}^{c_3 \dots c_j \dots c_k' \dots c_n; s_3 \dots s_n}, \tag{5.12}$$

where c_{12} labels the colour of the gluon which splits into the $q\bar{q}$ pair, and

$$\mathcal{S}^{q\bar{q}}_{jk}(p_1,p_2) = \frac{4T_R}{s_{12}^2}\frac{s_{1j}s_{2k}+s_{1k}s_{2j}-s_{jk}s_{12}}{s_{j(12)}s_{k(12)}}, \tag{5.13}$$

with

$$s_{i(12)} = s_{i1}+s_{i2}. \tag{5.14}$$

We note that the colour correlation is the same as in the single soft gluon case, since the pair of quark is ultimately linked to the rest of the diagram by a single gluon. Due to this fact, eq. (5.12) is highly similar to eq. (5.10).

For the case of two gluons of momenta p_1 and p_2, we separate the formula into an abelian piece and a non-abelian piece. The abelian piece corresponds to the two soft gluons being emitted from different hard partons, while the non-abelian piece adds the possibility that the two gluons come from the same gluon of momentum p_1+p_2. The resulting factorisation is [34, 58]

$$\mathscr{S}^{gg}_{12}|\mathcal{M}_{g_1g_2f_3\cdots f_n}|^2 = \left(\mathscr{S}^{gg,(ab)}_{12}+\mathscr{S}^{gg,(nab)}_{12}\right)|\mathcal{M}_{g_1g_2f_3\cdots f_n}|^2. \tag{5.15}$$

As we described before, the abelian part takes into account the emission of the two soft gluons from two different hard legs and hence has two copies of the eikonal factor, but with colour correlations involving up to four hard partons:

$$\begin{aligned}
&\mathscr{S}^{gg,(ab)}_{12}|\mathcal{M}_{g_1g_2f_3\cdots f_n}|^2 \\
&\quad = (\mu^{2\epsilon}g_s^2)^2\frac{1}{2}\sum_{i,j,k,l=3}^{n}\mathcal{S}_{ik}(p_1)\mathcal{S}_{jl}(p_2)\left[\mathcal{M}^{c_3\cdots c_i'\cdots c_j'\cdots c_k\cdots c_\ell\cdots c_n;s_3\cdots s_n}_{f_3\cdots f_n}\right]^* \\
&\qquad\qquad \left[\mathbf{T}^{c_1}_{c_i'c_i}\mathbf{T}^{c_1}_{c_kc_k'}\mathbf{T}^{c_2}_{c_j'c_j}\mathbf{T}^{c_2}_{c_\ell c_\ell'}+\mathbf{T}^{c_2}_{c_j'c_j}\mathbf{T}^{c_2}_{c_\ell c_\ell'}\mathbf{T}^{c_1}_{c_i'c_i}\mathbf{T}^{c_1}_{c_kc_k'}\right] \\
&\qquad\qquad \mathcal{M}^{c_3\cdots c_i\cdots c_j\cdots c_k'\cdots c_\ell'\cdots c_n;s_3\cdots s_n}_{f_3\cdots f_n}.
\end{aligned} \tag{5.16}$$

On the other hand, the non-abelian part features the same colour correlation as the single soft gluon and the soft pair of quarks cases, since it all come down to the colour correlation of the gluon with momentum

$p_1 + p_2$ from which the two soft gluons or quarks come in this case. However, the kinematic part is much more complex:

$$\mathscr{S}_{12}^{gg,(nab)}|\mathcal{M}_{g_1 g_2 f_3 \ldots f_n}|^2 = -(\mu^{2\epsilon} g_s^2)^2 \mathcal{C}_A \sum_{j,k=3}^{n} \mathcal{S}_{jk}^{gg}(p_1, p_2)$$
$$\left[\mathcal{M}_{f_3 \ldots f_n}^{c_3 \ldots c_j' \ldots c_k \ldots c_n; s_3 \ldots s_n}\right]^* \mathbf{T}_{c_j' c_j}^{c_{12}} \mathbf{T}_{c_k c_k'}^{c_{12}} \mathcal{M}_{f_3 \ldots f_n}^{c_3 \ldots c_j \ldots c_k' \ldots c_n; s_3 \ldots s_n}, \quad (5.17)$$

where

$$\mathcal{S}_{jk}^{gg}(p_1, p_2) = \mathcal{S}_{jk}^{(s.o.)}(p_1, p_2) - \frac{8 s_{jk}}{s_{12} s_{j(12)} s_{k(12)}}$$
$$+ 4 \frac{s_{j1} s_{k2} + s_{j2} s_{k1}}{s_{j(12)} s_{k(12)}} \left(\frac{1-\epsilon}{s_{12}^2} - \frac{1}{8} \mathcal{S}_{jk}^{(s.o.)}(p_1, p_2) \right), \quad (5.18)$$

and

$$\mathcal{S}_{jk}^{(s.o.)}(p_1, p_2) = \mathcal{S}_{jk}(p_2) \left(\mathcal{S}_{j2}(p_1) + \mathcal{S}_{k2}(p_1) - \mathcal{S}_{jk}(p_1) \right) \quad (5.19)$$

is the approximation of $\mathcal{S}_{jk}(p_1, p_2)$ in the strongly-ordered limit.

5.3. Soft limit of splitting functions

Having reviewed the behaviour of amplitudes and squared amplitudes in the single and double soft limits, we now focus on the behaviour of splitting functions under the same limits. As splitting functions are basically just limits of squared amplitudes, it is justified to expect them to display a similar behaviour. In this section, we consider n-parton processes, with the first m ones being collinear and the first or first two partons to be soft (respectively for the single soft or double soft cases). The single soft limit of the splitting function is then parametrised as follows:

$$z_1 \to \lambda z_1 , \qquad s_{1i} \to \lambda s_{1i} , \qquad \tilde{k}_1^\mu \to \lambda \tilde{k}_1^\mu , \qquad 1 < i \leq m , \quad (5.20)$$

while the double soft limit is parametrised as

$$z_1 \to \lambda z_1 \;\; , \;\; z_2 \to \lambda z_2 \;\; , \;\; \tilde{k}_1^\mu \to \lambda \tilde{k}_1^\mu \;\; , \;\; \tilde{k}_2^\mu \to \lambda \tilde{k}_2^\mu$$
$$s_{12} \to \lambda^2 s_{12} \;\; , \;\; s_{1i} \to \lambda s_{1i} \;\; , s_{2i} \to \lambda s_{2i} , \qquad 2 < i \leq m . \quad (5.21)$$

As for the collinear limit, we then simply expand the splitting function in the parameter λ and keep only the leading term in the Laurent series.

5.3.1. Single soft gluon

We start by the simplest case: one soft gluon. To obtain the behaviour of the splitting function in the soft limit, we exploit the fact that the soft and the collinear limits commute (as for the commutation of two collinear limits, this fact is easy to prove at tree-level):

$$\mathscr{S}_1\mathscr{C}_{1\ldots m}|\mathcal{M}_{g_1 f_2\ldots f_n}|^2 = \mathscr{C}_{1\ldots m}\mathscr{S}_1|\mathcal{M}_{g_1 f_2\ldots f_n}|^2. \tag{5.22}$$

The left hand side of eq. (5.22) is quite simply derived using the factorisation of squared amplitude in the collinear limit (c.f. eq. (2.16)):

$$\mathscr{S}_1\mathscr{C}_{1\ldots m}|\mathcal{M}_{g_1 f_2\ldots f_n}|^2 = \mathscr{S}_1\left(\left(\frac{2\mu^{2\epsilon}\, g_s^2}{s_{1\ldots m}}\right)^{m-1}\hat{P}^{ss'}_{f_1\ldots f_m}\right) \mathcal{T}^{ss'}_{f f_{m+1}\ldots f_n}(p, p_{m+1}, \ldots, p_n), \tag{5.23}$$

where $\mathcal{T}^{ss'}_{f f_{m+1}\ldots f_n}(p, p_{m+1}, \ldots, p_n)$ is not acted on by $\mathscr{S}_1$ since it does not depend on the soft parton. The right hand side on the other hand is more complex as we have to take the collinear limit of the squared amplitude in the soft limit, described in eq. (5.10). We can split the sum into four contributions:

- $m < j, k \leq n$: in this case, neither j nor k are in the collinear set; hence, these terms do not contribute because the eikonal factor is not singular in the collinear limit;
- $2 \leq j \leq m < k \leq n$: j is in the collinear set while k is not; the eikonal factor has a simple pole and reduces in the collinear limit to
$$\mathscr{C}_{1\ldots m}\mathscr{S}_{jk}(p_1) = -\frac{2\, z_j}{z_1\, s_{1j}}; \tag{5.24}$$
- $2 \leq k \leq m < j \leq n$: similar to the previous case with j and k exchanged;
- $2 \leq j, k \leq m$: both j and k are in the collinear set and the eikonal factor has a simple pole, as all three sub-energies involved have the same rescaling in the collinear limit.

Gathering all the pieces, we can write the right hand side of eq. (5.22) as

$$
\begin{aligned}
&\mathscr{C}_{1\dots m}\mathscr{S}_1|\mathcal{M}_{g_1 f_2\dots f_n}|^2 \\
&= \mu^{2\epsilon} g_s^2\, \mathcal{T}^{ss'}_{f f_{m+1}\dots f_n} \frac{1}{\mathcal{C}_f} \sum_{j,k=2}^{m} \mathcal{S}_{jk}(p_1) \left[\mathbf{Sp}^{c,c_2\dots c'_j\dots c_k\dots c_m;s'}_{f f_2\dots f_m}\right]^* \\
&\qquad\qquad \mathbf{T}^{c_1}_{c'_j c_j} \mathbf{T}^{c_1}_{c_k c'_k} \mathbf{Sp}^{c,c_2\dots c_j\dots c'_k\dots c_m;s}_{f f_2\dots f_m} \\
&- 2\mu^{2\epsilon} g_s^2 \sum_{k=2}^{m} \sum_{j=m+1}^{n} \frac{z_k}{z_1\, s_{1k}} \Big\{ \left[\mathcal{M}^{c,c_{m+1}\dots c'_j\dots c_n;s'}_{f f_{m+1}\dots f_n}\right]^* \left[\mathbf{Sp}^{c,c_2\dots c_k\dots c_m;s'}_{f f_2\dots f_m}\right]^* \\
&\qquad \mathbf{T}^{c_1}_{c'_j c_j} \mathbf{T}^{c_1}_{c_k c'_k} \mathbf{Sp}^{c',c_2\dots c'_k\dots c_m;s}_{f f_2\dots f_m} \mathcal{M}^{c',c_{m+1}\dots c_j\dots c_n;s}_{f f_{m+1}\dots f_n} + \left[\mathcal{M}^{c,c_{m+1}\dots c_j\dots c_n}_{f f_{m+1}\dots f_n}\right]^* \\
&\left[\mathbf{Sp}^{c,c_2\dots c'_k\dots c_m;s'}_{f f_2\dots f_m}\right]^* \mathbf{T}^{c_1}_{c'_k c_k} \mathbf{T}^{c_1}_{c_j c'_j} \mathbf{Sp}^{c',c_2\dots c_k\dots c_m;s}_{f f_2\dots f_m} \mathcal{M}^{c',c_{m+1}\dots c'_j\dots c_n;s}_{f f_{m+1}\dots f_n} \Big\}, \qquad (5.25)
\end{aligned}
$$

where, for readability, we keep the spin dependence of all quantities implicit, except for the spin indices of the parent parton, in order to keep track of spin correlations. To further simplify this equation and factorise $\mathcal{T}^{ss'}_{f f_{m+1}\dots f_n}$ as in the left hand side, we use colour conservation for the hard amplitude, which asserts that

$$
\sum_{i=m+1}^{n} \mathbf{T}^{c_1}_i = -\sum_{i=2}^{m} \mathbf{T}^{c_1}_i. \qquad (5.26)
$$

Applying this relation to eq. (5.25), we get

$$
\begin{aligned}
&\mathscr{C}_{1\dots m}\mathscr{S}_1|\mathcal{M}_{g_1 f_2\dots f_n}|^2 = \\
&= \mu^{2\epsilon} g_s^2\, \mathcal{T}^{ss'}_{f f_{m+1}\dots f_n} \frac{1}{\mathcal{C}_f} \sum_{j,k=2}^{m} \mathcal{S}_{jk}(p_1) \left[\mathbf{Sp}^{c,c_2\dots c'_j\dots c_k\dots c_m;s'}_{f f_2\dots f_m}\right]^* \\
&\qquad\qquad \mathbf{T}^{c_1}_{c'_j c_j} \mathbf{T}^{c_1}_{c_k c'_k} \mathbf{Sp}^{c,c_2\dots c_j\dots c'_k\dots c_m;s}_{f f_2\dots f_m} \\
&+ 2\mu^{2\epsilon} g_s^2\, \mathcal{T}^{ss'}_{f f_{m+1}\dots f_n} \frac{1}{\mathcal{C}_f} \sum_{j,k=2}^{m} \frac{z_k}{z_1\, s_{1k}} \Big\{ \left[\mathbf{Sp}^{c,c_2\dots c'_j\dots c_k\dots c_m;s'}_{f f_2\dots f_m}\right]^* \mathbf{T}^{c_1}_{c'_j c_j} \mathbf{T}^{c_1}_{c_k c'_k} \\
&\mathbf{Sp}^{c,c_2\dots c_j\dots c'_k\dots c_m;s}_{f f_2\dots f_m} + \left[\mathbf{Sp}^{c,c_2\dots c_j\dots c'_k\dots c_m;s'}_{f f_2\dots f_m}\right]^* \mathbf{T}^{c_1}_{c'_k c_k} \mathbf{T}^{c_1}_{c_j c'_j} \mathbf{Sp}^{c,c_2\dots c'_j\dots c_k\dots c_m;s}_{f f_2\dots f_m} \Big\} \\
&= \mu^{2\epsilon} g_s^2\, \mathcal{T}^{ss'}_{f f_{m+1}\dots f_n} \frac{1}{\mathcal{C}_f} \sum_{j,k=2}^{m} U_{jk;1} \left[\mathbf{Sp}^{c,c_2\dots c'_j\dots c_k\dots c_m;s'}_{f f_2\dots f_m}\right]^* \\
&\qquad\qquad \mathbf{T}^{c_1}_{c'_j c_j} \mathbf{T}^{c_1}_{c_k c'_k} \mathbf{Sp}^{c,c_2\dots c_j\dots c'_k\dots c_m;s}_{f f_2\dots f_m}, \qquad (5.27)
\end{aligned}
$$

where we defined

$$U_{jk;l} \equiv 2\left(-\frac{s_{jk}}{s_{jl}s_{kl}} + \frac{z_k}{z_l s_{kl}} + \frac{z_j}{z_l s_{jl}}\right). \tag{5.28}$$

We notice that $\mathcal{T}^{ss'}_{ff_{m+1}\cdots f_n}$ completely factorises and that the soft parton is only colour-correlated to the other collinear partons. This is a manifestation of colour-coherence: the cluster of collinear partons acts coherently as one single coloured object, and the hard partons cannot resolve its individual collinear constituents. Finally, we can put together the two sides of eq. (5.22) to find

$$\begin{aligned}
&\mathscr{S}_1\left[\left(\frac{2\mu^{2\epsilon}g_s^2}{s_{1\ldots m}}\right)^{m-1}\hat{P}^{ss'}_{g_1 f_2\ldots f_m}\right]\\
&= \mu^{2\epsilon}g_s^2\frac{1}{\mathcal{C}_f}\sum_{j,k=2}^{m}U_{jk;1}\left[\mathbf{Sp}^{c,c_2\ldots c'_j\ldots c_k\ldots c_m;s'}_{ff_2\ldots f_m}\right]^*\mathbf{T}^{c_1}_{c'_j c_j}\mathbf{T}^{c_1}_{c_k c'_k}\mathbf{Sp}^{c,c_2\ldots c_j\ldots c'_k\ldots c_m;s}_{ff_2\ldots f_m}.
\end{aligned} \tag{5.29}$$

This universal behaviour of splitting functions in the single soft limit is very reminiscent of the behaviour of squared amplitudes in the same limit (c.f. eq. (5.10)). Just like it was the case for squared amplitudes, we have to keep track of the colour correlations due to the soft gluon which happens at the amplitude level, the main difference being that the eikonal factor is replaced by the quantity $U_{jk;l}$. The factorisation in eq.. (5.29) is valid for an arbitrary number of collinear partons, and up to the colour correlations it is independent of the specific type or functional form of collinear amplitude.

5.3.2. Soft pair of quarks

We now turn to the case of a soft pair of quarks. Since the colour correlations for the soft pair of quark limit of a squared amplitude (c.f. eq. (5.12)) feature two-parton colour correlations as for the single soft gluon case (c.f. eq. (5.10)), the development of their respective soft limits of splitting functions is similar. More precisely, we split the double sum of eq. (5.12) into four contributions (according to whether or not the two indices of the double sum are in the collinear subset) and use colour conservation for the hard amplitude:

$$\sum_{i=m+1}^{n} \mathbf{T}_i^{c_{12}} = -\sum_{i=3}^{m} \mathbf{T}_i^{c_{12}}. \tag{5.30}$$

Using the commutativity of the soft and collinear limits, we arrive at an expression which is formally similar to eq. (5.29):

$$\begin{aligned}\mathscr{S}_{12}^{q\bar{q}} &\left[\left(\frac{2\mu^{2\epsilon}g_s^2}{s_{1\ldots m}}\right)^{m-1} \hat{P}^{ss'}_{q_1\bar{q}_2 f_3\cdots f_m}\right] \\ &= (\mu^{2\epsilon}g_s^2)^2 \frac{1}{\mathcal{C}_f} \sum_{j,k=3}^{m} U_{jk;12}^{q\bar{q}} \left[\mathbf{Sp}_{ff_3\ldots f_m}^{c,c_3\ldots c'_j\ldots c_k\ldots c_m;s'}\right]^* \\ &\qquad \mathbf{T}^{c_{12}}_{c'_j c_j} \mathbf{T}^{c_{12}}_{c_k c'_k} \mathbf{Sp}_{ff_3\ldots f_m}^{c,c_3\ldots c_j\ldots c'_k\ldots c_m;s}, \end{aligned} \tag{5.31}$$

where

$$\begin{aligned} U_{jk;12}^{q\bar{q}}(p_1,p_2) = \frac{4T_R}{s_{12}^2}\Bigg(&\frac{s_{1j}s_{2k}+s_{1k}s_{2j}-s_{jk}s_{12}}{s_{j(12)}s_{k(12)}} - \frac{z_1 s_{2j}+z_2 s_{1j}-z_j s_{12}}{(z_1+z_2)s_{j(12)}} \\ &- \frac{z_1 s_{2k}+z_2 s_{1k}-z_k s_{12}}{(z_1+z_2)s_{k(12)}} + \frac{2z_1 z_2}{(z_1+z_2)^2}\Bigg). \end{aligned} \tag{5.32}$$

Note that, unlike the soft gluon case, here the first two terms in the kinematic factor in eq. (5.13) contribute in the collinear limit even when neither j nor k are in the collinear set.

5.3.3. Two soft gluons

The case of two soft gluons in a splitting function is more involved, since the two soft gluon current features also four parton colour correlations. Hence, we start from the simpler case, which is the non-abelian part (see eq. (5.17)), which has only two parton correlations. Like for the two previous cases, we split the double sum into four contributions and repeat the same analysis. Similarly to the case of a soft pair of quarks, we still have contributions even when both j and k are not in the collinear set.

We find an expression which is yet again similar to eq. (5.29):

$$\mathscr{S}_{12}^{gg(nab)} \left[\left(\frac{2\mu^{2\epsilon} g_s^2}{s_{1\dots m}} \right)^{m-1} \hat{P}^{ss'}_{g_2 g_2 f_3 \cdots f_m} \right] = -(\mu^{2\epsilon} g_s^2)^2 \frac{1}{\mathcal{C}_f} \mathcal{C}_A \sum_{j,k=3}^{m} U^{gg(nab)}_{jk;12} \left[\mathbf{Sp}^{c,c_3\dots c'_j \dots c_k \dots c_m; s'}_{f f_3 \dots f_m} \right]^* \mathbf{T}^{c_{12}}_{c'_j c_j} \mathbf{T}^{c_{12}}_{c_k c'_k} \mathbf{Sp}^{c,c_3\dots c_j \dots c'_k \dots c_m; s}_{f f_3 \dots f_m}, \quad (5.33)$$

where

$$U^{gg(nab)}_{jk;12} = \mathcal{S}^{gg}_{jk}(p_1,p_2) - \mathcal{S}^{gg}_{j}(p_1,p_2) - \mathcal{S}^{gg}_{k}(p_1,p_2) + 4 \frac{2 z_1 z_2}{(z_1+z_2)^2} \frac{1-\epsilon}{s_{12}^2}, \quad (5.34)$$

with

$$\mathcal{S}^{gg}_{i}(p_1,p_2) = = \mathcal{S}^{(s.o.)}_{i}(p_1,p_2) + 4 \frac{z_2 s_{i1} + z_1 s_{i2}}{(z_1+z_2) s_{i(12)}} \left(\frac{1-\epsilon}{s_{12}^2} - \frac{1}{8} \mathcal{S}^{(s.o.)}_{i}(p_1,p_2) \right) - \frac{4}{s_{12}} \frac{2 z_i}{(z_1+z_2) s_{i(12)}}, \quad (5.35)$$

and

$$\mathcal{S}^{(s.o.)}_{i}(p_1,p_2) = -\frac{2 z_i}{z_2 s_{i2}} \left(-\frac{2 s_{i2}}{s_{i1} s_{12}} - \frac{2 z_2}{z_1 s_{12}} + \frac{2 z_i}{z_1 s_{i1}} \right). \quad (5.36)$$

As regards the abelian part of the two soft gluon current, which involves simply two copies of the eikonal factor but up to four parton colour correlations, the quadruple sum in eq. (5.16) may be split into six types of contributions:

- $m < i, j, k, \ell \leq n$: none of i, j, k, ℓ are in the collinear set, and so these terms do not contribute in the collinear limit, because the eikonal factors are not singular in the limit;
- $3 \leq i \leq m < j, k, \ell \leq n$, and likewise the other three cases where only one index runs in the collinear set: these terms do not contribute in the collinear limit, because one eikonal factor is not singular in the limit;

- $3 \le i,k \le m < j,\ell \le n$, and likewise the other case where only the pair (j,ℓ) runs through the collinear set: these terms do not contribute in the collinear limit, because one eikonal factor is not singular in the limit;

- $3 \le i,j \le m < k,\ell \le n$, and likewise the other three cases where one index from the pair (i,k) and one index from the pair (j,ℓ) run through the collinear set: each eikonal factor has a simple pole in the collinear limit, for example, for $3 \le i,j \le m < k,\ell \le n$, the eikonal factors reduce to

$$\mathscr{C}_{1\ldots m}\mathcal{S}_{ik}(p_1)\mathcal{S}_{j\ell}(p_2) = \frac{2\,z_i}{z_1\,s_{1i}}\,\frac{2\,z_j}{z_2\,s_{2j}}\,, \tag{5.37}$$

  and likewise for the other three cases;

- $3 \le i,j,k \le m < \ell \le n$, and likewise the other three cases where one index is outside of the collinear set: for $3 \le i,j,k \le m < \ell \le n$, we obtain

$$\mathscr{C}_{1\ldots m}\mathcal{S}_{ik}(p_1)\mathcal{S}_{j\ell}(p_2) = -\frac{2\,z_j}{z_2\,s_{2j}}\,\mathcal{S}_{ik}(p_1), \tag{5.38}$$

  and likewise for the other three cases;

- $3 \le i,j,k,\ell \le m$: each eikonal factor has a single pole like in the analogous case for the single soft limit.

Gathering once again the contributions outlined above, and using colour conservation for the hard amplitude as in eq. (5.30), the coefficient of the abelian part in eq. (5.16) of the double soft gluon limit becomes, as expected, the product of two single gluon coefficients $U_{jk;l}$, defined in eq. (5.28):

$$\mathscr{S}_{12}^{gg,(ab)} \left[\left(\frac{2\mu^{2\epsilon} g_s^2}{s_{1\dots m}} \right)^{m-1} \hat{P}^{ss'}_{g_1 g_2 f_3 \cdots f_m} \right]$$
$$= (\mu^{2\epsilon} g_s^2)^2 \frac{1}{\mathcal{C}_f} \frac{1}{2} \sum_{i,j,k,\ell=3}^{m} U_{ik;1}\, U_{j\ell;2} \left[\mathbf{Sp}^{c,c_3\dots c_i'\dots c_j'\dots c_k\dots c_\ell\dots c_m;s'}_{f f_3\dots f_m} \right]^*$$
$$\left[\mathbf{T}^{c_1}_{c_i' c_i} \mathbf{T}^{c_1}_{c_k c_k'} \mathbf{T}^{c_2}_{c_j' c_j} \mathbf{T}^{c_2}_{c_\ell c_\ell'} + \mathbf{T}^{c_2}_{c_j' c_j} \mathbf{T}^{c_2}_{c_\ell c_\ell'} \mathbf{T}^{c_1}_{c_i' c_i} \mathbf{T}^{c_1}_{c_k c_k'} \right] \mathbf{Sp}^{c,c_3\dots c_i\dots c_j\dots c_k'\dots c_\ell'\dots c_m;s}_{f f_3\dots f_m}. \tag{5.39}$$

The sum of eqs (5.33) and (5.39),

$$\mathscr{S}_{12}^{gg} \left[\left(\frac{2\mu^{2\epsilon} g_s^2}{s_{1\dots m}} \right)^{m-1} \hat{P}^{ss'}_{g_1 g_2 f_3 \cdots f_m} \right] =$$
$$= \left(\mathscr{S}_{12}^{gg,(ab)} + \mathscr{S}_{12}^{gg,(nab)} \right) \left[\left(\frac{2\mu^{2\epsilon} g_s^2}{s_{1\dots m}} \right)^{m-1} \hat{P}^{ss'}_{g_1 g_2 f_3 \cdots f_m} \right], \tag{5.40}$$

yields the double-soft gluon limit of an m-parton collinear splitting function.

5.4. Applications of soft limit of splitting functions

After having detailed how a generic splitting function behaves in the soft limit, we specialise these formulas to up to four partons. We focus mainly on the cases where all but two of the collinear partons are soft. In that case, the remaining functions **Sp** are splitting the parent parton into only two partons and have only one colour structure. This means that we are able to recombine the functions **Sp** into splitting functions, thus giving us relations between splitting functions only. We will start by the simplest cases and, step by step, end up with soft limit of our quadruple collinear splitting functions.

5.4.1. Single soft limit of double collinear splitting function

We start with an almost too simple case. We consider a splitting function $\hat{P}_{g_1 f_2}$, where the gluon g_1 is soft. By virtue of eq. (5.29), we have

$$\mathscr{S}_1 \left[\left(\frac{2\mu^{2\epsilon} g_s^2}{s_{1\ldots m}} \right) \hat{P}^{ss'}_{g_1 f_2} \right] = \mu^{2\epsilon} g_s^2 \frac{1}{\mathcal{C}_f} U_{22;1} \left[\mathbf{Sp}^{c,c'_2;s'}_{ff_2} \right]^* \mathbf{T}^{c_1}_{c'_2 c_2} \mathbf{T}^{c_1}_{c_2 c''_2} \mathbf{Sp}^{c,c''_2;s}_{ff_2} , \tag{5.41}$$

as both indices in the double sum can only take the value 2. Here we can solve the colour correlations immediately, using eq. (5.3),

$$\mathbf{T}^{c_1}_{c'_2 c_2} \mathbf{T}^{c_1}_{c_2 c''_2} = \left(\mathbf{T}^{\mathbf{2}}_{\mathbf{2}} \right)_{c'_2 c''_2} = \mathcal{C}_2 \delta_{c'_2 c''_2} , \tag{5.42}$$

where $\mathcal{C}_2$ is the Casimir of the parton 2. The Kronecker symbol that appears allows us to sum over the colour of parton 2 in eq. (5.41) to make the splitting function appear, according to eq. (2.18):

$$\frac{1}{\mathcal{C}_f} \left[\mathbf{Sp}^{c,c'_2;s'}_{ff_2} \right]^* \mathbf{Sp}^{c,c''_2;s}_{ff_2} \delta_{c'_2 c''_2} = \hat{P}^{ss'}_{f_2} . \tag{5.43}$$

The splitting function that appear in the right hand side of the last equation is the splitting of one parton to one parton, which is trivial:

$$\hat{P}^{ss'}_{f_2} = \delta^{ss'} . \tag{5.44}$$

Putting everything together in eq. (5.41), we finally have

$$\mathscr{S}_1 \left[\hat{P}^{ss'}_{g_1 f_2} \right] = 2 \frac{z_2}{z_1} \mathcal{C}_2 \delta^{ss'} . \tag{5.45}$$

5.4.2. Single soft limit of triple collinear splitting function

We now apply the same idea as before to the first example of non-trivial of soft-collinear limit: the soft limit of triple collinear splitting functions.

We one again start from eq. (5.29), but this time the indices in the double sum can take the values 2 or 3:

$$\begin{aligned}
&\mathscr{S}_1\left[\left(\frac{2\mu^{2\epsilon}g_s^2}{s_{123}}\right)^2\hat{P}^{ss'}_{g_1f_2f_3}\right]\\
&=\frac{\mu^{2\epsilon}g_s^2}{\mathcal{C}_f}\left\{U_{22;1}\left[\mathbf{Sp}^{c,c_2'c_3;s'}_{ff_2f_3}\right]^*\mathbf{T}^{c_1}_{c_2'c_2}\mathbf{T}^{c_1}_{c_2c_2''}\mathbf{Sp}^{c,c_2''c_3;s}_{ff_2f_3}\right.\\
&\qquad\qquad+U_{23;1}\left[\mathbf{Sp}^{c,c_2'c_3;s'}_{ff_2f_3}\right]^*\mathbf{T}^{c_1}_{c_2'c_2}\mathbf{T}^{c_1}_{c_3c_3'}\mathbf{Sp}^{c,c_2c_3';s}_{ff_2f_3}\\
&\qquad\qquad+U_{23;1}\left[\mathbf{Sp}^{c,c_2c_3';s'}_{ff_2f_3}\right]^*\mathbf{T}^{c_1}_{c_3'c_3}\mathbf{T}^{c_1}_{c_2c_2'}\mathbf{Sp}^{c,c_2'c_3;s}_{ff_2f_3}\\
&\qquad\qquad\left.+U_{33;1}\left[\mathbf{Sp}^{c,c_2c_3';s'}_{ff_2f_3}\right]^*\mathbf{T}^{c_1}_{c_3'c_3}\mathbf{T}^{c_1}_{c_3c_3''}\mathbf{Sp}^{c,c_2c_3'';s}_{ff_2f_3}\right\},
\end{aligned}\tag{5.46}$$

where we used the fact that $U_{jk;1}$ is symmetric under $j \leftrightarrow k$. The first and last term in this equation have colour structure which can be directly evaluated as

$$\mathbf{T}^{c_1}_{c_2'c_2}\mathbf{T}^{c_1}_{c_2c_2''}=\mathcal{C}_2\delta_{c_2'c_2''},\tag{5.47}$$

and the same thing with 2 replaced by 3. On the other hand, the second and third term in eq. (5.46) will give rise to $\mathbf{T}_2\cdot\mathbf{T}_3$ and $\mathbf{T}_3\cdot\mathbf{T}_2$, which are equal as colour charges of different partons commute. These colour correlations can still be evaluated using colour conservation:

$$\mathbf{T}_P+\mathbf{T}_2+\mathbf{T}_3=0\Rightarrow\mathbf{T}_2\cdot\mathbf{T}_3=\frac{\mathbf{T}_P^2-\mathbf{T}_2^2-\mathbf{T}_3^2}{2},\tag{5.48}$$

where $\mathbf{T}_P$ is the colour charge of the parent parton. We can thus simplify eq. (5.46):

$$\begin{aligned}
&\mathscr{S}_1\left[\left(\frac{2\mu^{2\epsilon}g_s^2}{s_{123}}\right)^2\hat{P}^{ss'}_{g_1f_2f_3}\right]\\
&\quad=\mu^{2\epsilon}g_s^2\left[U_{22;1}\mathcal{C}_2+U_{23;1}(\mathcal{C}_P-\mathcal{C}_2-\mathcal{C}_3)+U_{33;1}\mathcal{C}_3\right]\left(\frac{2\mu^{2\epsilon}g_s^2}{s_{23}}\right)\hat{P}^{ss'}_{f_2f_3}\,.
\end{aligned}\tag{5.49}$$

To obtain the factorisation of a specific splitting function, one simply needs to replace in this equation the coefficients $U_{jk;1}$ by their value given in eq. (5.28) and the Casimirs $\mathcal{C}_i$ by $\mathcal{C}_F$ if parton i is a quark and $\mathcal{C}_A$ if parton i is a gluon. The result we found are in agreement with ref [34].

5.4.3. Soft $q\bar{q}$ pair limit of quadruple collinear splitting function

The first non-trivial example of a soft pair of quark limit is for quadruple collinear splitting functions. We are hence looking for the limit of splitting functions of the form $\hat{P}^{ss'}_{q_1\bar{q}_2f_3f_4}$. Looking at eq. (5.31), we realise that it involves the same kind of colour correlations as eq. (5.29), two-parton colour correlations, so that the factorisation of the splitting function in the soft limit in the case of two soft partons or a single gluon are identical up to replacing the factors $U_{jk;1}$ from eq. (5.28) with $U^{q\bar{q}}_{jk;12}$ from eq. (5.32) and changing the span of the indices j and k from running $\{2,3\}$ to $\{3,4\}$. This gives us the following formula:

$$\mathscr{S}^{q\bar{q}}_{12}\left[\left(\frac{2\mu^{2\epsilon}g_s^2}{s_{1234}}\right)^3\hat{P}^{ss'}_{q_1\bar{q}_2f_3f_4}\right] = (\mu^{2\epsilon}g_s^2)^2\left[U^{q\bar{q}}_{33;12}\mathcal{C}_3 + U^{q\bar{q}}_{34;12}(\mathcal{C}_P - \mathcal{C}_3 - \mathcal{C}_4) + U^{q\bar{q}}_{44;12}\mathcal{C}_4\right] \left(\frac{2\mu^{2\epsilon}g_s^2}{s_{34}}\right)\hat{P}^{ss'}_{f_3f_4}. \quad (5.50)$$

Once again, this formula is then easily applied to any quadruple collinear splitting function, as it only requires to input the values of the coefficients $U^{q\bar{q}}_{jk;12}$ (which are always the same irregardless of the flavours of the partons) and the Casimirs of the parent parton and partons 3 and 4.

5.4.4. Two soft gluon limit of quadruple collinear splitting function

Finally, we turn to the limit where two gluons are going soft in a quadruple collinear splitting function. This case is more involved than the previous ones as it features up to four parton colour correlations. We start by considering the non-abelian part which has only two parton colour correlations. This time again, as it was the case for the soft pair of quark limit, we have the same colour correlations as the single soft limit. Indeed, eq. (5.33) is the same as eq. (5.31), with $U^{gg(nab)}_{jk;12}$ from eq. (5.34) instead of $U^{q\bar{q}}_{jk;12}$ from eq. (5.32). Hence, we can immediately write

$$\begin{aligned}
&\mathscr{S}^{gg(nab)}_{12}\left[\left(\frac{2\mu^{2\epsilon}g_s^2}{s_{1234}}\right)^3 \hat{P}^{ss'}_{g_1g_2f_3f_4}\right] \\
&= -(\mu^{2\epsilon}g_s^2)^2\,\mathcal{C}_A\,\left[U^{gg(nab)}_{33;12}\mathcal{C}_3 + U^{gg(nab)}_{34;12}(\mathcal{C}_P - \mathcal{C}_3 - \mathcal{C}_4) + U^{gg(nab)}_{44;12}\mathcal{C}_4\right] \\
&\qquad \left(\frac{2\mu^{2\epsilon}g_s^2}{s_{34}}\right)\hat{P}^{ss'}_{f_3f_4}. \qquad (5.51)
\end{aligned}$$

For the abelian part, we expand the quadruple sum in eq. (5.39) with $3 \leq i, j, k, \ell \leq 4$, and after using colour conservation,

$$\mathbf{T}_P + \mathbf{T}_3 + \mathbf{T}_4 = 0 \qquad (5.52)$$

we obtain

$$\begin{aligned}
&\mathscr{S}^{gg(ab)}_{12}\left[\left(\frac{2\mu^{2\epsilon}g_s^2}{s_{1234}}\right)^3 \hat{P}^{ss'}_{g_1g_2f_3f_4}\right] \\
&= (\mu^{2\epsilon}g_s^2)^2\,\left[U_{33;1}\mathcal{C}_3 + U_{34;1}(\mathcal{C}_P - \mathcal{C}_3 - \mathcal{C}_4) + U_{44;1}\mathcal{C}_4\right] \\
&\qquad \left[U_{33;2}\mathcal{C}_3 + U_{34;2}(\mathcal{C}_P - \mathcal{C}_3 - \mathcal{C}_4) + U_{44;2}\mathcal{C}_4\right]\left(\frac{2\mu^{2\epsilon}g_s^2}{s_{34}}\right)\hat{P}^{ss'}_{f_3f_4}, \qquad (5.53)
\end{aligned}$$

with the coefficients $U_{jk;l}$ defined in eq. (5.28).

The double soft gluon limit of a quadruple collinear function is then given by the sum of eqs (5.51) and (5.53):

$$\mathscr{S}^{gg}_{12}\left[\hat{P}^{ss'}_{g_1g_2f_3f_4}\right] = \left(\mathscr{S}^{gg(ab)}_{12} + \mathscr{S}^{gg(nab)}_{12}\right)\left[\hat{P}^{ss'}_{g_1g_2f_3f_4}\right]. \qquad (5.54)$$

As it was the case in the previous limits, this formula can be directly applied to any quadruple collinear splitting function.

5.5. Summary and results

In this chapter, we presented the soft-collinear limit, which allows us to explore the soft limit of splitting functions. We showed how the splitting functions behave almost identically to squared amplitudes (with of course different kinematic coefficients), with one change due to colour-coherence. Indeed, this property makes the non-collinear partons unable to resolve the individual collinear partons, and the colour correlations then only happen between the hard collinear partons. In addition to this result, we checked the soft limits of quark-parent splitting functions, and these have been found to behave exactly as expected.

Conclusions and Outlook

In this thesis, we presented our work on the quadruple collinear splitting functions, where we computed those for the first time, and explored some of their properties.

In Chapter 3, we exposed our most central result: the splitting functions themselves. We detailed the symmetries of these functions and their colour structure. Indeed, the computation of the quadruple collinear splitting functions required a deep understanding of their composition, but, above all, this process was made simpler by our gauge choice. As we insisted in Chapter 2, the choice of a physical gauge was crucial since it allowed us to directly extract the splitting functions from subgraphs that factorise from the main process in the collinear limit. This trick left us to compute the square of 5-point processes (1 splitting to 4) and take the limit. Our results are an important addition to the effort to build a subtraction scheme at N^{3}LO, since it was the penultimate missing piece, the last missing piece being the double soft limit at one loop. Due to their sheer size, this thesis does not include the quadruple collinear splitting functions but they can instead be found online [77].

In Chapter 4, we started our study of the properties of splitting functions by looking at the sub-collinear limit. The purpose of that study was twofold. One the one hand, it consolidated our trust in our results as it provided a strong sanity check. Indeed, our results having the expected behaviour for all possible collinear limits leaves close to no room for mistakes to happen. In the context of this thesis, we checked all the collinear limits of the quadruple collinear splitting functions and they were all found to match the expected value. On the other hand, this study of the sub-collinear limit allowed us to explore this particular corner of phase-space and to better understand the mathematical properties of these functions. This lead us to the introduction of the splitting tensors, which are new functions that appear in the factorisation of the splitting functions in the collinear limit, and to the computation of the triple collinear splitting tensors, which were never computed before. Since the splitting tensors are essentially just splitting functions with one open leg and splitting functions are limits of squared amplitudes with one open leg, we should not be surprised by the results of this chapter as they basically indicate that splitting functions behave like squared amplitudes.

In Chapter 5, we explored another interesting limit of the splitting functions: the soft limit. The reasons to do so are exactly the same as for the sub-collinear limits: to provide more strength to the trust in our results and to explore the mathematics of the soft-collinear limits. In the context of this thesis, we checked the soft limits of the quark-parent splitting functions and found them to match the expected results. This limit added a new ingredient to the mix: colour correlations. For the soft limit that we considered, the colour correlations were mostly two-parton colour correlations but they could go as high as four-parton. Once again, due to the nature of the splitting functions, it was no surprise that their behaviour in the soft limit is highly reminiscent of the one of squared amplitudes. The biggest twist to that analogy is probably colour-coherence: the fact that in the soft-collinear limit, the soft partons only colour-correlate the hard collinear partons.

Looking forward, there is still plenty of work to be done related to this thesis. First, as we mentioned before, the knowledge of the quadruple collinear limit was only the penultimate missing block to the building of a subtraction scheme at N^{3}LO. The next logical step would then be to look for the double soft limit at one loop, as it would achieve this goal of fully understanding the structure of IR divergences at N^{3}LO in QCD.

Next, as it was suggested in [58], one could extend these results to a supersymmetric version of QCD, $\mathscr{N} = 1$ Super-QCD, to further reinforce our trust in our results. Indeed, something intriguing happens then: the splitting functions in this theory could be obtained from the QCD ones by putting $\mathcal{C}_A = \mathcal{C}_F = 2T_R$ and symmetrising over the quark states to have the gluino states (the gluino being the leptonic super-partner of the gluon); then, in $D = 4$, the splitting of a gluon into all possible final states should be the same as the splitting of a gluino into all final states, providing an identity involving all splitting functions at once. Since it involves functions that are computed from QCD splitting functions, verifying this identity would provide another strong check of our results.

A | Lower Order Splitting Functions

In this appendix, we give the expressions of the splitting functions for $m = 2$ and $m = 3$ (c.f. for example [58, 89]). We recall the parametrisation of the collinear limit (cf. eq. (2.5)):

$$p_i = x_i p + k_i - \frac{k_i^2}{2x_i}\frac{n}{n \cdot p}, \tag{A.1}$$

as well as the boost-invariant variables (cf. eq. (2.6)):

$$z_i = \frac{x_i}{\sum_{j=1}^m x_j}, \tag{A.2}$$

$$\tilde{k}_i = k_i - z_i \sum_{j=1}^m k_j. \tag{A.3}$$

For $m = 2$ the corresponding splitting amplitudes read

$$\begin{aligned}
\langle \hat{P}_{qg} \rangle &= \mathcal{C}_F \left(\frac{1+z^2}{1-z} - \epsilon(1-z) \right), \\
\hat{P}^{\mu\nu}_{q\bar{q}} &= T_R \left(-g^{\mu\nu} + 4z(1-z)\frac{\tilde{k}^\mu \tilde{k}^\nu}{\tilde{k}^2} \right), \\
\hat{P}^{\mu\nu}_{gg} &= 2\mathcal{C}_A \left(-g^{\mu\nu} \left(\frac{z}{1-z} + \frac{1-z}{z} \right) - 2(1-\epsilon)z(1-z)\frac{\tilde{k}^\mu \tilde{k}^\nu}{\tilde{k}^2} \right),
\end{aligned} \tag{A.4}$$

where $z = z_1 = 1 - z_2$ and $\tilde{k} = \tilde{k}_1 = -\tilde{k}_2$.

For $m = 3$, there is five independent splitting functions. The simplest of the quark-initiated ones is

$$\langle \hat{P}_{\bar{q}'q'q} \rangle = \frac{1}{2} T_R \mathcal{C}_F \frac{s_{123}}{s_{12}} \Big(-\frac{t_{12,3}^2}{s_{12}s_{123}} + \frac{4z_3 + (z_1 - z_2)^2}{z_1 + z_2} + (1 - 2\epsilon)\left(z_1 + z_2 - \frac{s_{12}}{s_{123}} \right) \Big), \quad \text{(A.5)}$$

with

$$t_{ij,k} = 2\frac{z_i s_{jk} - z_j s_{ik}}{z_i + z_j} + \frac{z_i - z_j}{z_i + z_j} s_{ij}. \quad \text{(A.6)}$$

We also have a case with quarks all of the same flavour:

$$\langle \hat{P}_{\bar{q}qq} \rangle = \Big(\langle \hat{P}_{\bar{q}'q'q} \rangle + (2 \leftrightarrow 3) \Big) + \langle \hat{P}^{(id)}_{\bar{q}qq} \rangle, \quad \text{(A.7)}$$

with

$$\langle \hat{P}^{(id)}_{\bar{q}qq} \rangle = \mathcal{C}_F \left(\mathcal{C}_F - \frac{1}{2}\mathcal{C}_A \right) \Bigg[(1 - \epsilon)\left(2\frac{s_{23}}{s_{12}} - \epsilon \right) + \frac{s_{123}}{s_{12}} \Bigg(\frac{1 + z_1^2}{1 - z_2} - \frac{2z_2}{1 - z_3} - \epsilon \left(\frac{(1 - z_3)^2}{1 - z_2} + 1 + z_1 - \frac{2z_2}{1 - z_3} \right) - \epsilon^2 (1 - z_3) \Bigg) - \frac{s_{123}^2}{s_{12}s_{13}} \frac{z_1}{2} \left(\frac{1 + z_1^2}{(1 - z_2)(1 - z_3)} - \epsilon \left(1 + 2\frac{1 - z_2}{1 - z_3} - \epsilon^2 \right) \right) \Bigg] + (2 \leftrightarrow 3). \quad \text{(A.8)}$$

For the last of the quark-parent splitting functions with $m = 3$, we get

$$\langle \hat{P}_{ggq} \rangle = \mathcal{C}_F^2 \langle \hat{P}^{(ab)}_{ggq} \rangle + \mathcal{C}_A \mathcal{C}_F \langle \hat{P}^{(nab)}_{ggq} \rangle, \quad \text{(A.9)}$$

with

$$\langle \hat{P}^{(ab)}_{ggq} \rangle = \Bigg[\frac{s_{123}^2}{2s_{13}s_{23}} z_3 \left(\frac{1 + z_3^2}{z_1 z_2} - \epsilon \frac{z_1^2 + z_2^2}{z_1 z_2} - \epsilon(1 - \epsilon) \right) + \frac{s_{123}}{s_{13}} \left(\frac{z_3(1 - z_1) + (1 - z_2)^3}{z_1 z_2} + \epsilon^2 (1 + z_3) - \epsilon (z_1^2 + z_1 z_2 + z_2^2) \frac{1 - z_2}{z_1 z_2} \right) + (1 - \epsilon)\left(\epsilon - (1 - \epsilon \frac{s_{23}}{s_{13}} \right) \Bigg] + (1 \leftrightarrow 2), \quad \text{(A.10)}$$

and

$$
\begin{aligned}
\langle \hat{P}^{(nab)}_{ggq} \rangle = \Bigg[&(1-\epsilon)\left(\frac{t^2_{12,3}}{4s^2_{12}} + \frac{1}{4} - \frac{\epsilon}{2}\right) + \frac{s^2_{123}}{2s_{12}s_{13}}\Bigg(\frac{(1-z_3)^2(1-\epsilon)+2z_3}{z_2} \\
&+ \frac{z_2^2(1-\epsilon)+2(1-z_2)}{1-z_3}\Bigg) - \frac{s^2_{123}}{4s_{13}s_{23}} z_3 \Bigg(\frac{(1-z_3)^2(1-\epsilon)+2z_3}{z_1 z_2} + \epsilon(1-\epsilon)\Bigg) \\
&+ \frac{s_{123}}{2s_{12}}\Bigg((1-\epsilon)\frac{z_1(2-2z_1+z_1^2)-z_2(6-6z_2+z_2^2)}{z_2(1-z_3)} + 2\epsilon \frac{z_3(z_1-2z_2)-z_2}{z_2(1-z_3)}\Bigg) \\
&+ \frac{s_{123}}{2s_{13}}\Bigg((1-\epsilon)\frac{(1-z_2)^3+z_3^2-z_2}{z_2(1-z_3)} - \epsilon\left(\frac{2(1-z_2)(z_2-z_3)}{z_2(1-z_3)} - z_1 + z_2\right) \\
&- \frac{z_3(1-z_1)+(1-z_2)^3}{z_1 z_2} + \epsilon(1-z_2)\left(\frac{z_1^2+z_2^2}{z_1 z_2} - \epsilon\right)\Bigg)\Bigg] + (1 \leftrightarrow 2).
\end{aligned}
\tag{A.11}
$$

Then, for the gluon-parent splitting functions, we have first

$$
\hat{P}^{\mu\nu}_{gq\bar{q}} = T_R \mathcal{C}_F \hat{P}^{\mu\nu\ (ab)}_{gq\bar{q}} + T_R \mathcal{C}_A \hat{P}^{\mu\nu\ (nab)}_{gq\bar{q}},
\tag{A.12}
$$

with

$$
\begin{aligned}
\hat{P}^{\mu\nu(ab)}_{gq\bar{q}} = -g^{\mu\nu}&\left(-2 + \frac{2s_{123}s_{23}+(1-\epsilon)(s_{123}-s_{23})^2}{s_{12}s_{13}}\right) \\
&+ \frac{4s_{123}}{s_{12}s_{13}}\left(\tilde{k}_3^\mu \tilde{k}_2^\nu + \tilde{k}_2^\mu \tilde{k}_3^\nu - (1-\epsilon)\tilde{k}_1^\mu \tilde{k}_1^\nu\right),
\end{aligned}
\tag{A.13}
$$

and

$$
\begin{aligned}
\hat{P}^{\mu\nu(nab)}_{gq\bar{q}} = \frac{1}{4}\Bigg(&\frac{s_{123}}{s^2_{23}}\left[g^{\mu\nu}\frac{t^2_{23,1}}{s_{123}} - 16\frac{z_2^2 z_3^2}{z_1(1-z_1)}\left(\frac{\tilde{k}_2}{z_2} - \frac{\tilde{k}_3}{z_3}\right)^\mu \left(\frac{\tilde{k}_2}{z_2} - \frac{\tilde{k}_3}{z_3}\right)^\nu\right] \\
&+ \frac{s_{123}}{s_{12}s_{13}}\left[2s_{123}g^{\mu\nu} - 4\left(\tilde{k}_2^\mu \tilde{k}_3^\nu + \tilde{k}_3^\mu \tilde{k}_2^\nu - (1-\epsilon)\tilde{k}_1^\mu \tilde{k}_1^\nu\right)\right] \\
&- g^{\mu\nu}\left[-(1-2\epsilon) + 2\frac{s_{123}}{s_{12}}\frac{1-z_3}{z_1(1-z_1)} + 2\frac{s_{123}}{s_{23}}\frac{1-z_1+2z_1^2}{z_1(1-z_1)}\right] \\
&+ \frac{s_{123}}{s_{12}s_{23}}\Bigg[-2s_{123}g^{\mu\nu}\frac{z_2(1-2z_1)}{z_1(1-z_1)} - 16\tilde{k}_3^\mu \tilde{k}_3^\nu \frac{z_2^2}{z_1(1-z_1)} + 8(1-\epsilon)\tilde{k}_2^\mu \tilde{k}_2^\nu \\
&+ 4(\tilde{k}_2^\mu \tilde{k}_3^\nu + \tilde{k}_3^\mu \tilde{k}_2^\nu)\left(\frac{2z_2(z_3-z_1}{z_1(1-z_1)} + (1-\epsilon)\right)\Bigg]\Bigg) + (2 \leftrightarrow 3).
\end{aligned}
\tag{A.14}
$$

Finally, for the last triple splitting function, we have

$$
\begin{aligned}
\hat{P}^{\mu\nu}_{ggg} = \mathcal{C}_A^2 \Bigg(& \frac{s_{123}(1-\epsilon)}{s_{12}s_{13}} \Bigg[2z_1 \left(\tilde{k}_2^\mu \tilde{k}_2^\nu \frac{1-2z_3}{z_3(1-z_3)} + \tilde{k}_3^\mu \tilde{k}_3^\nu \frac{1-2z_2}{z_2(1-z_2)} \right) \\
& - \frac{3}{4}(1-\epsilon) g^{\mu\nu} + \frac{s_{123}}{s_{12}} g^{\mu\nu} \frac{1}{z_3} \left[\frac{2(1-z_3)+4z_3^2}{1-z_3} - \frac{1-2z_3(1-z_3)}{z_1(1-z_1)} \right] \\
& + \frac{(1-\epsilon)}{4s_{12}^2} \left[-g^{\mu\nu} t_{12,3}^2 + 16 s_{123} \frac{z_1^2 z_2^2}{z_3(1-z_3)} \left(\frac{\tilde{k}_2}{z_2} - \frac{\tilde{k}_1}{z_1} \right)^\mu \left(\frac{\tilde{k}_2}{z_2} - \frac{\tilde{k}_1}{z_1} \right)^\nu \right] \\
& + \frac{s_{123}}{2(1-\epsilon)} g^{\mu\nu} \left(\frac{4z_2z_3 + 2z_1(1-z_1) - 1}{(1-z_2)(1-z_3)} - \frac{1-2z_1(1-z_1)}{z_2z_3} \right) \\
& + (\tilde{k}_2^\mu \tilde{k}_3^\nu + \tilde{k}_3^\mu \tilde{k}_2^\nu) \left(\frac{2z_2(1-z_2)}{z_3(1-z_3)} - 3 \right) \Bigg] \Bigg) \\
& + (5 \text{ permutations}). \qquad \text{(A.15)}
\end{aligned}
$$

B | Splitting Tensors

In this appendix, we give the expressions of the splitting tensors for $m = 2$ and $m = 3$. Note that, due to its size, the three-gluon splitting tensor $H_{ggg}^{\rho\sigma;\mu\nu}$ is too lengthy to be presented on paper, but we make it available in computer-readable form [77]. For $m = 2$, we have

$$H_{gq}^{\rho\sigma} = \mathcal{C}_F \left[\frac{1}{2} (1-z)\, d^{\rho\sigma}(p,n) - 2 \frac{z}{1-z} \frac{\tilde{k}^\rho \tilde{k}^\sigma}{\tilde{k}^2} \right], \tag{B.1}$$

$$\begin{aligned} H_{gg}^{\rho\sigma;\mu\nu} = 2\mathcal{C}_A \Bigg[& \frac{1-z}{2z} (g^{\mu\rho} g^{\nu\sigma} + g^{\nu\rho} g^{\mu\sigma}) \\ & + \frac{z}{1-z} g^{\mu\nu} \frac{\tilde{k}^\rho \tilde{k}^\sigma}{\tilde{k}^2} - z(1-z) d^{\rho\sigma}(p,n) \frac{\tilde{k}^\mu \tilde{k}^\nu}{\tilde{k}^2} \Bigg], \end{aligned} \tag{B.2}$$

where $z = z_1 = 1 - z_2$ and $\tilde{k} = \tilde{k}_1 = -\tilde{k}_2$.

For $m = 3$, we first present the splitting tensor $H_{g_{(12)} g_3 q_4}$, where we consider that it comes from a quadruple splitting function where the two first partons are collinear. We therefore added a subscript (12) to denote the on-shell momentum of the gluon sub-parent. We separate the colour structure of the splitting tensor as follows

$$H_{ggq}^{\rho\sigma} = \mathcal{C}_F^2 \, H_{ggq}^{\rho\sigma\,(\mathrm{ab})} + \mathcal{C}_A \, \mathcal{C}_F \, H_{ggq}^{\rho\sigma\,(\mathrm{nab})}, \tag{B.3}$$

and give the expression of the abelian and non-abelian parts in term of the coefficients introduced in eq. (4.19). Furthermore, we define the shorthand

$$z_{1\ldots j} = z_1 + \ldots + z_j, \qquad \bar{z}_i = 1 - z_i, \qquad \tilde{k}_{1\ldots j} = \tilde{k}_1 + \ldots + \tilde{k}_j. \quad \text{(B.4)}$$

In what follows, we have eliminated z_{12} and $\tilde{k}_{12}$ using the constraints. The coefficients of the abelian piece of $H_{g_{(12)}g_3q_4}$ read

$$\begin{aligned} A^{(\mathrm{ab})} = \frac{1}{2z_3}\Bigg\{ & \frac{s_{(12)3}^2(2(\bar{z}_4 + z_3) - (D-2)z_3)z_4}{2s_{34}s_{(12)4}} + \frac{s_{34}(\bar{z}_3^2 - z_4^2)}{s_{(12)4}} \\ & + s_{(12)3}\left(\frac{3z_4\bar{z}_4 - (1+z_3)z_3}{s_{34}} + \frac{\bar{z}_3^2 + (1 + z_3 - 2z_4)z_4}{s_{(12)4}}\right) \\ & + (2 - z_3)z_4 - 3z_4^2 + \bar{z}_3 + s_{(12)3}z_3\bar{z}_4(D-2)\frac{1}{2}\left(\frac{1}{s_{34}} + \frac{1}{s_{(12)4}}\right) \\ & - \frac{s_{(12)4}(z_3(1 + z_{34}) - 2z_4\bar{z}_4)}{s_{34}}\Bigg\}, \end{aligned} \quad \text{(B.5)}$$

$$\begin{aligned} B_{33}^{(\mathrm{ab})} = \frac{s_{(12)34}^2 z_4}{s_{34}z_3(1 - z_{34})^2}\Bigg\{ & \frac{(D-2)(z_3z_4 + \bar{z}_4^2)z_3 + 4z_4}{s_{(12)4}} \\ & + \frac{z_4 s_{34}(4\bar{z}_3 + (D-2)z_3^2)}{s_{(12)4}^2}\Bigg\}, \end{aligned} \quad \text{(B.6)}$$

$$\begin{aligned} B_{44}^{(\mathrm{ab})} = \frac{s_{(12)34}^2 \bar{z}_3}{s_{34}z_3(1 - z_{34})^2}\Bigg\{ & \frac{s_{34}(4\bar{z}_3 + (D-2)z_3^2)\bar{z}_3}{s_{(12)4}^2} \\ & - \frac{z_3^2(D-2)(z_{34} - 2) - 4z_4)}{s_{(12)4}}\Bigg\}, \end{aligned} \quad \text{(B.7)}$$

$$\begin{aligned} B_{34}^{(\mathrm{ab})} \equiv B_{43}^{(\mathrm{ab})} = \frac{s_{(12)34}^2}{2s_{34}z_3(1 - z_{34})^2}\Bigg\{ & \frac{2s_{34}\bar{z}_3z_4(4\bar{z}_3 + (D-2)z_3^2)}{s_{(12)4}^2} \\ & + \frac{(D-2)\left(\bar{z}_4^2 - z_3z_4\left(2z_3 + 2z_4 - 5\right) - z_3\right)z_3 + 4z_4\left(\bar{z}_3 + z_4\right)}{s_{(12)4}}\Bigg\}. \end{aligned} \quad \text{(B.8)}$$

On the other hand, the coefficients of the non-abelian part of the splitting tensor $H_{g_{(12)}g_3q_4}$ can be written (following eq. (4.19)) as

$$
\begin{aligned}
A^{(\mathrm{nab})} &= \frac{s_{(12)4}^2}{\bar{z}_4 s_{(12)3}}\left(\frac{z_3^2}{\bar{z}_4 s_{(12)3}} - \frac{z_3\bar{z}_4 - 2\bar{z}_4^2 - z_3^2}{4s_{3,4}}\right) - \frac{s_{3,4}s_{(12)4}}{s_{(12)3}^2}\frac{2z_3\,(1-z_{34})}{\bar{z}_4^2} \\
&+ \frac{s_{3,4}^2\,(1-z_{34})^2}{\bar{z}_4 s_{(12)3}}\left(\frac{(z_3+\bar{z}_4)}{4z_3 s_{(12)4}} + \frac{1}{\bar{z}_4 s_{(12)3}}\right) - \frac{s_{3,4}\,(1-z_{34})}{4s_{(12)3}}\left(\frac{z_3\,(z_4+7)}{\bar{z}_4^2}\right. \\
&\left. - \frac{3\bar{z}_4}{z_3} - \frac{4}{\bar{z}_4}\right) - \frac{s_{3,4}\,(1-z_{34})}{8s_{(12)4}}\left((D-2) + \frac{2(z_3+\bar{z}_4)(z_3+3z_4-2)}{z_3\bar{z}_4}\right) \\
&+ \frac{s_{(12)3}^2}{8s_{34}s_{(12)4}}\left(z_4(D-2) - \frac{2z_4(z_3+\bar{z}_4)}{z_3}\right) - \frac{s_{(12)3}}{8s_{(12)4}}\left((D-2)\,(\bar{z}_3-2z_4)\right. \\
&\left. + 2z_4 + \frac{2z_3(1-2z_4)}{\bar{z}_4} + 2\frac{z_4\,(4-3z_4)-1}{z_3}\right) - \frac{s_{(12)3}}{8s_{3,4}}\left((D-2)\,(z_3-z_4)\right. \\
&\left. - \frac{2z_3(1-2z_4)}{\bar{z}_4} + \frac{2\bar{z}_4(3z_4-z_3)}{z_3}\right) + \frac{s_{(12)4}}{8s_{3,4}}\left(2 - 2(z_4-z_3)\frac{2\bar{z}_4^2+z_3^2}{z_3\bar{z}_4}\right. \\
&\left. - (D-2)z_3\right) + \frac{s_{(12)4}}{4s_{(12)3}}\left(\frac{z_3(4z_3+(z_3-\bar{z}_4)(z_4+3))}{\bar{z}_4^2} + \frac{2\bar{z}_4^2}{z_3}\right) \\
&+ \frac{1}{8}(D-2)\,(1+z_4) + \frac{1}{4}\,(2z_4-1)\left(1-\frac{3\bar{z}_4}{z_3}\right) - \frac{z_3\,(1+z_4)\,(1-z_{34})}{2\bar{z}_4^2}
\end{aligned}
\tag{B.9}
$$

$$
\begin{aligned}
B_{33}^{(\mathrm{nab})} &= \frac{s_{(12)34}^2}{2(1-z_{34})^2}\left\{\frac{2\bar{z}_4(4z_4+(D-2)\bar{z}_4^2)}{s_{(12)3}^2} - \frac{4z_4(z_3-2\bar{z}_4)}{s_{34}s_{(12)3}\bar{z}_4}\right. \\
&- \frac{z_4(4\bar{z}_3+\bar{z}_4^2(D-2)(\bar{z}_4+z_3)+4(1-2z_4)z_4)}{s_{(12)3}s_{(12)4}\bar{z}_4} - \frac{4z_4^2}{s_{34}s_{(12)4}z_3} \\
&\left. + \left(\frac{\bar{z}_4}{s_{(12)3}} - \frac{z_4}{s_{(12)4}}\right)\frac{(D-2)(z_4(z_{34}-2)+1)}{s_{34}}\right\},
\end{aligned}
\tag{B.10}
$$

$$
\begin{aligned}
B_{44}^{(\mathrm{nab})} &= \frac{s_{(12)34}^2}{2(1-z_{34})^2}\left\{\frac{2z_3^2(4z_4+(D-2)\bar{z}_4^2)}{s_{(12)3}^2\bar{z}_4} - \frac{\bar{z}_3(4z_4+(D-2)(2-z_{34})z_3^2)}{s_{34}s_{(12)4}z_3}\right. \\
&+ \frac{\bar{z}_3}{s_{(12)3}s_{(12)4}}\left(\frac{4\,(z_3\,(2z_3-3)+\bar{z}_4)}{z_3} - (D-2)(\bar{z}_4+z_3)z_3\right) \\
&\left. + \frac{1}{s_{34}s_{(12)3}}\left(4+4z_3\left(\frac{z_3}{\bar{z}_4}-2\right) + (D-2)(2-z_{34})z_3^2\right)\right\},
\end{aligned}
\tag{B.11}
$$

$$
\begin{aligned}
B_{34}^{(\mathrm{nab})} &\equiv B_{43}^{(\mathrm{nab})} = \frac{s_{(12)34}^2}{4(1-z_{34})^2}\left\{\frac{4z_3(\bar{z}_4^2(D-2)+4z_4)}{s_{(12)3}^2}\right. \\
&- \frac{4z_4(z_4+\bar{z}_3)+z_3(D-2)(z_4(2z_3-1)(2-z_{34})+\bar{z}_3)}{z_3 s_{34}s_{(12)4}}
\end{aligned}
$$

$$
\begin{aligned}
&+ \frac{1}{z_3 \bar{z}_4 s_{(12)3} s_{(12)4}} \Bigg(4\bar{z}_4^2 z_4 - \bar{z}_4 z_3 (4 + (D-2)\bar{z}_4^2 + 20 z_4) \\
&\qquad\qquad + 2z_3^2 (z_4(6 - 8z_4 - (D-2)\bar{z}_4^2) + 4) \Bigg) \\
&- \frac{z_3(8 + \bar{z}_4^2 (D-2)(2z_4 - 3) - 4z_4) - 4\bar{z}_4(1 + 2z_4)}{\bar{z}_4 s_{34} s_{(12)3}} \\
&- \frac{z_3^2 (s_{34} - s_{(12)4})(\bar{z}_4 (D-2)(2z_4 - 1) + 4)}{\bar{z}_4 s_{34} s_{(12)3} s_{(12)4}} \Bigg\} .
\end{aligned}
\tag{B.12}
$$

In the remainder of this section, we provide explicit results for the splitting tensor $H^{\rho\sigma;\mu\nu}_{g\bar{q}q}$. We can write it in terms of an abelian and non-abelian part:

$$
H^{\rho\sigma;\mu\nu}_{g\bar{q}q} = T_R\, \mathcal{C}_F\, H^{\rho\sigma,\mu\nu\ (\mathrm{ab})}_{g\bar{q}q} + T_R\, \mathcal{C}_A\, H^{\rho\sigma,\mu\nu\ (\mathrm{nab})}_{g\bar{q}q} . \tag{B.13}
$$

The coefficients in eq. (4.28) belonging to the abelian piece of $H^{\rho\sigma;\mu\nu}_{g_{(12)}\bar{q}_3 q_4}$ are given by

$$
A^{\ (\mathrm{ab})} = -\frac{\left(s_{(12)3} + s_{(12)4}\right)^2}{2 s_{(12)3} s_{(12)4}} , \tag{B.14}
$$

$$
B_{33}^{(\mathrm{ab})} \equiv B_{34}^{(\mathrm{ab})} \equiv B_{43}^{(\mathrm{ab})} \equiv B_{44}^{(\mathrm{ab})} = -\frac{2 s_{(12)34}}{s_{(12)3} s_{(12)4}} , \tag{B.15}
$$

$$
C_{33}^{(\mathrm{ab})} = -\frac{2 s_{(12)34} \left(z_4 s_{(12)3} - \bar{z}_4 s_{(12)4}\right)^2}{s_{(12)3}^2 s_{(12)4}^2 (1 - z_{34})^2} , \tag{B.16}
$$

$$
C_{44}^{(\mathrm{ab})} = -\frac{2 s_{(12)34} \left(z_3 s_{(12)4} - \bar{z}_3 s_{(12)3}\right)^2}{s_{(12)3}^2 s_{(12)4}^2 (1 - z_{34})^2} , \tag{B.17}
$$

$$
C_{34}^{(\mathrm{ab})} \equiv C_{43}^{(\mathrm{ab})} = \frac{2 s_{(12)34} \left(z_3 s_{(12)4} - \bar{z}_3 s_{(12)3}\right) \left(z_4 s_{(12)3} - \bar{z}_4 s_{(12)4}\right)}{s_{(12)3}^2 s_{(12)4}^2 (1 - z_{34})^2} , \tag{B.18}
$$

$$
D_{3333}^{(\mathrm{ab})} = -\frac{8 {z_4}^2}{s_{(12)4}^2 (1 - z_{34})^2} , \tag{B.19}
$$

$$
D_{4444}^{(\mathrm{ab})} = -\frac{8 {z_3}^2}{s_{(12)3}^2 (1 - z_{34})^2} , \tag{B.20}
$$

$$
D_{3334}^{(\mathrm{ab})} \equiv D_{3343}^{(\mathrm{ab})} = -\frac{8 z_4 \bar{z}_3}{s_{(12)4}^2 (1 - z_{34})^2} , \tag{B.21}
$$

$$
D_{3433}^{(\mathrm{ab})} \equiv D_{4333}^{(\mathrm{ab})} = -\frac{8 z_4 \bar{z}_4}{s_{(12)3} s_{(12)4} (1 - z_{34})^2} , \tag{B.22}
$$

$$D^{(\mathrm{ab})}_{4434} \equiv D^{(\mathrm{ab})}_{4443} = -\frac{8 z_3 \bar{z}_4}{s^2_{(12)3}(1-z_{34})^2}\,, \tag{B.23}$$

$$D^{(\mathrm{ab})}_{3444} \equiv D^{(\mathrm{ab})}_{4344} = -\frac{8 z_3 \bar{z}_3}{s_{(12)3}s_{(12)4}(1-z_{34})^2}\,, \tag{B.24}$$

$$\begin{aligned} D^{(\mathrm{ab})}_{3434} &\equiv D^{(\mathrm{ab})}_{4343} \equiv D^{(\mathrm{ab})}_{4334} \equiv D^{(\mathrm{ab})}_{3443} \\ &= 4\,\frac{z_3\bar{z}_4 + z_4\bar{z}_3 - 1}{s_{(12)3}s_{(12)4}(1-z_{34})^2}\,, \end{aligned} \tag{B.25}$$

$$D^{(\mathrm{ab})}_{4433} = -\frac{8\bar{z}_4^2}{s^2_{(12)3}(1-z_{34})^2}\,, \tag{B.26}$$

$$D^{(\mathrm{ab})}_{3344} = -\frac{8\bar{z}_3^2}{s^2_{(12)4}(1-z_{34})^2}\,, \tag{B.27}$$

$$E^{(\mathrm{ab})}_{33} = -\frac{2z_4}{s_{(12)4}(1-z_{34})}\,, \tag{B.28}$$

$$E^{(\mathrm{ab})}_{44} = -\frac{2z_3}{s_{(12)3}(1-z_{34})}\,, \tag{B.29}$$

$$E^{(\mathrm{ab})}_{34} = -\frac{2\bar{z}_4}{s_{(12)3}(1-z_{34})}\,, \tag{B.30}$$

$$E^{(\mathrm{ab})}_{43} = -\frac{2\bar{z}_3}{s_{(12)4}(1-z_{34})}\,, \tag{B.31}$$

$$F^{\,(\mathrm{ab})} = -1\,, \tag{B.32}$$

while the non-abelian coefficients read

$$A^{\,(\mathrm{nab})} = \frac{1}{2}\,, \tag{B.33}$$

$$B^{(\mathrm{nab})}_{33} = \frac{s_{(12)34}\left(s_{34}+s_{(12)4}\right)}{s_{34}s_{(12)3}s_{(12)4}}\,, \tag{B.34}$$

$$B^{(\mathrm{nab})}_{34} \equiv B^{(\mathrm{nab})}_{43} = \frac{s_{(12)34}\left(s_{(12)34}+s_{34}\right)}{2s_{34}s_{(12)3}s_{(12)4}}\,, \tag{B.35}$$

$$B^{(\mathrm{nab})}_{44} = \frac{s_{(12)34}\left(s_{34}+s_{(12)3}\right)}{s_{34}s_{(12)3}s_{(12)4}}\,, \tag{B.36}$$

$$C^{(\mathrm{nab})}_{33} = -\frac{s_{(12)34}\left(\bar{z}_4\left(2z_4 s_{34}+s_{(12)4}\right)+z_4 s_{(12)3}\right)}{s_{34}s_{(12)3}s_{(12)4}(1-z_{34})^2}\,, \tag{B.37}$$

$$C^{(\mathrm{nab})}_{44} = -\frac{s_{(12)34}\left(\bar{z}_3\left(2z_3 s_{34}+s_{(12)3}\right)+z_3 s_{(12)4}\right)}{s_{34}s_{(12)3}s_{(12)4}(1-z_{34})^2}\,, \tag{B.38}$$

$$C^{(\mathrm{nab})}_{34} \equiv C^{(\mathrm{nab})}_{43} = -\frac{s_{(12)34}}{(1-z_{34})^2}\left(\frac{\bar{z}_4\bar{z}_3+z_4 z_3}{s_{(12)3}s_{(12)4}} + \frac{\bar{z}_3+z_4}{2s_{34}s_{(12)4}} + \frac{\bar{z}_4+z_3}{2s_{34}s_{(12)3}}\right),$$

$$D_{3333}^{(\mathrm{nab})} = -\frac{8{z_4}^2\left(s_{34}+s_{(12)4}\right)}{{s_{34}}^2 s_{(12)4}(1-z_{34})^2}\,, \tag{B.39}$$

$$D_{4444}^{(\mathrm{nab})} = -\frac{8{z_3}^2\left(s_{34}+s_{(12)3}\right)}{{s_{34}}^2 s_{(12)3}(1-z_{34})^2}\,, \tag{B.40}$$

$$D_{3334}^{(\mathrm{nab})} \equiv D_{3343}^{(\mathrm{nab})} = -\frac{8z_4\bar{z}_3\left(s_{34}+s_{(12)4}\right)}{{s_{34}}^2 s_{(12)4}(1-z_{34})^2}\,, \tag{B.41}$$

$$D_{3433}^{(\mathrm{nab})} \equiv D_{4333}^{(\mathrm{nab})} = \frac{4z_4\bar{z}_4}{s_{(12)4}(1-z_{34})^2}\left(\frac{s_{34}+2s_{(12)4}}{s_{34}^2}+\frac{s_{34}+s_{(12)4}}{s_{34}s_{(12)3}}\right), \tag{B.42}$$

$$D_{4434}^{(\mathrm{nab})} \equiv D_{4443}^{(\mathrm{nab})} = -\frac{8z_3\bar{z}_4\left(s_{34}+s_{(12)3}\right)}{{s_{34}}^2 s_{(12)3}(1-z_{34})^2}\,, \tag{B.43}$$

$$D_{3444}^{(\mathrm{nab})} \equiv D_{4344}^{(\mathrm{nab})} = \frac{4z_3\bar{z}_3}{s_{(12)4}(1-z_{34})^2}\left(\frac{s_{34}+2s_{(12)4}}{s_{34}^2}+\frac{s_{34}+s_{(12)4}}{s_{34}s_{(12)3}}\right), \tag{B.44}$$

$$\begin{aligned} D_{3434}^{(\mathrm{nab})} &\equiv D_{4343}^{(\mathrm{nab})} \equiv D_{4334}^{(\mathrm{nab})} \equiv D_{3443}^{(\mathrm{nab})} \\ &= 2\,\frac{\bar{z}_4\bar{z}_3+z_3z_4}{(1-z_{34})^2}\left(\frac{2}{s_{34}^2}+\frac{s_{(12)34}}{s_{(12)3}s_{(12)4}s_{34}}\right)\,, \end{aligned} \tag{B.45}$$

$$D_{4433}^{(\mathrm{nab})} = -\frac{8\bar{z}_4^2\left(s_{34}+s_{(12)3}\right)}{{s_{34}}^2 s_{(12)3}(1-z_{34})^2}\,, \tag{B.46}$$

$$D_{3344}^{(\mathrm{nab})} = -\frac{8\bar{z}_3^2\left(s_{34}+s_{(12)4}\right)}{{s_{34}}^2 s_{(12)4}(1-z_{34})^2}\,, \tag{B.47}$$

$$E_{33}^{(\mathrm{nab})} = \frac{2z_4^2(s_{(12)3}+s_{34})-4z_3z_4s_{(12)4}}{(1-z_{34})z_{34}s_{34}}\left(\frac{1}{s_{(12)4}}+\frac{1}{s_{34}}\right)+\frac{2z_4^2s_{(12)3}}{(1-z_{34})z_{34}s_{34}^2}\,, \tag{B.48}$$

$$E_{44}^{(\mathrm{nab})} = \frac{2z_3^2(s_{(12)4}+s_{34})-4z_3z_4s_{(12)3}}{(1-z_{34})z_{34}s_{34}}\left(\frac{1}{s_{(12)3}}+\frac{1}{s_{34}}\right)+\frac{2z_3^2s_{(12)4}}{(1-z_{34})z_{34}s_{34}^2}\,, \tag{B.49}$$

$$\begin{aligned} E_{34}^{(\mathrm{nab})} &= \frac{s_{34}+s_{(12)4}}{2s_{34}s_{(12)3}z_{34}}-\frac{(s_{34}+s_{(12)3})}{2s_{34}s_{(12)4}}\left(\frac{4z_4\bar{z}_3}{(1-z_{34})z_{34}}+\frac{1}{z_{34}}\right) \\ &\qquad +\frac{4\bar{z}_3}{s_{34}(1-z_{34})z_{34}}\left(z_3-\frac{1}{2}z_4-\frac{s_{(12)3}z_4-s_{(12)4}z_3}{s_{34}}\right)\,, \end{aligned} \tag{B.50}$$

$$\begin{aligned} E_{43}^{(\mathrm{nab})} &= \frac{s_{34}+s_{(12)3}}{2s_{34}s_{(12)4}z_{34}}-\frac{(s_{34}+s_{(12)4})}{2s_{34}s_{(12)3}}\left(\frac{4z_3\bar{z}_4}{(1-z_{34})z_{34}}+\frac{1}{z_{34}}\right) \\ &\qquad +\frac{4\bar{z}_4}{s_{34}(1-z_{34})z_{34}}\left(z_4-\frac{1}{2}z_3+\frac{s_{(12)3}z_4-s_{(12)4}z_3}{s_{34}}\right)\,, \end{aligned} \tag{B.51}$$

$$
\begin{aligned}
F^{\,(\mathrm{nab})} = {} & \frac{1}{4} - \frac{\left(z_3 s_{(12)4} - z_4 s_{(12)3}\right)^2}{{s_{34}}^2 z_{34}^2} + \frac{\left(s_{34} + s_{(12)4}\right)\left(s_{34} - z_3 s_{(12)4}\right)}{2 s_{34} s_{(12)3} z_{34}} \\
& - \frac{s_{34} + s_{(12)3}}{2 s_{(12)4}} + \frac{s_{(12)4}\left(z_{34}\left(4 - 3 z_4\right) - 8 {z_3}^2\right)}{2 s_{34} z_{34}^2} + \frac{3\left(1 - z_{34}\right)}{2 z_{34}} + \frac{z_3 z_4}{z_{34}^2} \\
& + (3 \leftrightarrow 4)\,.
\end{aligned}
\tag{B.52}
$$

Bibliography

[1] T. W. Kibble, "The standard model of particle physics," *European Review*, vol. 23, no. 1, pp. 36–44, 2015.

[2] S. Dittmaier *et al.*, "Handbook of LHC Higgs Cross Sections: 1. Inclusive Observables," 2011.

[3] S. Dittmaier *et al.*, "Handbook of LHC Higgs Cross Sections: 2. Differential Distributions," 2012.

[4] J. R. Andersen *et al.*, "Handbook of LHC Higgs Cross Sections: 3. Higgs Properties," 2013.

[5] D. de Florian *et al.*, "Handbook of LHC Higgs Cross Sections: 4. Deciphering the Nature of the Higgs Sector," 2016.

[6] D. Graudenz, M. Spira, and P. M. Zerwas, "QCD corrections to Higgs boson production at proton proton colliders," *Phys. Rev. Lett.*, vol. 70, pp. 1372–1375, 1993.

[7] M. Spira, A. Djouadi, D. Graudenz, and P. M. Zerwas, "Higgs boson production at the LHC," *Nucl. Phys.*, vol. B453, pp. 17–82, 1995.

[8] C. Anastasiou, C. Duhr, F. Dulat, F. Herzog, and B. Mistlberger, "Higgs Boson Gluon-Fusion Production in QCD at Three Loops," *Phys. Rev. Lett.*, vol. 114, p. 212001, 2015.

[9] B. Mistlberger, "Higgs boson production at hadron colliders at N^3LO in QCD," *JHEP*, vol. 05, p. 028, 2018.

[10] C. Anastasiou, C. Duhr, F. Dulat, E. Furlan, T. Gehrmann, F. Herzog, A. Lazopoulos, and B. Mistlberger, “High precision determination of the gluon fusion Higgs boson cross-section at the LHC,” *JHEP*, vol. 05, p. 058, 2016.

[11] F. A. Dreyer and A. Karlberg, “Vector-Boson Fusion Higgs Production at Three Loops in QCD,” *Phys. Rev. Lett.*, vol. 117, no. 7, p. 072001, 2016.

[12] F. A. Dreyer and A. Karlberg, “Vector-Boson Fusion Higgs Pair Production at N^{3}LO,” *Phys. Rev.*, vol. D98, no. 11, p. 114016, 2018.

[13] C. Duhr, F. Dulat, and B. Mistlberger, “Higgs production in bottom-quark fusion to third order in the strong coupling,” 2019.

[14] L. Cieri, X. Chen, T. Gehrmann, E. W. N. Glover, and A. Huss, “Higgs boson production at the LHC using the q_T subtraction formalism at N^{3}LO QCD,” *JHEP*, vol. 02, p. 096, 2019.

[15] F. Dulat, B. Mistlberger, and A. Pelloni, “Precision predictions at N^{3}LO for the Higgs boson rapidity distribution at the LHC,” *Phys. Rev.*, vol. D99, no. 3, p. 034004, 2019.

[16] J. Currie, T. Gehrmann, E. W. N. Glover, A. Huss, J. Niehues, and A. Vogt, “N^{3}LO corrections to jet production in deep inelastic scattering using the Projection-to-Born method,” *JHEP*, vol. 05, p. 209, 2018.

[17] X. Chen, J. Cruz-Martinez, T. Gehrmann, E. W. N. Glover, and M. Jaquier, “NNLO QCD corrections to Higgs boson production at large transverse momentum,” *JHEP*, vol. 10, p. 066, 2016.

[18] R. Boughezal, F. Caola, K. Melnikov, F. Petriello, and M. Schulze, “Higgs boson production in association with a jet at next-to-next-to-leading order,” *Phys. Rev. Lett.*, vol. 115, no. 8, p. 082003, 2015.

[19] R. Boughezal, C. Focke, W. Giele, X. Liu, and F. Petriello, “Higgs boson production in association with a jet at NNLO using jettiness subtraction,” *Phys. Lett.*, vol. B748, pp. 5–8, 2015.

[20] T. Binoth and G. Heinrich, "An automatized algorithm to compute infrared divergent multiloop integrals," *Nucl. Phys.*, vol. B585, pp. 741–759, 2000.

[21] C. Anastasiou and A. Daleo, "Numerical evaluation of loop integrals," *JHEP*, vol. 10, p. 031, 2006.

[22] S. Catani and M. Grazzini, "An NNLO subtraction formalism in hadron collisions and its application to Higgs boson production at the LHC," *Phys. Rev. Lett.*, vol. 98, p. 222002, 2007.

[23] R. Boughezal, X. Liu, and F. Petriello, "N-jettiness soft function at next-to-next-to-leading order," *Phys. Rev.*, vol. D91, no. 9, p. 094035, 2015.

[24] J. Gaunt, M. Stahlhofen, F. J. Tackmann, and J. R. Walsh, "N-jettiness Subtractions for NNLO QCD Calculations," *JHEP*, vol. 09, p. 058, 2015.

[25] A. Gehrmann-De Ridder, T. Gehrmann, and E. W. N. Glover, "Antenna subtraction at NNLO," *JHEP*, vol. 09, p. 056, 2005.

[26] A. Daleo, T. Gehrmann, and D. Maitre, "Antenna subtraction with hadronic initial states," *JHEP*, vol. 04, p. 016, 2007.

[27] A. Gehrmann-De Ridder, T. Gehrmann, and E. W. N. Glover, "Gluon-gluon antenna functions from Higgs boson decay," *Phys. Lett.*, vol. B612, pp. 49–60, 2005.

[28] A. Gehrmann-De Ridder, T. Gehrmann, and E. W. N. Glover, "Quark-gluon antenna functions from neutralino decay," *Phys. Lett.*, vol. B612, pp. 36–48, 2005.

[29] A. Daleo, A. Gehrmann-De Ridder, T. Gehrmann, and G. Luisoni, "Antenna subtraction at NNLO with hadronic initial states: initial-final configurations," *JHEP*, vol. 01, p. 118, 2010.

[30] T. Gehrmann and P. F. Monni, "Antenna subtraction at NNLO with hadronic initial states: real-virtual initial-initial configurations," *JHEP*, vol. 12, p. 049, 2011.

[31] R. Boughezal, A. Gehrmann-De Ridder, and M. Ritzmann, "Antenna subtraction at NNLO with hadronic initial states: double real radiation for initial-initial configurations with two quark flavours," *JHEP*, vol. 02, p. 098, 2011.

[32] A. Gehrmann-De Ridder, T. Gehrmann, and M. Ritzmann, "Antenna subtraction at NNLO with hadronic initial states: double real initial-initial configurations," *JHEP*, vol. 10, p. 047, 2012.

[33] J. Currie, E. W. N. Glover, and S. Wells, "Infrared Structure at NNLO Using Antenna Subtraction," *JHEP*, vol. 04, p. 066, 2013.

[34] G. Somogyi, Z. Trocsanyi, and V. Del Duca, "Matching of singly- and doubly-unresolved limits of tree-level QCD squared matrix elements," *JHEP*, vol. 06, p. 024, 2005.

[35] G. Somogyi, Z. Trocsanyi, and V. Del Duca, "A Subtraction scheme for computing QCD jet cross sections at NNLO: Regularization of doubly-real emissions," *JHEP*, vol. 01, p. 070, 2007.

[36] G. Somogyi and Z. Trocsanyi, "A Subtraction scheme for computing QCD jet cross sections at NNLO: Regularization of real-virtual emission," *JHEP*, vol. 01, p. 052, 2007.

[37] G. Somogyi and Z. Trocsanyi, "A Subtraction scheme for computing QCD jet cross sections at NNLO: Integrating the subtraction terms. I.," *JHEP*, vol. 08, p. 042, 2008.

[38] U. Aglietti, V. Del Duca, C. Duhr, G. Somogyi, and Z. Trocsanyi, "Analytic integration of real-virtual counterterms in NNLO jet cross sections. I.," *JHEP*, vol. 09, p. 107, 2008.

[39] G. Somogyi, "Subtraction with hadronic initial states at NLO: An NNLO-compatible scheme," *JHEP*, vol. 05, p. 016, 2009.

[40] P. Bolzoni, S.-O. Moch, G. Somogyi, and Z. Trocsanyi, "Analytic integration of real-virtual counterterms in NNLO jet cross sections. II.," *JHEP*, vol. 08, p. 079, 2009.

[41] P. Bolzoni, G. Somogyi, and Z. Trocsanyi, “A subtraction scheme for computing QCD jet cross sections at NNLO: integrating the iterated singly-unresolved subtraction terms,” *JHEP*, vol. 01, p. 059, 2011.

[42] V. Del Duca, G. Somogyi, and Z. Trocsanyi, “Integration of collinear-type doubly unresolved counterterms in NNLO jet cross sections,” *JHEP*, vol. 06, p. 079, 2013.

[43] G. Somogyi, “A subtraction scheme for computing QCD jet cross sections at NNLO: integrating the doubly unresolved subtraction terms,” *JHEP*, vol. 04, p. 010, 2013.

[44] M. Czakon, “A novel subtraction scheme for double-real radiation at NNLO,” *Phys. Lett.*, vol. B693, pp. 259–268, 2010.

[45] M. Czakon, “Double-real radiation in hadronic top quark pair production as a proof of a certain concept,” *Nucl. Phys.*, vol. B849, pp. 250–295, 2011.

[46] M. Czakon and D. Heymes, “Four-dimensional formulation of the sector-improved residue subtraction scheme,” *Nucl. Phys.*, vol. B890, pp. 152–227, 2014.

[47] M. Czakon, A. van Hameren, A. Mitov, and R. Poncelet, “Single-jet inclusive rates with exact color at $\mathcal{O}\left(\alpha_s^4\right)$,” *JHEP*, vol. 10, p. 262, 2019.

[48] F. Caola, K. Melnikov, and R. Roentsch, “Nested soft-collinear subtractions in NNLO QCD computations,” *Eur. Phys. J.*, vol. C77, no. 4, p. 248, 2017.

[49] F. Caola, M. Delto, H. Frellesvig, and K. Melnikov, “The double-soft integral for an arbitrary angle between hard radiators,” *Eur. Phys. J.*, vol. C78, no. 8, p. 687, 2018.

[50] M. Delto and K. Melnikov, “Integrated triple-collinear counter-terms for the nested soft-collinear subtraction scheme,” *JHEP*, vol. 05, p. 148, 2019.

[51] F. Caola, K. Melnikov, and R. Roentsch, "Analytic results for color-singlet production at NNLO QCD with the nested soft-collinear subtraction scheme," *Eur. Phys. J.*, vol. C79, no. 5, p. 386, 2019.

[52] F. Caola, K. Melnikov, and R. Roentsch, "Analytic results for decays of color singlets to gg and $q\bar{q}$ final states at NNLO QCD with the nested soft-collinear subtraction scheme," 2019.

[53] M. Cacciari, F. A. Dreyer, A. Karlberg, G. P. Salam, and G. Zanderighi, "Fully Differential Vector-Boson-Fusion Higgs Production at Next-to-Next-to-Leading Order," *Phys. Rev. Lett.*, vol. 115, no. 8, p. 082002, 2015. [Erratum: Phys. Rev. Lett.120,no.13,139901(2018)].

[54] J. M. Henn and B. Mistlberger, "Four-Gluon Scattering at Three Loops, Infrared Structure, and the Regge Limit," *Phys. Rev. Lett.*, vol. 117, no. 17, p. 171601, 2016.

[55] O. Almelid, C. Duhr, and E. Gardi, "Three-loop corrections to the soft anomalous dimension in multileg scattering," *Phys. Rev. Lett.*, vol. 117, no. 17, p. 172002, 2016.

[56] O. Almelid, C. Duhr, E. Gardi, A. McLeod, and C. D. White, "Bootstrapping the QCD soft anomalous dimension," *JHEP*, vol. 09, p. 073, 2017.

[57] J. M. Campbell and E. W. N. Glover, "Double unresolved approximations to multiparton scattering amplitudes," *Nucl. Phys.*, vol. B527, pp. 264–288, 1998.

[58] S. Catani and M. Grazzini, "Infrared factorization of tree level QCD amplitudes at the next-to-next-to-leading order and beyond," *Nucl. Phys.*, vol. B570, pp. 287–325, 2000.

[59] V. Del Duca, A. Frizzo, and F. Maltoni, "Factorization of tree QCD amplitudes in the high-energy limit and in the collinear limit," *Nucl. Phys.*, vol. B568, pp. 211–262, 2000.

[60] D. A. Kosower, "Multiple singular emission in gauge theories," *Phys. Rev.*, vol. D67, p. 116003, 2003.

[61] Z. Bern, L. J. Dixon, D. C. Dunbar, and D. A. Kosower, "One loop n point gauge theory amplitudes, unitarity and collinear limits," *Nucl. Phys.*, vol. B425, pp. 217–260, 1994.

[62] Z. Bern, V. Del Duca, and C. R. Schmidt, "The Infrared behavior of one loop gluon amplitudes at next-to-next-to-leading order," *Phys. Lett.*, vol. B445, pp. 168–177, 1998.

[63] D. A. Kosower and P. Uwer, "One loop splitting amplitudes in gauge theory," *Nucl. Phys.*, vol. B563, pp. 477–505, 1999.

[64] Z. Bern, V. Del Duca, W. B. Kilgore, and C. R. Schmidt, "The infrared behavior of one loop QCD amplitudes at next-to-next-to leading order," *Phys. Rev.*, vol. D60, p. 116001, 1999.

[65] S. Catani and M. Grazzini, "The soft gluon current at one loop order," *Nucl. Phys.*, vol. B591, pp. 435–454, 2000.

[66] T. G. Birthwright, E. W. N. Glover, V. V. Khoze, and P. Marquard, "Multi-gluon collinear limits from MHV diagrams," *JHEP*, vol. 05, p. 013, 2005.

[67] C. Duhr, "Applications of twistor methods in QCD," Master's thesis, Université catholique de Louvain, 2006.

[68] S. Catani, D. Colferai, and A. Torrini, "Triple (and quadruple) soft-gluon radiation in QCD hard scattering," 2019.

[69] S. Catani, D. de Florian, and G. Rodrigo, "The Triple collinear limit of one loop QCD amplitudes," *Phys. Lett.*, vol. B586, pp. 323–331, 2004.

[70] S. Badger, F. Buciuni, and T. Peraro, "One-loop triple collinear splitting amplitudes in QCD," *JHEP*, vol. 09, p. 188, 2015.

[71] Z. Bern, L. J. Dixon, and D. A. Kosower, "Two-loop $g \to gg$ splitting amplitudes in QCD," *JHEP*, vol. 08, p. 012, 2004.

[72] S. D. Badger and E. W. N. Glover, "Two loop splitting functions in QCD," *JHEP*, vol. 07, p. 040, 2004.

[73] C. Duhr, T. Gehrmann, and M. Jaquier, "Two-loop splitting amplitudes and the single-real contribution to inclusive Higgs production at N^3LO," *JHEP*, vol. 02, p. 077, 2015.

[74] C. Duhr and T. Gehrmann, "The two-loop soft current in dimensional regularization," *Phys. Lett.*, vol. B727, pp. 452–455, 2013.

[75] Y. Li and H. X. Zhu, "Single soft gluon emission at two loops," *JHEP*, vol. 11, p. 080, 2013.

[76] L. J. Dixon, E. Herrmann, K. Yan, and H. X. Zhu, "Soft gluon emission at two loops in full color," *JHEP*, vol. 05, p. 135, 2020.

[77] "Quadruple Collinear Splitting Amplitudes supplementary material." `https://people.phys.ethz.ch/~pheno/quadruple_collinear`. Accessed: 2020-08-19.

[78] V. Del Duca, C. Duhr, R. Haindl, A. Lazopoulos, and M. Michel, "Tree-level splitting amplitudes for a quark into four collinear partons," *JHEP*, vol. 02, p. 189, 2020.

[79] V. Del Duca, C. Duhr, R. Haindl, A. Lazopoulos, and M. Michel, "Tree-level splitting amplitudes for a gluon into four collinear partons," 7 2020.

[80] W. Konetschny and W. Kummer, "Unitarity in the Ghost Free Axial Gauge," *Nucl. Phys. B*, vol. 108, pp. 397–408, 1976.

[81] S. Catani and M. Grazzini, "Collinear factorization and splitting functions for next-to-next-to-leading order QCD calculations," *Phys. Lett.*, vol. B446, pp. 143–152, 1999.

[82] D. Amati, R. Petronzio, and G. Veneziano, "Relating Hard QCD Processes Through Universality of Mass Singularities," *Nucl. Phys.*, vol. B140, pp. 54–72, 1978.

[83] D. Amati, R. Petronzio, and G. Veneziano, "Relating Hard QCD Processes Through Universality of Mass Singularities. 2.," *Nucl. Phys.*, vol. B146, pp. 29–49, 1978.

[84] R. K. Ellis, H. Georgi, M. Machacek, H. D. Politzer, and G. G. Ross, "Factorization and the Parton Model in QCD," *Phys. Lett.*, vol. 78B, pp. 281–284, 1978.

[85] R. Ellis, H. Georgi, M. Machacek, H. Politzer, and G. G. Ross, "Perturbation theory and the parton model in qcd," *Nuclear Physics B*, vol. 152, no. 2, pp. 285 – 329, 1979.

[86] J. M. Campbell and E. W. N. Glover, "Double unresolved approximations to multiparton scattering amplitudes," *Nucl. Phys.*, vol. B527, pp. 264–288, 1998.

[87] A. Bassetto, M. Ciafaloni, and G. Marchesini, "Jet Structure and Infrared Sensitive Quantities in Perturbative QCD," *Phys. Rept.*, vol. 100, pp. 201–272, 1983.

[88] S. Catani, "New Techniques for Calculating Higher-Order QCD Corrections," in *Proceedings, Workshop on New Techniques for Calculating Higher Order QCD Corrections, Zurich, Switzerland, 16-18 Dec 1992*, (Zürich), 1992.

[89] G. Altarelli and G. Parisi, "Asymptotic Freedom in Parton Language," *Nucl. Phys.*, vol. B126, pp. 298–318, 1977.